www.advtechconsultants.com

Supercritical Fluids and Injection Processes of Relevance to High-Pressure Combustion

Bruce Chehroudi, PhD

Vice President of Research and Development
Advanced Technology Consultants
www.advtechconsultants.com
ChehroudiB@aol.com

Kolloquium Thermo- und Fluiddynamik (KTF)
ETH
Swiss Federal Institute of Technology Zurich

February 18, 2009

ATC Advanced Technology Consultants

www.advtechconsultants.com

Table of Contents

ATC Advanced Technology Consultants
www.advtechconsultants.com

Motivation

- High combustion chamber pressure and temperature generally reflect to high efficiency and/or thrust in diesel, gas turbine, and rockets.

- The Space Shuttle main engine thrust chamber pressure is about 22.3 MPa.
  - This is supercritical for the liquid H_2 (1.28/32.94) and liquid O_2 (5.04/154.6). (Pc in MPa / Tc in K)
  - The combustion chamber pressure for Vulcain (Ariane 5) with liquid H_2 /liquid O_2 can reach up to 10 MPa while a record pressure of nearly 28.2 MPa has been reported

- Understanding mechanism of acoustic combustion instabilities under such a high pressure environment has been a challenge

- Limited information is available for jets injected under these conditions where injectant finds itself in a thermodynamic supercritical environment.

Advanced Technology Consultants

www.advtechconsultants.com

Combustion Instability in Liquid Rocket Engine (LRE)

Viewing Direction

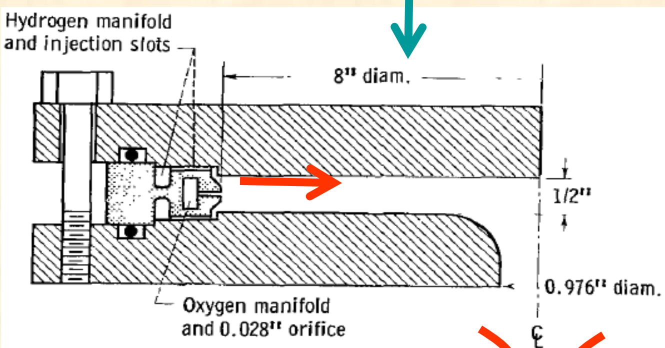

LOX Core

- **The LOX core was found to decrease in length during a combustion instability event**
- **LOX core large scale sinusoidal structure**

Heidmann, NASA TN D-2725, 1965
NASA Lewis Film C-226, 1965

Combustion Instability: Nature of the Problem

www.advtechconsultants.com

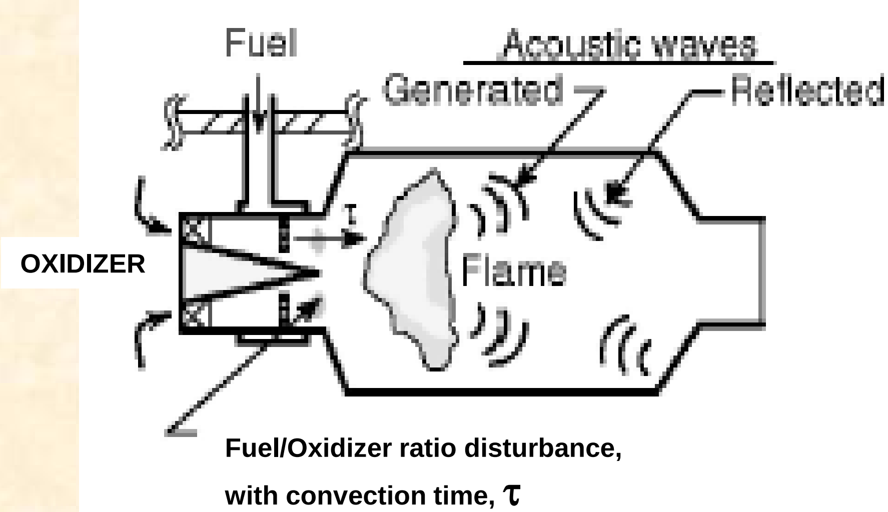

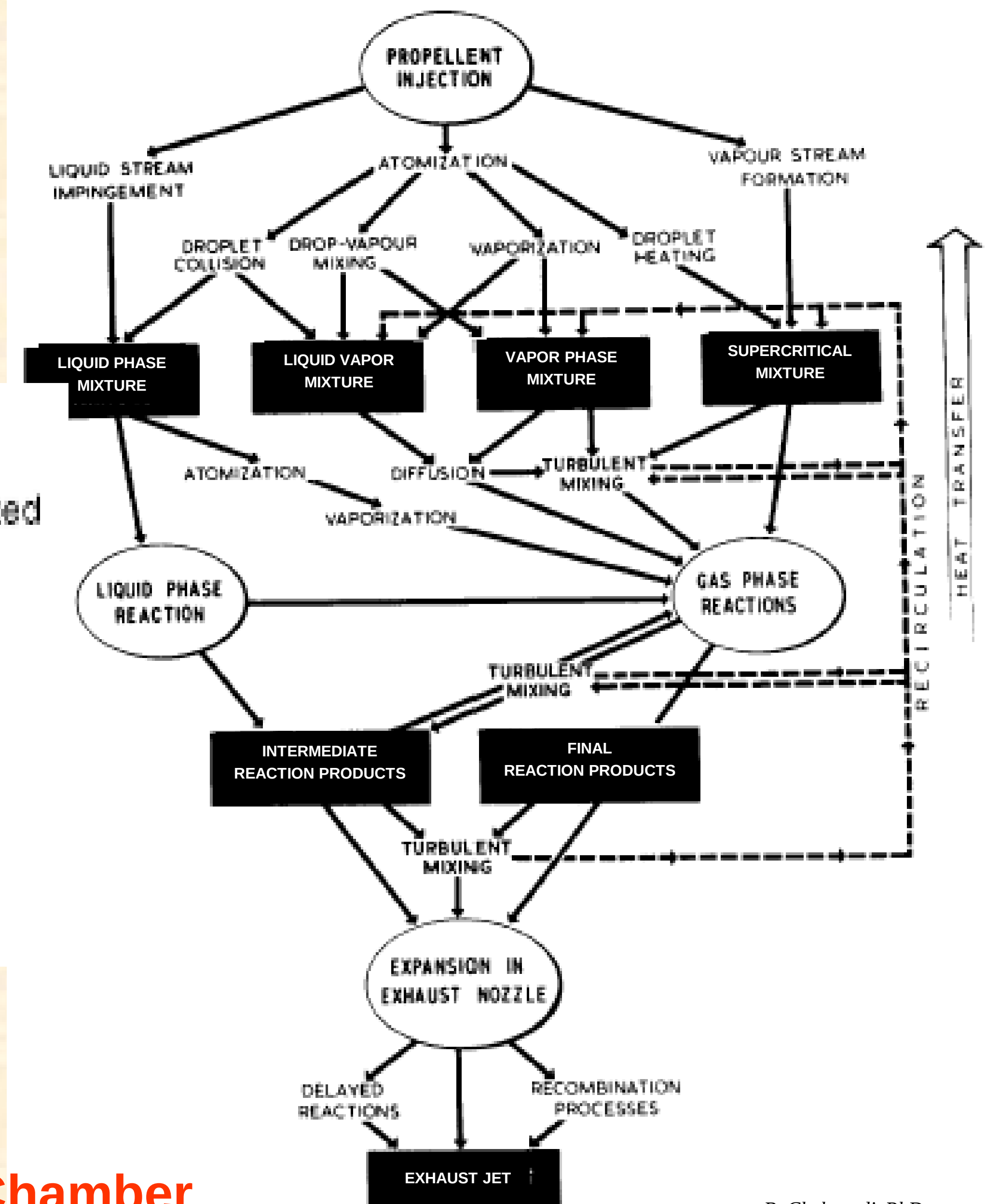

Rocket Engine Thrust Chamber

Mechanism of Combustion Instability in LRE

ATC Advanced Technology Consultants
www.advtechconsultants.com

Fred Culick (CalTech)

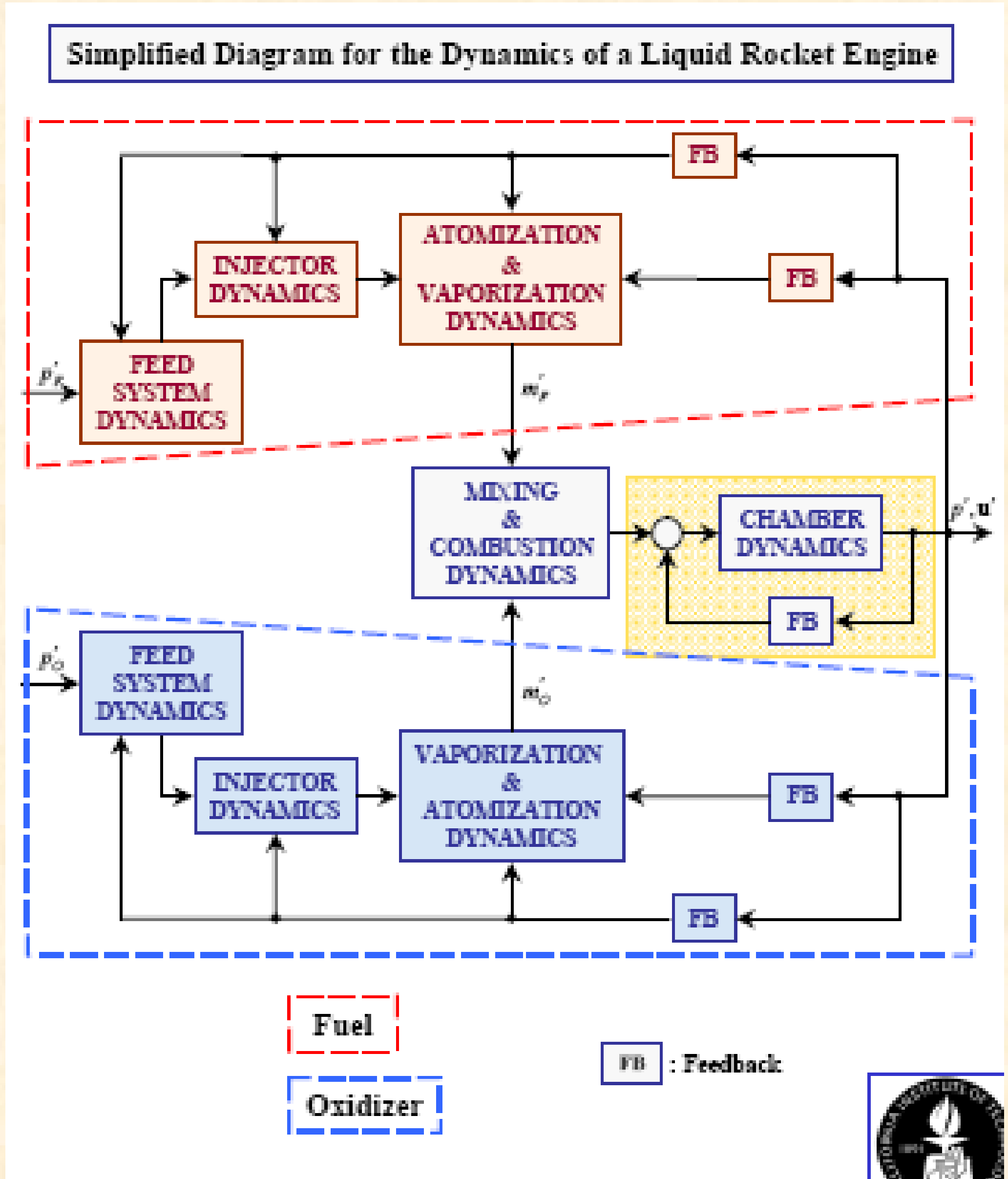

What Is The Physics?

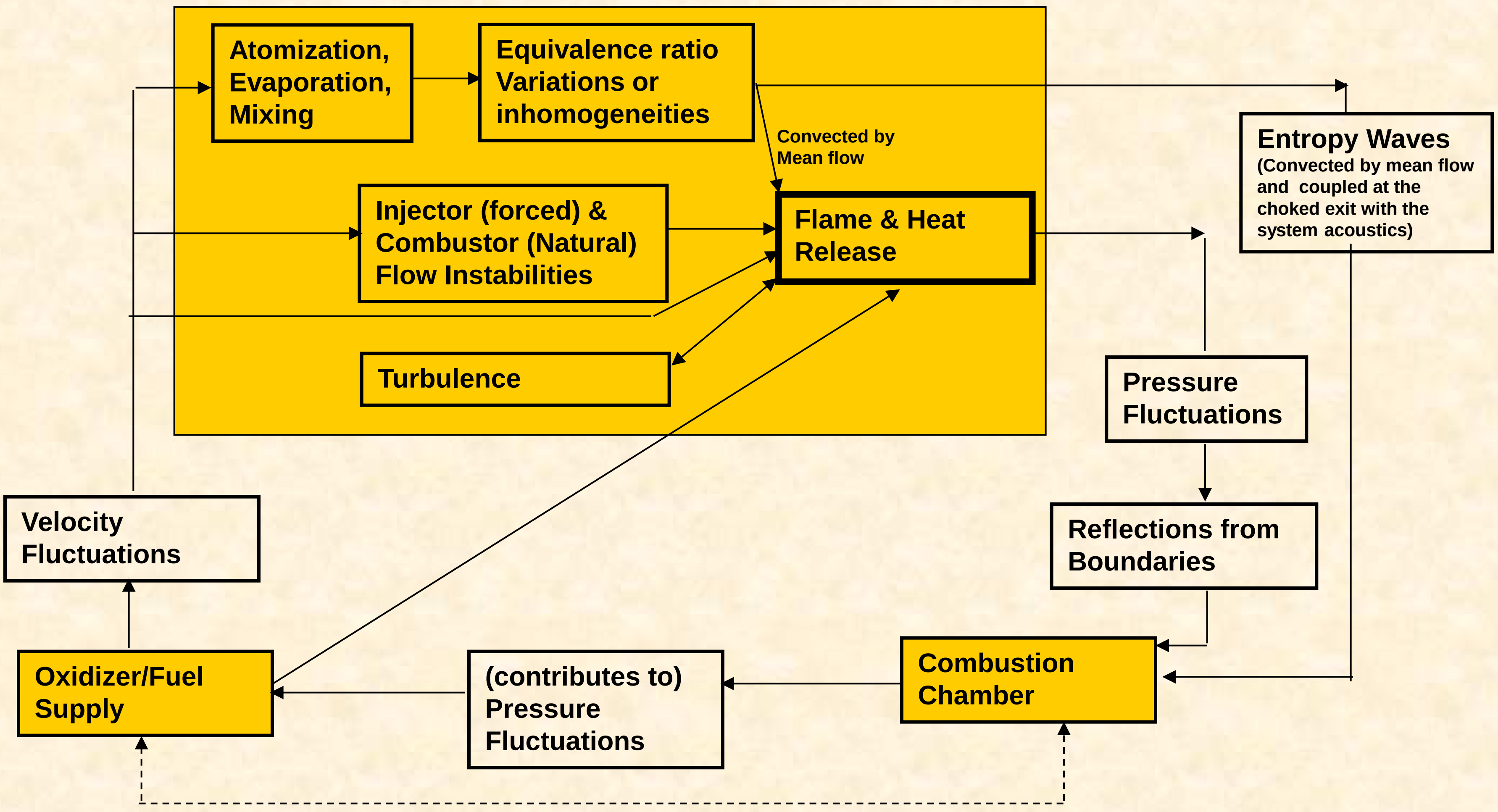

Entropy waves: The adiabatic flame temperature of richer (leaner) pockets of mixture is higher (lower) than average. Thus, equivalence ratio fluctuations will lead to fluctuations in the hot gas temperature downstream of the flame (i.e., so-called entropy waves)

Pressure Oscillations

ATC Advanced Technology Consultants
www.advtechconsultants.com

"Like Doublet Injector with a Monotuned 1T Resonator" without Baffles

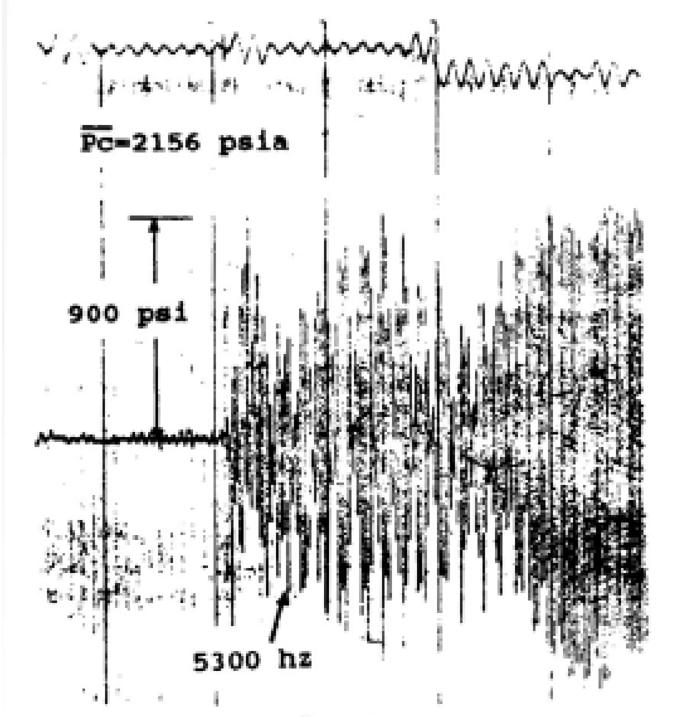

"Like Doublet Injector with a 16 cm High Baffle" without 1T-mode Acoustic Cavities

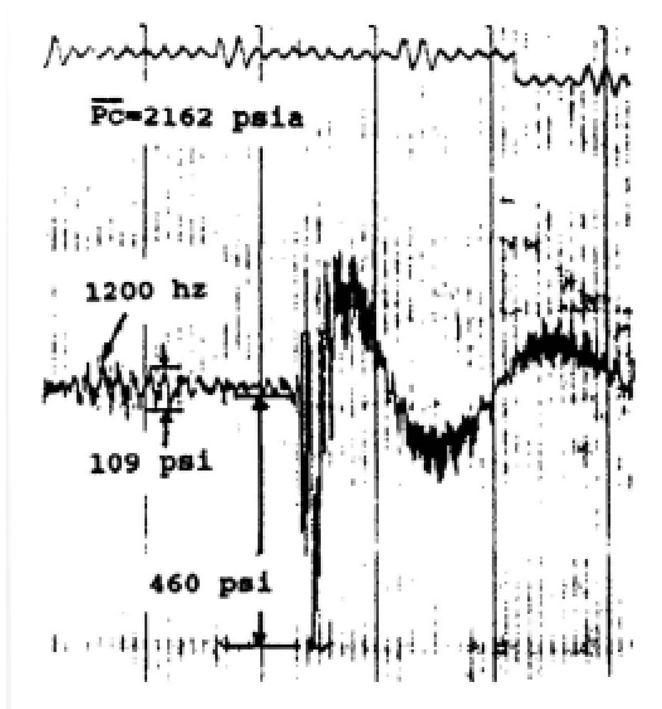

Advanced Technology Consultants

www.advtechconsultants.com

Combustor as a Feedback Amplifier

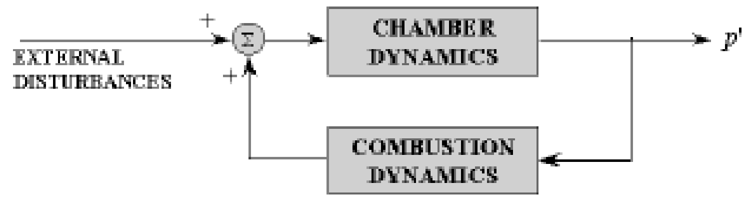

FIGURE 1.1. Schematic diagram of a combustion system as a feedback amplifier.

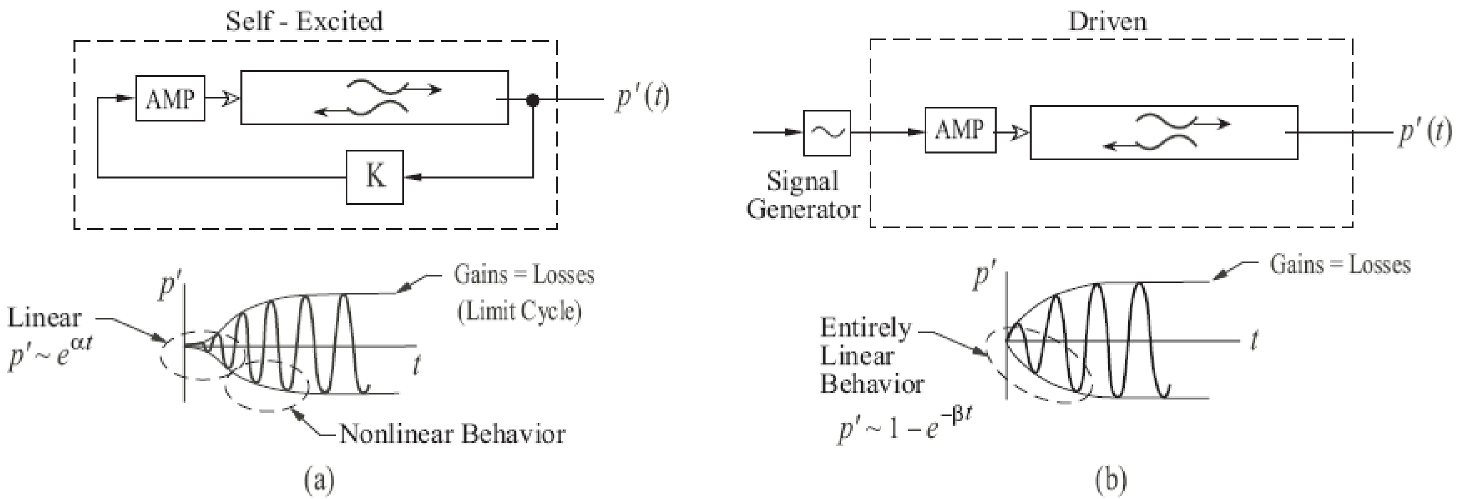

FIGURE 1.34. Transient behavior of (a) self-excited linearly unstable motions; (b) forced motions.

Data of the sort sketched in Figure 1.34 leave no doubt that the unstable motions in combustion chambers are self-excited, having the characteristics shown in Figure 1.34(a). The physical origin of this behavior is the dependence of the energy gains and losses on the motions themselves. For combustion instabilities, the 'system' is the dynamical system whose behavior is measured by the instrument sensing the pressure oscillations. Thus, in view of earlier remarks, the dynamical system is in some sense the system of acoustical motions in the chamber coupled to the mean flow and combustion processes (recall Figure 1.1).

ATC Advanced Technology Consultants

www.advtechconsultants.com

Historical Note on Combustion Instability in LRE

- Two classes of instabilities:
  - "*Nonacousic*": chugging represented as low-frequency pulsations (p ~ uniform) in a lumped-parameter system containing time lags, especially due to the propellant supply system
  - "*Acoustic*": high frequency, caused by coupling between the combustion processes and the unsteady motions

- Acoustic combustion instability has been one of the most complex phenomena in liquid rocket engines, and therefore
  - difficult to fully understand, control, and predict particularly in the design of large-output rockets
- The difficulty arises from the emergence of oscillatory combustion with rapidly increasing and large pressure amplitudes.
  - This leads to local burnout of the combustion chamber walls and injector plates which is caused through extreme heat-transfer rates by high-frequency pressure and gas velocity fluctuations
- Resonance acoustic modes of the thrust chamber, amongst them the transverse modes being the most troublesome, are excited through the energy provided by the combustion.
- The amplification process is thought to include
  - a feedback of information from the acoustic field to the injector or near-injector phenomena which in turn tends to reinforce the combustion-to-acoustic-field energy transfer processes.
- The underlying physics of this energy transfer is the widely cited general principle by *Lord Rayleigh*
  - He stated that the interaction between the combustion heat release and the acoustic field is the strongest if heat is added in a region of space *and* at the time when the acoustic amplitude is the highest.
- Although this view (*i.e., Rayleigh's*) has been useful, evidences gathered by past investigations attributed combustion instability to a complex interaction of the external acoustic field with the fuel injection (or near-injector) processes as a feedback mechanism, thereby leading to incidences of instability in rocket engines.

ATC Advanced Technology Consultants

www.advtechconsultants.com

Historical Note on Combustion Instability in LRE

TUESDAY, AUGUST 28, 2001: Six weeks after its next-generation Ariane 5 rocket malfunctioned, Arianespace is ready for its next commercial satellite launch, albeit using the older workhorse Ariane 4 booster. Officials have cleared the Ariane 4 for blastoff at 0646 GMT (2:46 a.m. EDT) Thursday from the ELA-2 launch complex at the Guiana Space Center in Kourou, French Guiana on South America's northeastern coast. Investigators probing the July 12 failure of the Ariane 5 blamed the mishap on "combustion instability" during ignition of the rocket's upper stage. The pressure spike caused an inproper mixture of fuel and oxidizer feeing to the stage's engine, resulting in reduced thrust and a premature engine shutdown when the oxidizer was used up 80 seconds sooner than planned. The rocket's two satellite cargos were deployed into an orbit vastly lower than planned due to the upper stage trouble.

3.1 Summary of the F-1 Program

Reference: Olefein and Yang, (1993) *J. Propulsion and Power*, Vol. 9, No. 5, (pp. 657–677)

- LOX/HC (PR-1, kerosene)
- Summary of Development
  - Lineage E-1(1950s) → MA-2(Atlas) → H-1(Saturn I)
  - Experience with combustion instabilities in F-1

PERIOD	NUMBER OF TESTS	NUMBER OF CI	REMARKS
1959–1960	44	20	$(\Delta p)_{p-p} \geq \bar{p}$
1960–1960	—	—	• Linear or Nonlinear Instability identified: "self-triggering" • Baffles required for dynamic stability
1962–1965	207	—	• Preliminary Flight Rating Tests (PFRT): 11 injectors
	422	—	• Flight Rating Tests (FRT): 46 injectors
	703	—	• Qualification: 51 injectors
TOTAL	1376		108 injectors

ATC Advanced Technology Consultants

www.advtechconsultants.com

Liquid Rocket Combustion Chamber

Rocket Thrust Chamber

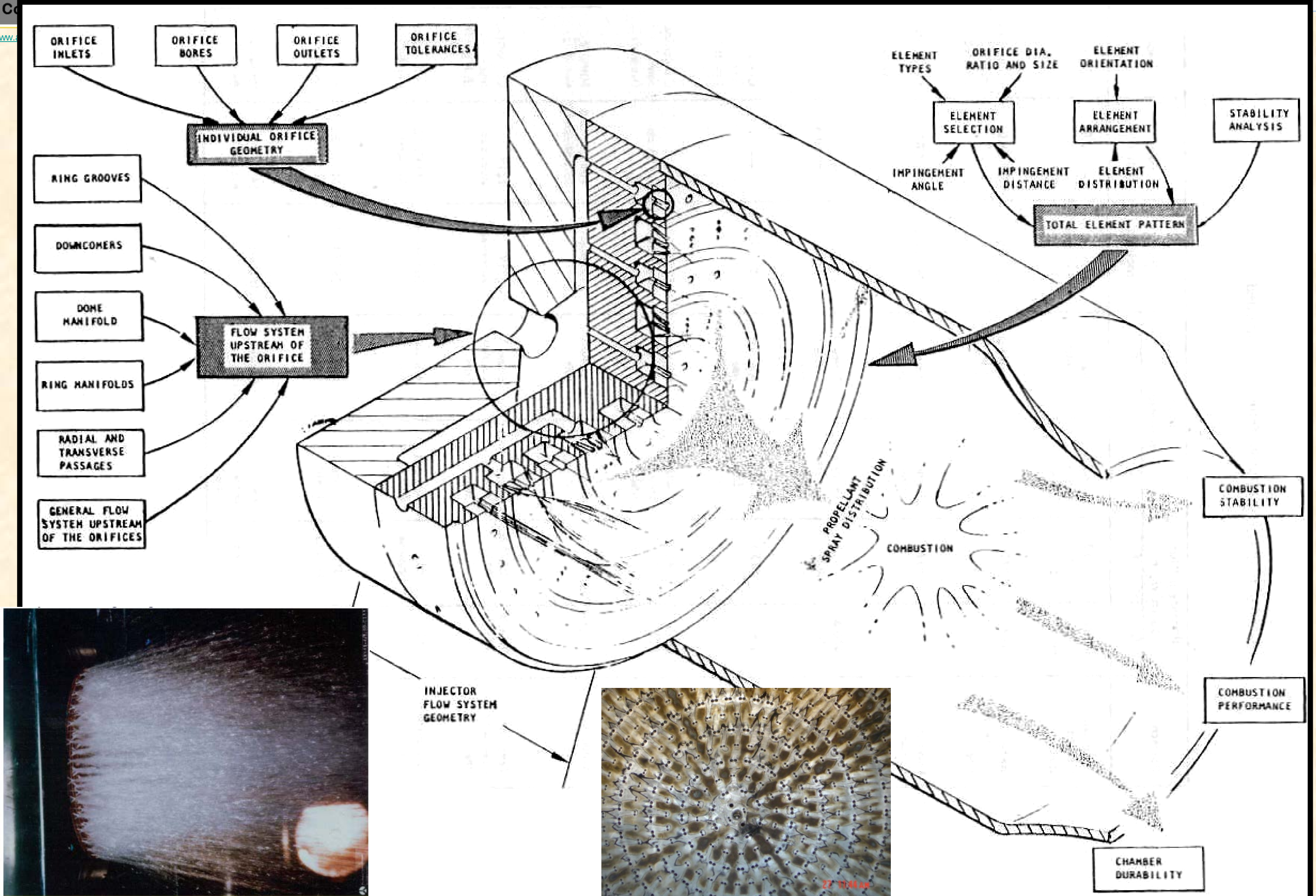

water flow test of F-1 engine injection system

Rocket Engine Thrust Chamber

B. Chehroudi, PhD

ATC Advanced Technology Consultants

www.advtechconsultants.com

Rocket Thrust Chamber

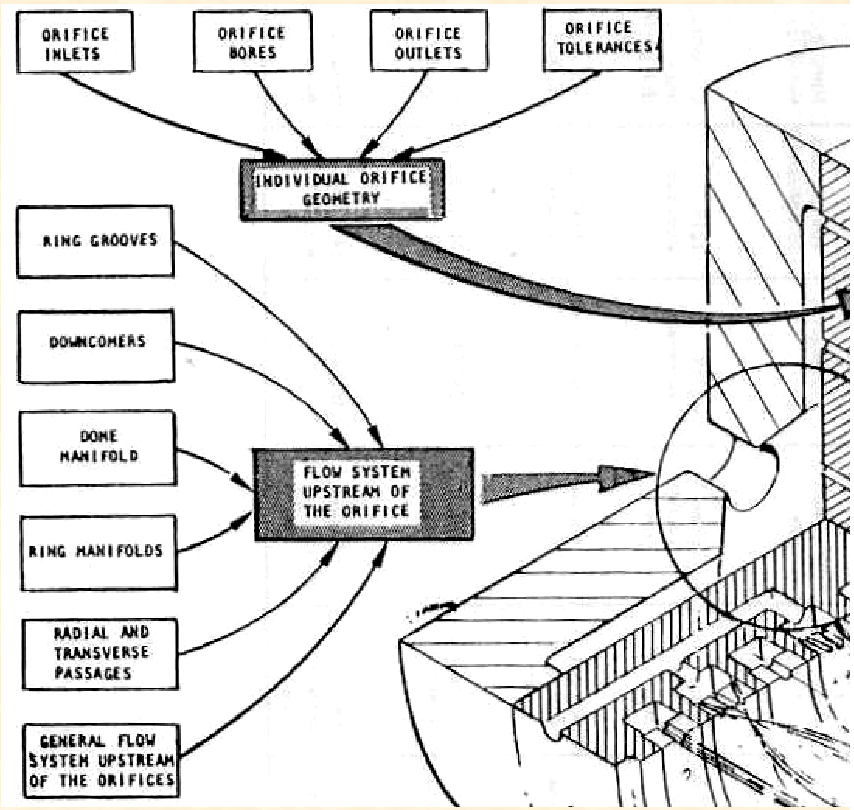

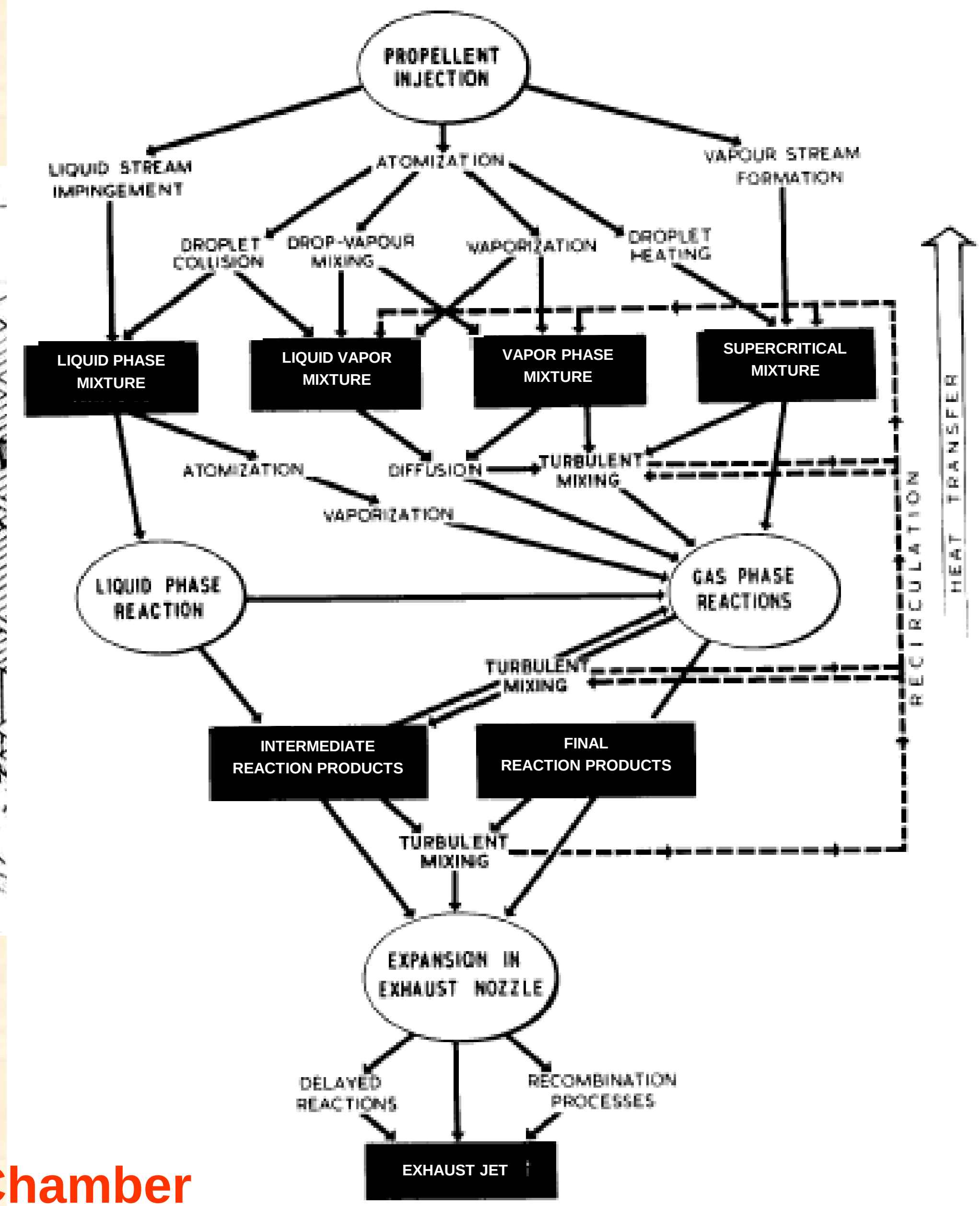

Rocket Engine Thrust Chamber

ATC
Advanced Technology Consultants

www.advtechconsultants.com

Rocket Engine

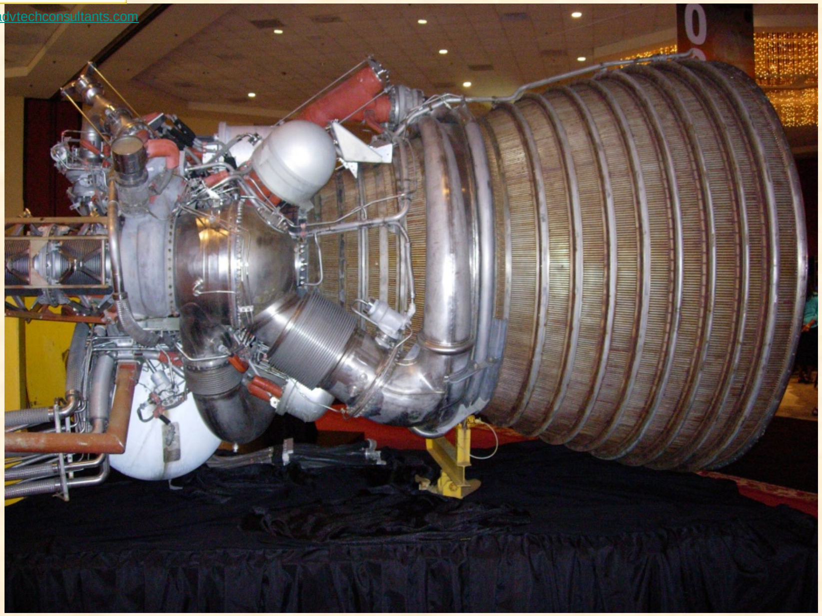

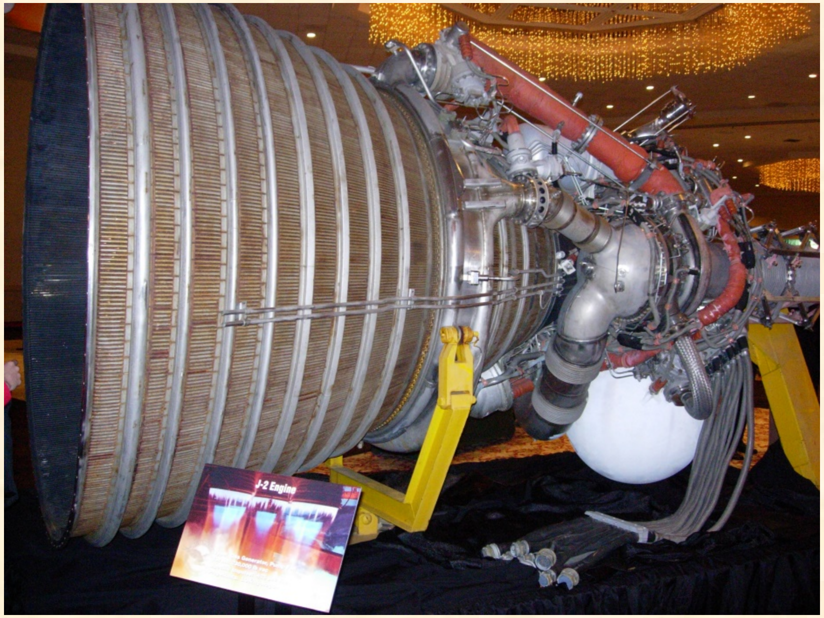

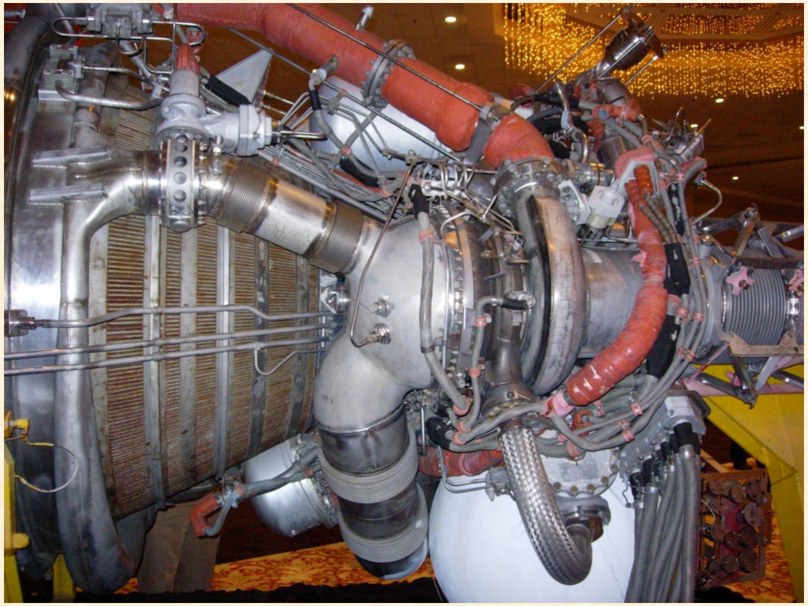

Overall Characteristics

ROCKET vs. TURBINE ENGINES	
TURBINE ENGINES	**ROCKE ENGINES**
Internal operating pressure ~ 300 psi	Internal operating pressures ~ 6000 psi
Turbine temperature ~ 3300F	Turbine temperatures ~ 1250 F
T/W ~ 6 AT T ~ 40,000 lbf	T/W ~ 65 AT T ~450,000 lbf
Room Temperature propellant	Cryogenic propellants (-280F to -423F)
Mission time at max thrust ~25%	Mission time at max thrust ~ 95%
Idle to max thrust time <~ 5s	Idle to max thrust ~ 1s

- Diagnostics for combustion instability studies must then deal With the Following requirements
  - Deposits (soot, etc.) on the walls
  - High temperature
  - High pressure
  - Fast-response
  - Dense liquid spray

Features of SSME Engine

ATC Advanced Technology Consultants
www.advtechconsultants.com

AFRL THE AIR FORCE RESEARCH LABORATORY LEAD | DISCOVER | DEVELOP | DELIVER

Overview:

The Space Shuttle Main Engine (SSME) is the world's most reliable and highly tested large rocket engine ever built. The SSMEs have achieved 100% flight success, and a demonstrated reliability of 0.9995. The SSME is a reusable, staged-combustion cycle engine utilizing liquid hydrogen fuel to achieve high performance never previously attained in a production rocket engine. The SSME is the only operational, reusable liquid booster engine designed for human space flight.

The first flight of the upgraded Block II SSME will be in 2001.

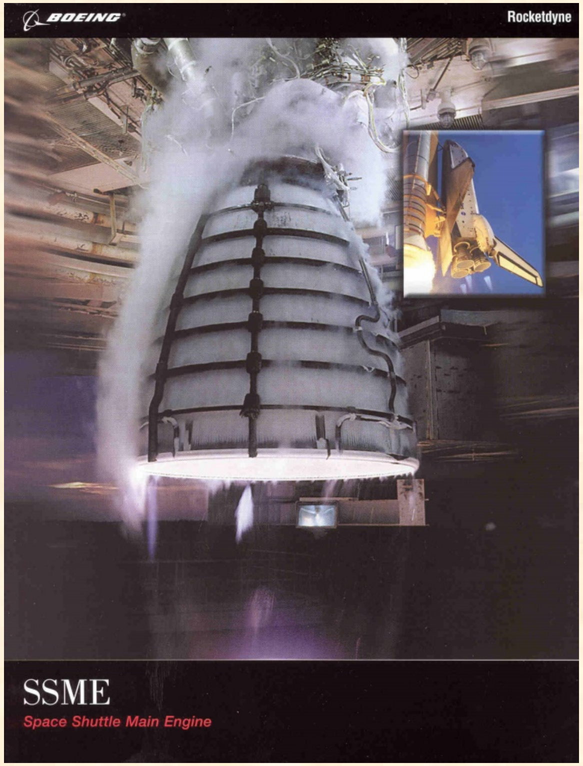

Performance

Block II Space Shuttle Main Engine (full power level)

Maximum Thrust: (109% Power Level)		
	At Sea Level:	418,000 lb
	In Vacuum:	512,300 lb
Throttle Range:	67% – 109%	
Pressures:	Hydrogen Pump Discharge:	6,276 psia
	Oxygen Pump Discharge:	7,268 psia
	Chamber Pressure:	2,994 psia
Specific Impulse: (In Vacuum)	452.3 sec	
Power: High Pressure Pumps		
	Hydrogen:	71,140 hp
	Oxygen:	23,260 hp
Area Ratio:	69:1	
Weight:	7,774 lb	
Mixture Ratio: (O/F)	6.03:1	
Dimensions:	168 in. long 96 in. wide	
Propellants:	Fuel:	Liquid Hydrogen
	Oxidizer:	Liquid Oxygen

ATC
Advanced Technology Consultants
www.advtechconsultants.com

Features of RD-180 Engine

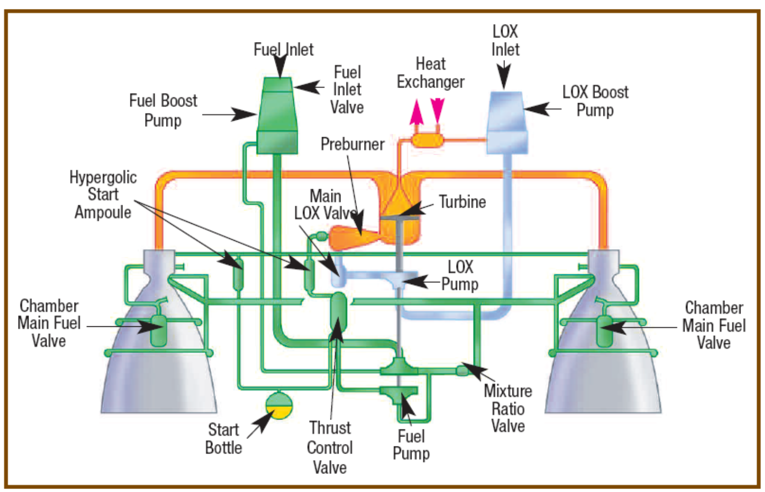

Characteristics (100% power)		
Nominal Thrust:	(sea level) (vacuum)	860,200 lb 933,400 lb
Specific impulse: (sea level)	311.3 sec	
Vacuum specific impulse:	337.8 sec	
Chamber Pressure:	3,722 psia	
Nozzle area ratio:	36.4:1	
Mixture ratio:	2.72	
Length:	140 in.	
Diameter:	124 in	
Throttle Range:	47% – 100%	
Dry weight:	12,081 lb (5,480 kg)	

Description

- Staged-combustion cycle engine
- Liquid oxygen/kerosene propellants
- 2 thrust chambers (gimbal +/-8 degrees)
- 1 oxygen-rich preburner
- High-pressure turbopump assembly
  - 2-stage fuel pump • single-stage oxygen pump • single turbine
- Hypergolic ignition
- Self-contained hydraulic system powered with kerosene from fuel pump
- Minimal interfaces with launch pad and vehicle
- 70% RD-170 parts

Liquid Rocket Injectors

ATC Advanced Technology Consultants

www.advtechconsultants.com

Major Kinds of Rocket Injectors

THE AIR FORCE RESEARCH LABORATORY — LEAD | DISCOVER | DEVELOP | DELIVER

Common Injection Element Configurations

Element Designation	Element Configuration (Flow Direction)	Characteristics	Engine Application
Concentric Tube	GAS, LIQ, GAS	• Very good wall compatibility • Very high performance with LOX/H_2 • Good stability characteristics with LOX/H_2 • Fuel is gas • Small annular gap requires care in fabrication and is sensitive to contamination	• Shuttle main and preburners • J-2 • Orbit Transfer Vehicle

Concentric Tube with Liquid Swirl	GAS, LIQ, RECESS	• Same as concentric tube except:
		  • Improved mixing and atomization
		  • More complex element
		  • Stability characteristics in large engines unknown
		  • Possible wall compatibility issue with some designs
		• Gas can also be swirled
			• RL-10

Unlike Pentad (4 on 1)	LIQ, GAS, LIQ	• Applicable to very high or low mixture or density ratios • Good mixing and atomization • Difficult to manifold	• Experimental
Unlike Doublet (1 on 1)	OX, FUEL, IMP DIST	• Good overall mixing and atomization (High Performance) • Simple to manifold • Subject to blowapart with hypergolic propellants	• LEM ascent engine • Delta launch vehicle • Almost all high response attitude control engines using storable propellants
Unlike Triplet (2 on 1)	OX, FUEL, OX	• Good overall mixing and atomization (High Performance) • Symmetric spray pattern • Subject to blowapart with hypergolic propellants • Fuel can be gas • Pattern can be reversed	• Agena upper stage • Rocketdyne LEM descent engine design • LOX/RP1 gas generators
Like Doublet (1 on 1)	OX, FUEL, FUEL, OX	• Easy to manifold • Excellent for chamber wall compatibility • Not subject to blowapart • Less effective atomization and mixing than unlike impinging elements	• Titan I and II first stage • Redstone, Jupiter, Thor, Atlas boosters • Shuttle OMES • H-1, F-1 engines
Showerhead	OX, FUEL	• Often employed for fuel boundary layer cooling of chamber wall • Easy to manifold • Poor atomization and mixing (Low Performance)	• Aerobee sustainer • X-15 • Pioneer
Variable Area (Pintle)	FUEL, OX	• Throttleable over wide range • Complex fabrication • Lower performance	• LEM descent engine • Lance sustainer

Splash Plate	SPLASH PLATE, OX, FUEL	• Less sensitive to design tolerances
		• Generally larger elements
			• Lance booster (early version)
			  • Saturn SIVB ullage control
			  • Apollo CM RCS (SE-8)
			  • Gemini SC maneuvering, attitude control and reentry engines

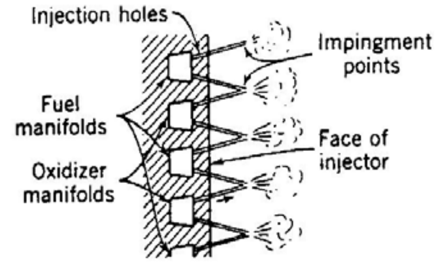

Doublet impinging stream pattern

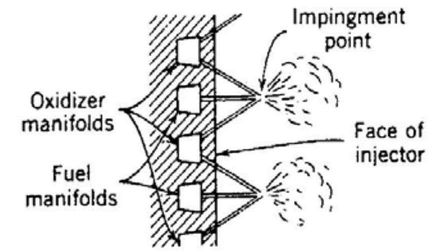

Triplet impinging stream pattern

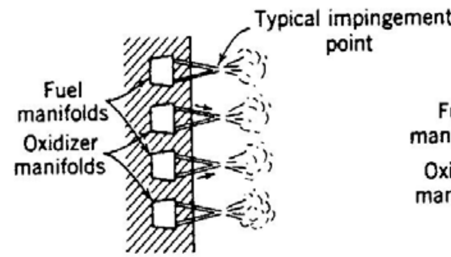

Self-impinging stream pattern

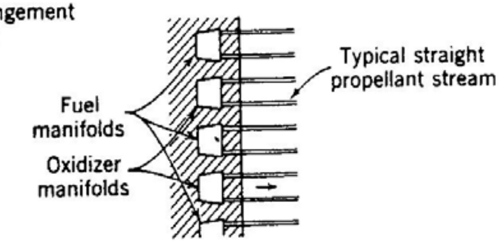

Shower head stream pattern

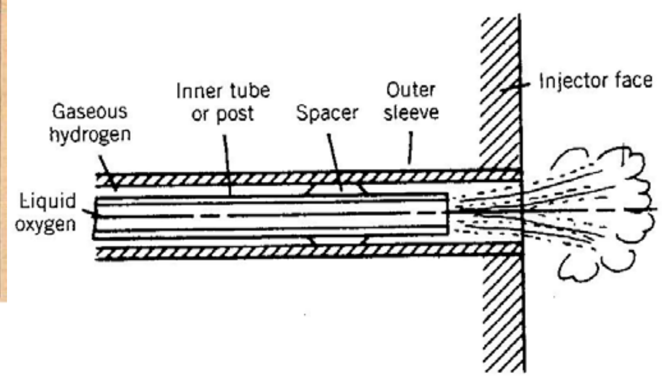

Hollow post and sleeve element

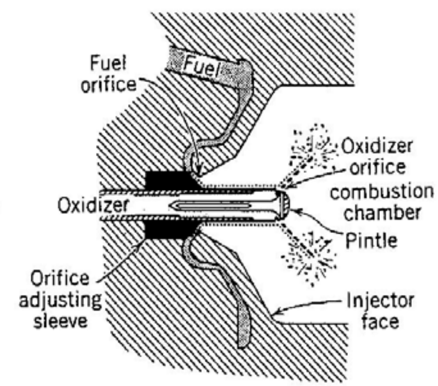

Variable injection area concentric tube injector

From Sutton, “Rocket Propulsion Elements,” 6th ed., pg 299, Wylie 1992

Major Kinds of Rocket Injectors

Type	Element Configuration	Advantages	Disadvantages	Engine Application
Unlike Doublet (1 on 1)		•Proven dependability •Good overall mixing •Simple to manifold •Extensive studied	•Subject to blowapart with hypergolic propellants •Wall compatibility problems due to mixture-ratio gradients	•LEM ascent engine •Delta launch vehicle
Unlike Triplet (2 on 1)		•Good overall mixing •Resultant spray direction is axial •Proven dependability	•Subject to blowapart with hypergolic •Wall compatibility is good only when fuel is used in outer orifices	•Agena upper stage, Gemini
Unlike Quadlet (2 on 2)		•Can be used near wall •Resultant spray direction is axial •Proven dependability	•Subject to blowapart with hypergolic propellants •Difficult to manifold •Not well characterized	•Titan III first, second stage •Titan II, second stage
Like Doublet (1 on 1)		•Easy to manifold •Good mixing, Very stable •Not subject to blowapart •Well understood	•Requires increased axial distance to mix •Sensitive to design tolerances	•Titan I,II first stage •Jupiter, Thor, Atlas •H-1, F-1 engines
Concentric Tube	Fuel O Fuel	•Very good wall compatibility •Low pressure drop	•Poor mixing •Difficult to fabricate •Tends to become unstable when throttled	•Russia use extensively

Common Injection Element Configurations

Element Designation	Element Configuration (Flow Direction)	Characteristics	Engine Application
Concentric Tube	GAS LIQ GAS	• Very good wall compatibility • Very high performance with LOX/H_2 • Good stability characteristics with LOX/H_2 • Fuel is gas • Small annular gap requires care in fabrication and is sensitive to contamination	• Shuttle main and preburners • J-2 • Orbit Transfer Vehicle
Concentric Tube with Liquid Swirl	GAS LIQ d_O d_F RECESS	• Same as concentric tube except: • Improved mixing and atomization • More complex element • Stability characteristics in large engines unknown • Possible wall compatibility issue with some designs • Gas can also be swirled	• RL-10
Unlike Pentad (4 on 1)	LIQ GAS LIQ	• Applicable to very high or low mixture or density ratios • Good mixing and atomization • Difficult to manifold	• Experimental
Unlike Doublet (1 on 1)	OX FUEL IMP DIST	• Good overall mixing and atomization (High Performance) • Simple to manifold • Subject to blowapart with hypergolic propellants	• LEM ascent engine • Delta launch vehicle • Almost all high response attitude control engines using storable propellants
Unlike Triplet (2 on 1)	OX FUEL OX	• Good overall mixing and atomization (High Performance) • Symmetric spray pattern • Subject to blowapart with hypergolic propellants • Fuel can be gas • Pattern can be reversed	• Agena upper stage • Rocketdyne LEM descent engine design • LOX/RPl gas generators
Like Doublet (1 on 1)	OX FUEL FUEL OX	• Easy to manifold • Excellent for chamber wall compatibility • Not subject to blowapart • Less effective atomization and mixing than unlike impinging elements	• Titan I and II first stage • Redstone, Jupiter, Thor, Atlas boosters • Shuttle OMES • H-1, F-1 engines
Showerhead	OX FUEL	• Often employed for fuel boundary layer cooling of chamber wall • Easy to manifold • Poor atomization and mixing (Low Performance)	• Aerobee sustainer • X-15 • Pioneer
Variable Area (Pintle)	FUEL OX	• Throttleable over wide range • Complex fabrication • Lower performance	• LEM descent engine • Lance sustainer
Splash Plate	SPLASH PLATE OX FUEL	• Less sensitive to design tolerances • Generally larger elements	• Lance booster (early version) • Saturn SIVB ullage control • Apollo CM RCS (SE-8) • Gemini SC maneuvering attitude control and reentry engines

From Sutton, "Rocket Propulsion Elements," 6th ed., pg 299, Wylie 1992

ATC
Advanced Technology Consultants
www.advtechconsultants.com

Water Testing Rocket Injectors

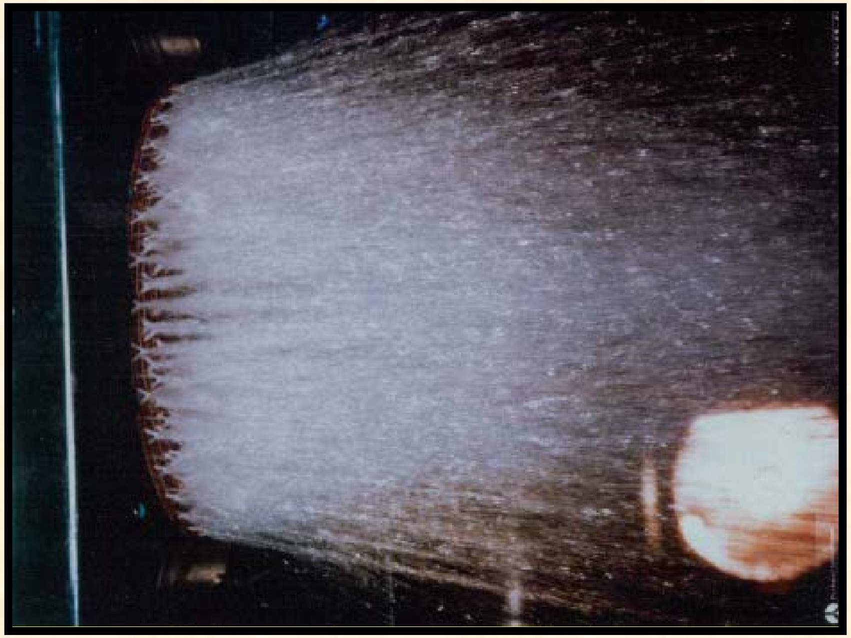

Water flow test of F-1 engine injector system

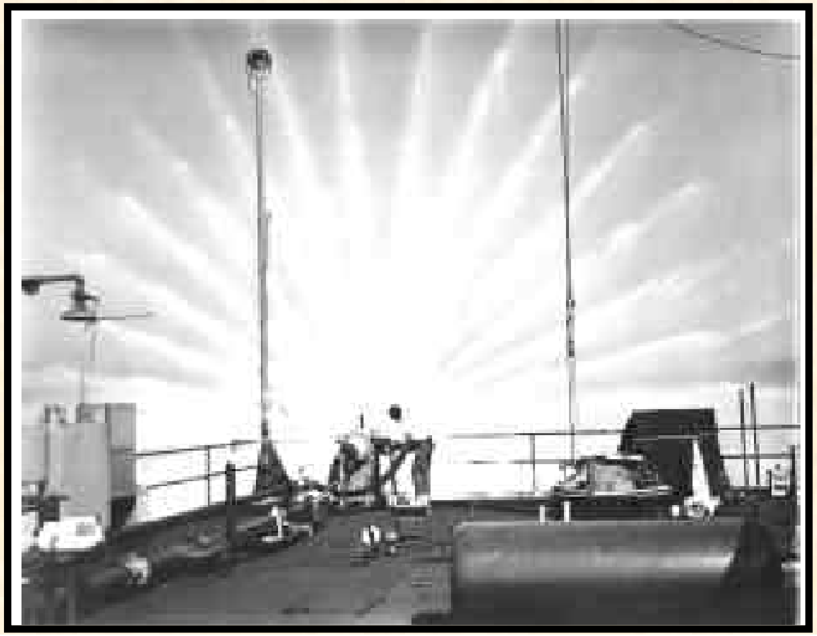

Water flow test of pintle injector for Air Force 250,000 lbf Engine

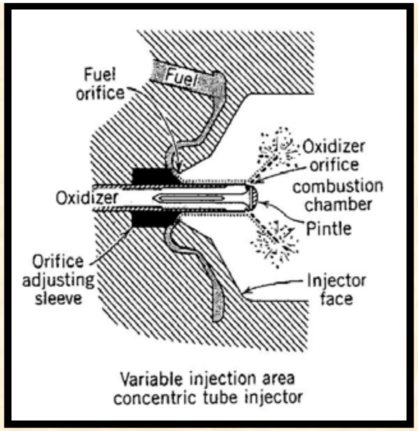

Like Doublet (1 on 1)	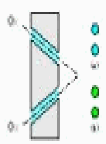	•Easy to manifold •Good mixing, Very stable •Not subject to blowapart •Well understood	•Requires increased axial distance to mix •Sensitive to design tolerances	•Titan I,II first stage •Jupiter, Thor, Atlas •H-1, F-1 engines

B. Chehroudi, PhD

ATC Advanced Technology Consultants

www.advtechconsultants.com

Space Shuttle Main Engine Injector

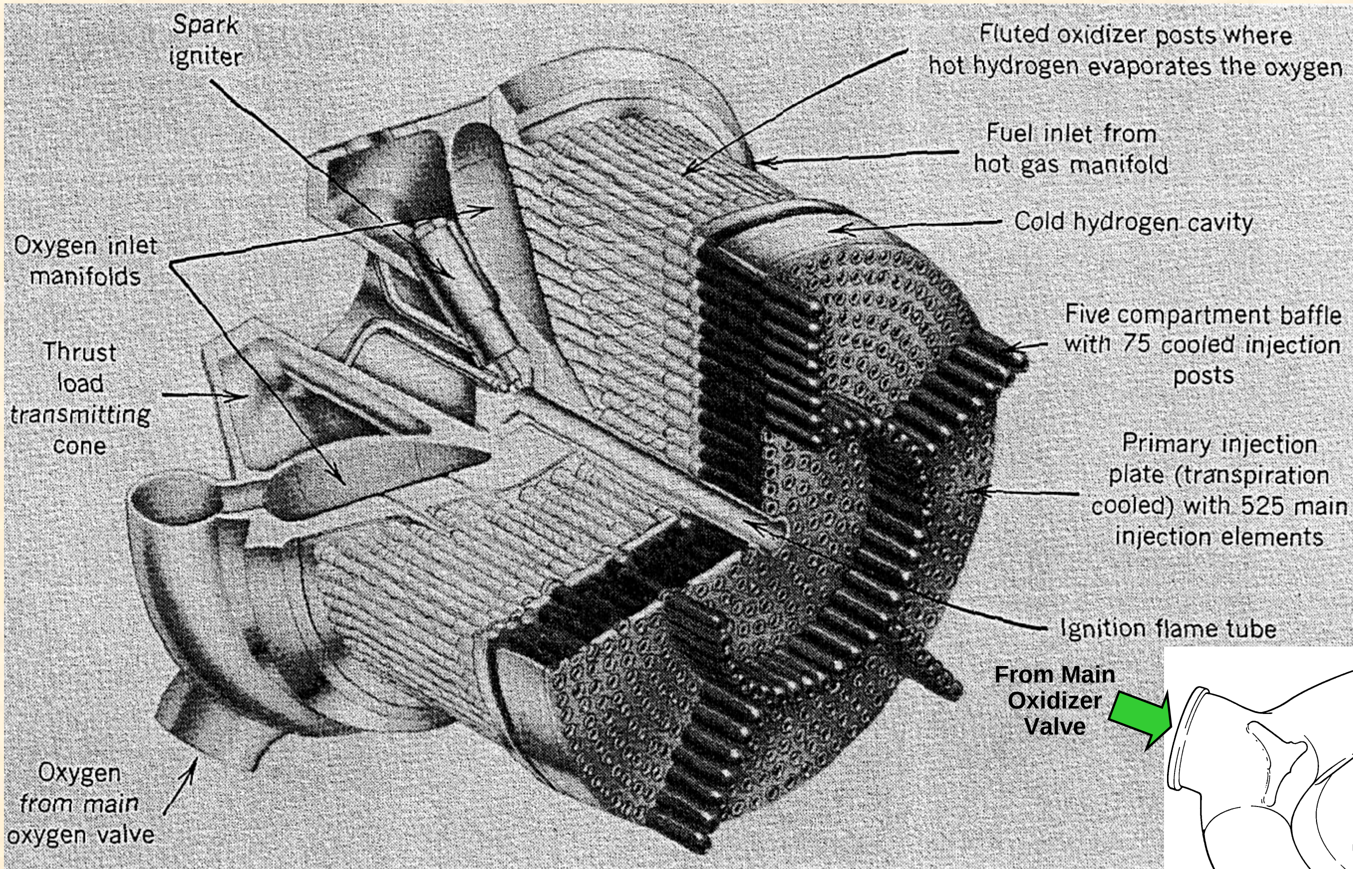

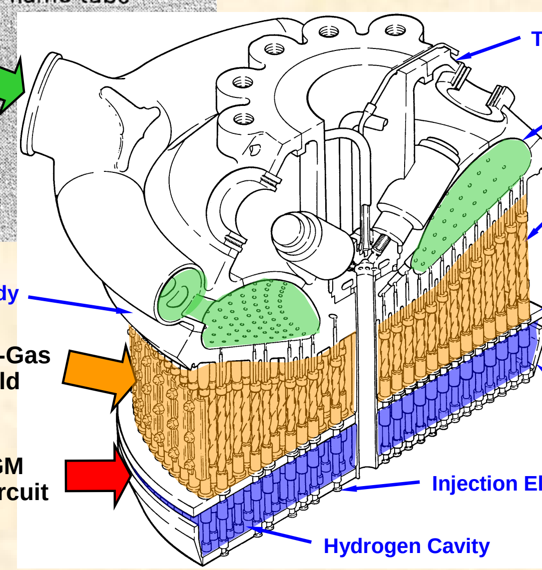

Coaxial Injector

From Sutton, "Rocket Propulsion Elements," 6th ed., pg 277, Wylie 1992

Injector Requirements

- Complete combustion in the shortest possible length
  - Main injectors: performance vs weight tradeoffs
  - Preburners/GG's: downstream component interactions, eg, turbine blades, etc
- Acoustically stable
  - Chamber modes
  - Feed system coupling
- Chamber/wall compatibility
  - Heat transfer/cooling
  - Oxygen blanching
  - Lifetime

– Manage pressure drop
– Throttling
– Ignitable; minimum ignition transients
– Cost, weight
– The "ilities:"
  - Reliability
  - Maintainability
  - Manufacturability
  - Durability
  - Operability
  - *PREDICTABILITY*

ATC
Advanced
Technology
Consultants

Liquid Rockets
and
Supercritical Fluids

Thermodynamic Critical Point

ATC Advanced Technology Consultants

www.advtechconsultants.com

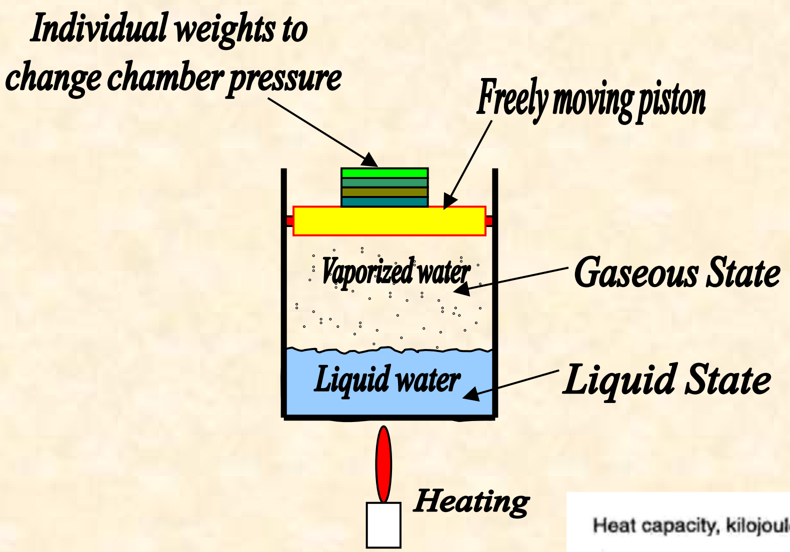

- Very large C_p at Critical Point (CP)
- Surface tension vanishes
- Heat of vaporization vanishes above CP
- Distinction between liquid and gas phases disappears above CP
- For mixtures: Critical mixing T & P (critical lines for 2-component)

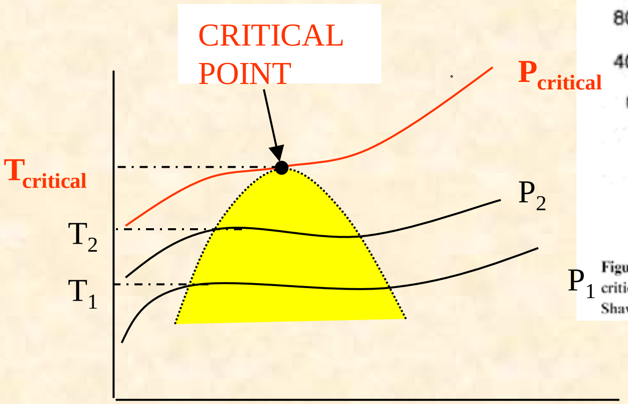

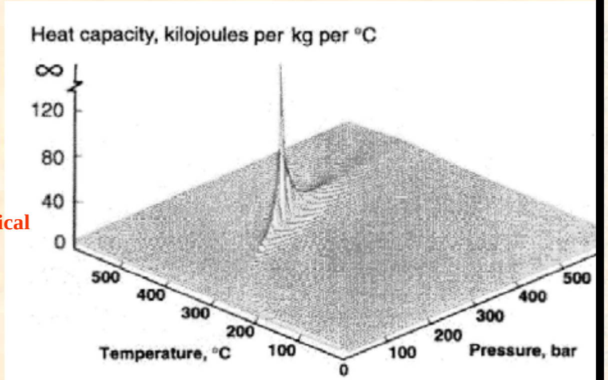

Figure 5. Behavior of heat capacity as a function temperature and pressure near critical point of water (Critical pressure and temperature values are 221 bar and 374 Shaw et al. (1991).

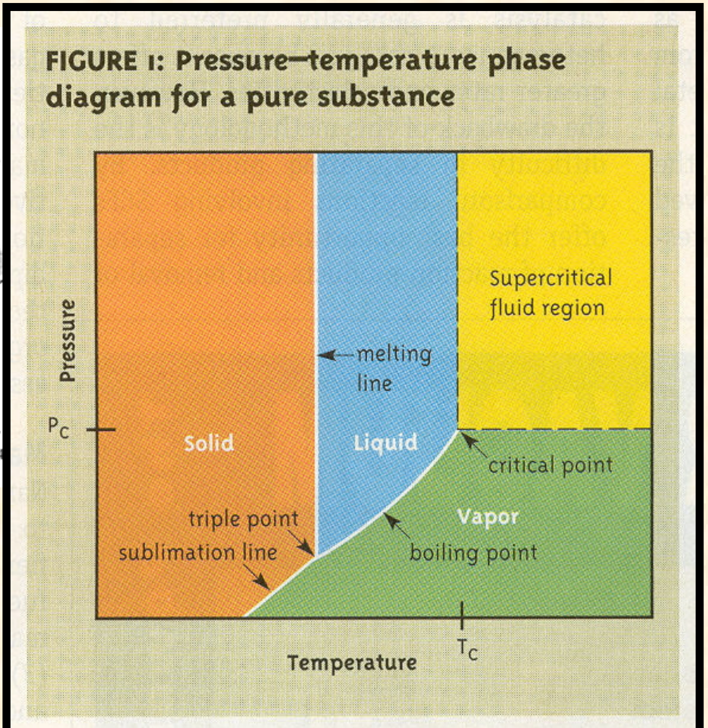

Chehroudi, B., 2006. Supercritical Fluids: Nanotechnology and Select Emerging Applications, *Invited Review Paper*, special volume dedicated to Supercritical Fluids, *Combustion Science and Technology*, Vol. 178, No. 1-3, January 2006, pp. 555-621(67).

Thermodynamic Critical Point

ATC Advanced Technology Consultants

www.advtechconsultants.com

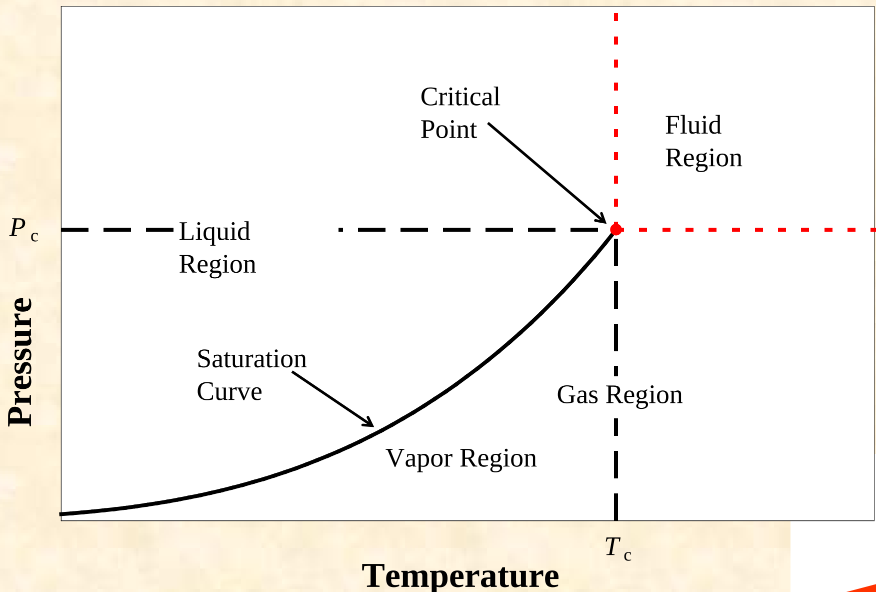

Single Species Phase Diagram

- **Phase change only over saturation curve**
- **Critical Pressure N_2 = 3.4 MPa (493 psia)**
- **Critical Temp. N_2 = 126.2 K (-233 °F)**

Binary Mixture (N_2 – H_2) Phase Diagram

- **Blue points are measured data[1]**
- **Max. measured P_c of mixture 58 MPa (8400 psia) = 17P_c of N_2**

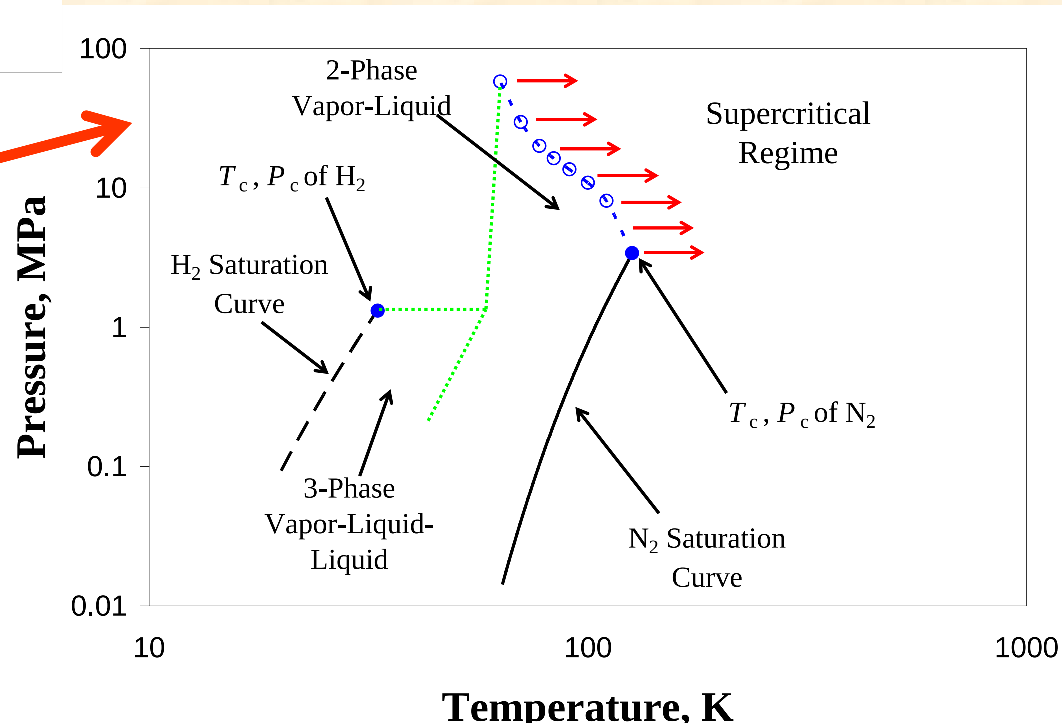

[1] Street, W. B., and Calado, J. C. G., J. Chem. Thermodynamics, Vol. 10, 1978, pp 1089-1100.

ATC Advanced Technology Consultants
www.advtechconsultants.com

Critical Properties of Some Substances

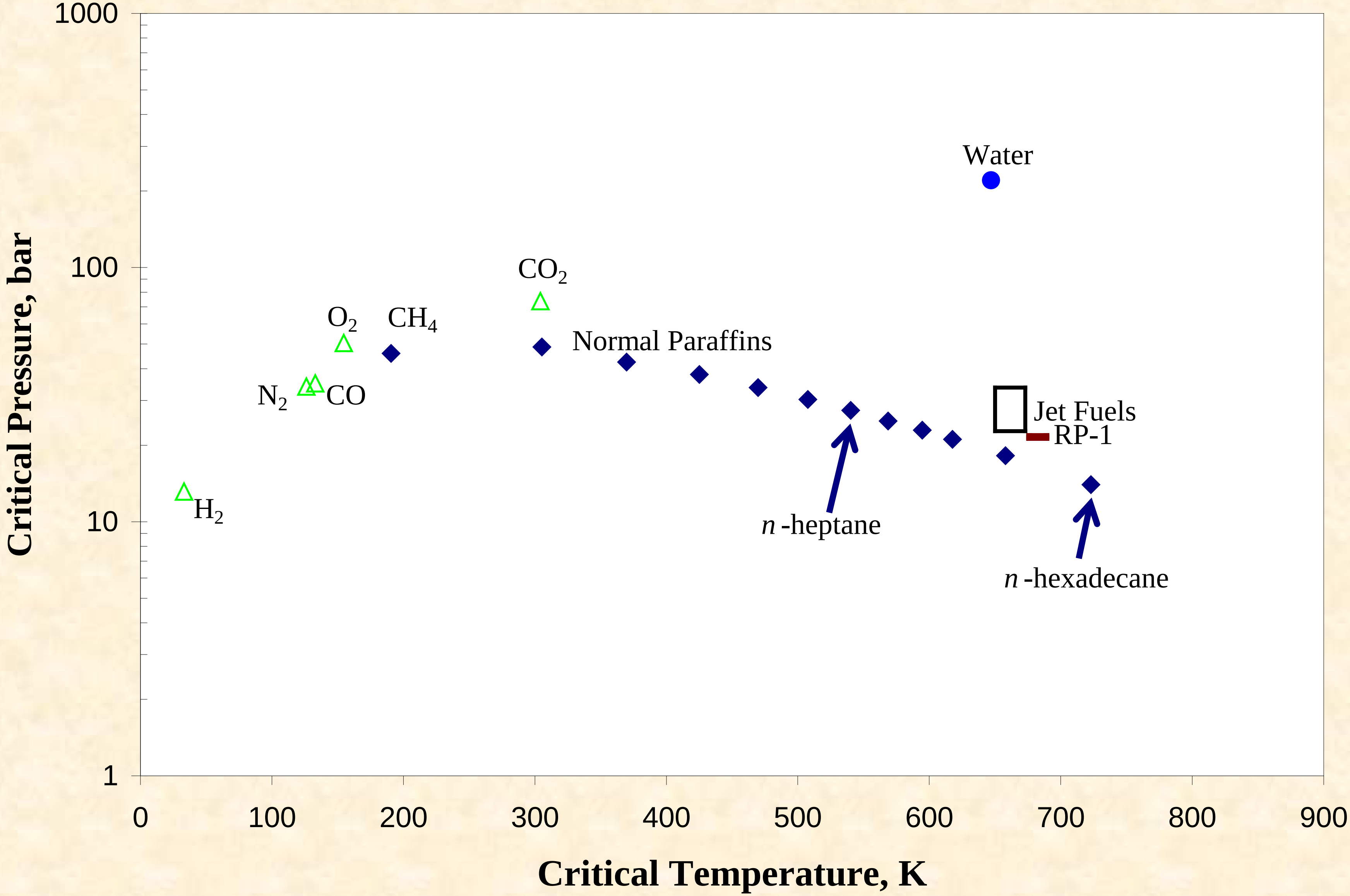

ATC Advanced Technology Consultants

www.advtechconsultants.com

Critical Properties & Engine Conditions

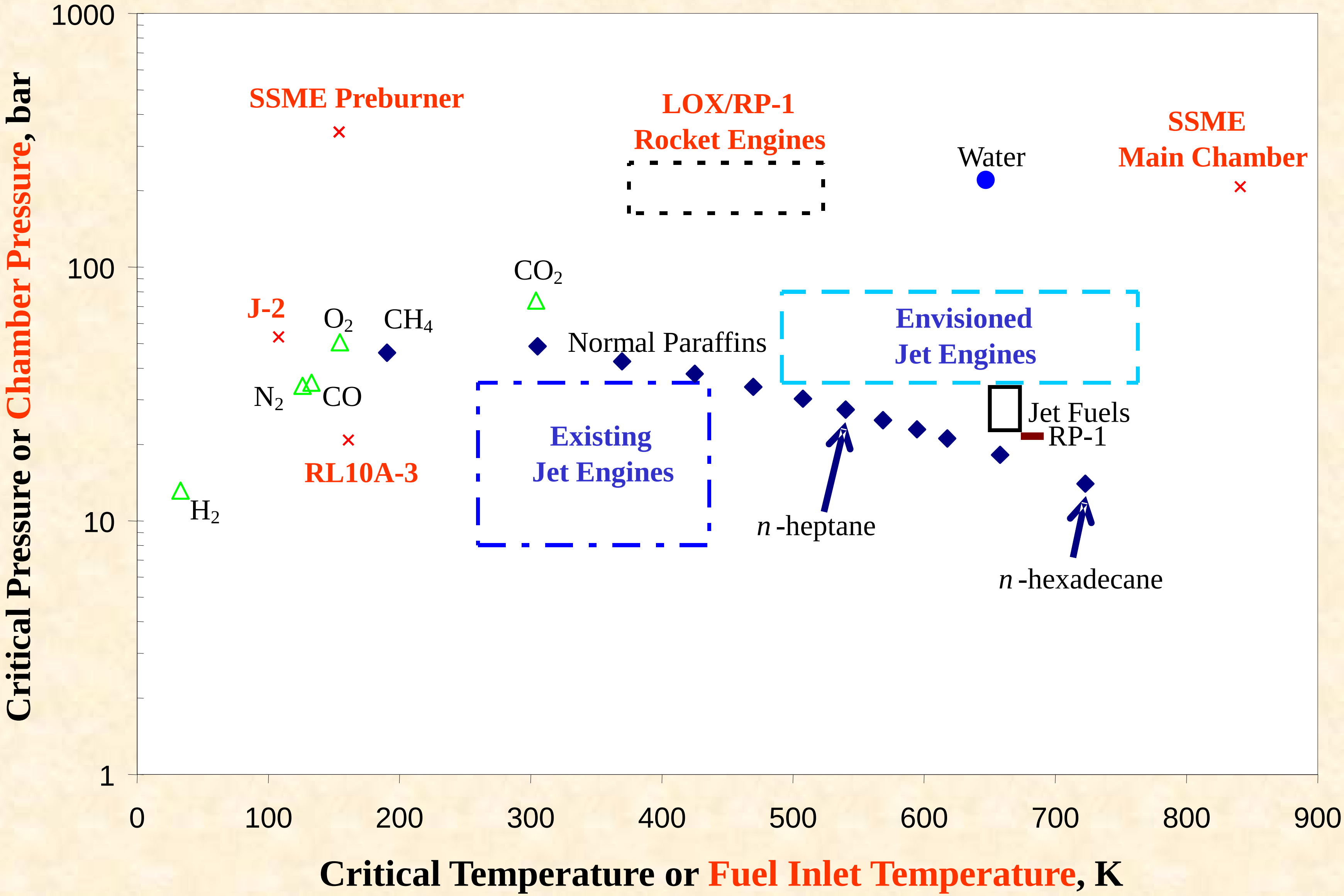

ATC Advanced Technology Consultants

www.advtechconsultants.com

More Information on Emerging Applications of Supercritical Fluids

Combustion Science and Technology
Publication details, including instructions for authors and subscription information:
http://www.informaworld.com/smpp/title~content=t713456315

SUPERCRITICAL FLUIDS: NANOTECHNOLOGY AND SELECT EMERGING APPLICATIONS

B. Chehroudi [a]
[a] Engineering Research Consultants, Lancaster, California, USA

Online Publication Date: 01 January 2006
To cite this Article: Chehroudi, B. (2006) 'SUPERCRITICAL FLUIDS: NANOTECHNOLOGY AND SELECT EMERGING APPLICATIONS', Combustion Science and Technology, 178:1, 555 - 621
To link to this article: DOI: 10.1080/00102200500294247
URL: http://dx.doi.org/10.1080/00102200500294247

Combust. Sci. and Tech., 178: 555–621, 2006

ISSN: 0010-2202 print/1563-521X online
DOI: 10.1080/00102200500294247

Taylor & Francis
Taylor & Francis Group

SUPERCRITICAL FLUIDS: NANOTECHNOLOGY AND SELECT EMERGING APPLICATIONS

B. CHEHROUDI*

Engineering Research Consultants, Lancaster, California, USA

In this paper, a selected list of emerging applications of supercritical fluids (SCFs) are presented. In particular, demonstrated facts for the promise of the nanoscale science and technology and its overlap or interface with the SCFs technology are presented. It is argued that nanoengineered materials at the nanoscale have mechanical, optical, chemical, and electrical properties quite different from the bulk material. Examples of enhanced performance of many such materials when they are used in practical applications are given. SCFs, in particular carbon dioxide, on account of their special properties such as zero surface tension, low viscosity, and high solubility, enable them to play a critical role in many advanced technology applications. For example, as miniaturization efforts approach the nanoscale, surface tension forces become an important factor in many nanotechnology processes such as lithography in the electronic industry. In particular, the zero-surface-tension property of the SCFs presents them as a natural choice for nanotechnology

It is not just a "phenomenon", it is a "technology"

www.advtechconsultants.com

Supercritical Test Facility

Experimental Setup

ATC Advanced Technology Consultants

www.advtechconsultants.com

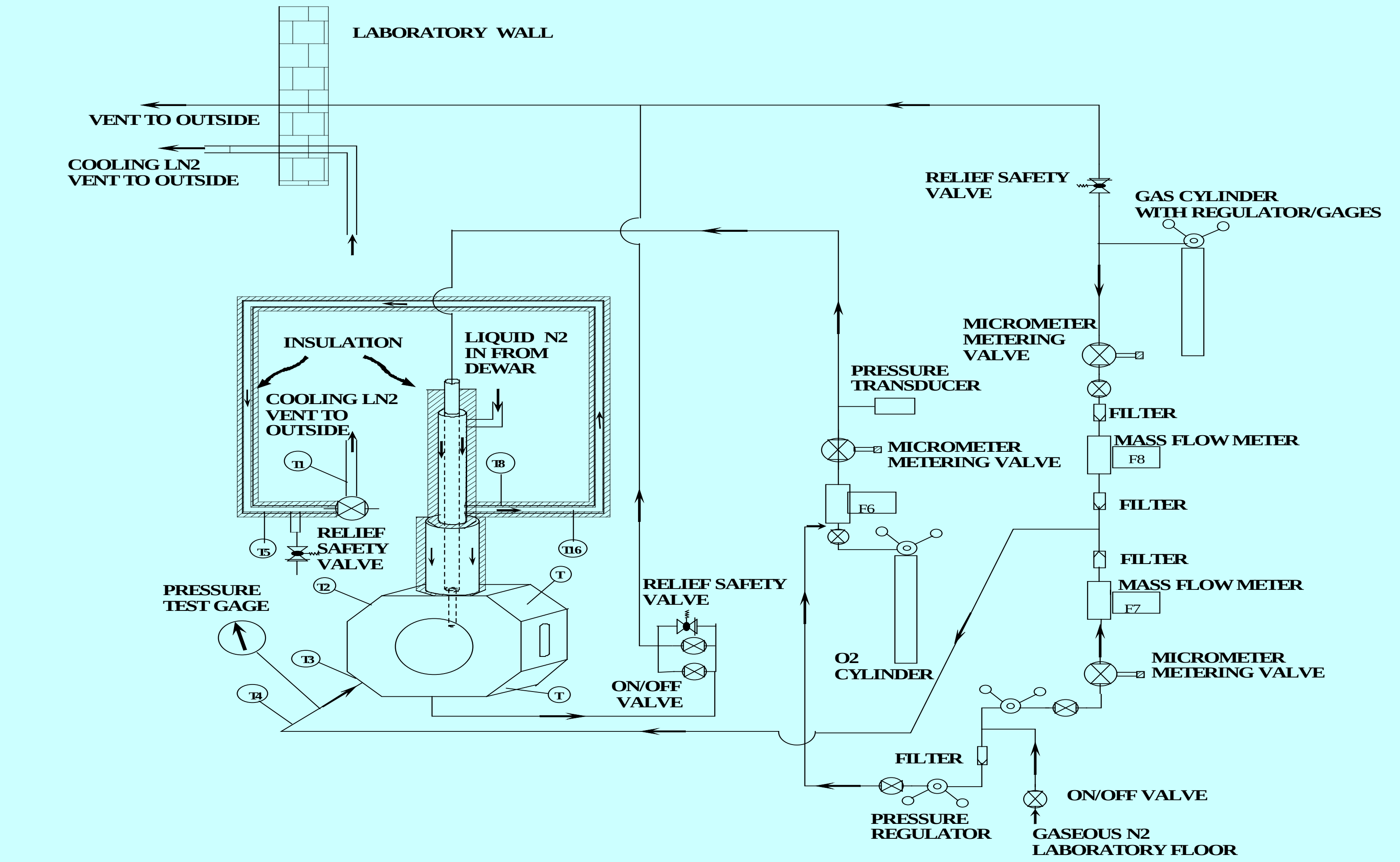

Figure 1. Schematic diagram of experimental setup for sub- to supercritical jet injection.

ATC
Advanced Technology Consultants
www.advtechconsultants.com

Pictures of the Injector Assembly and High-Pressure Chamber

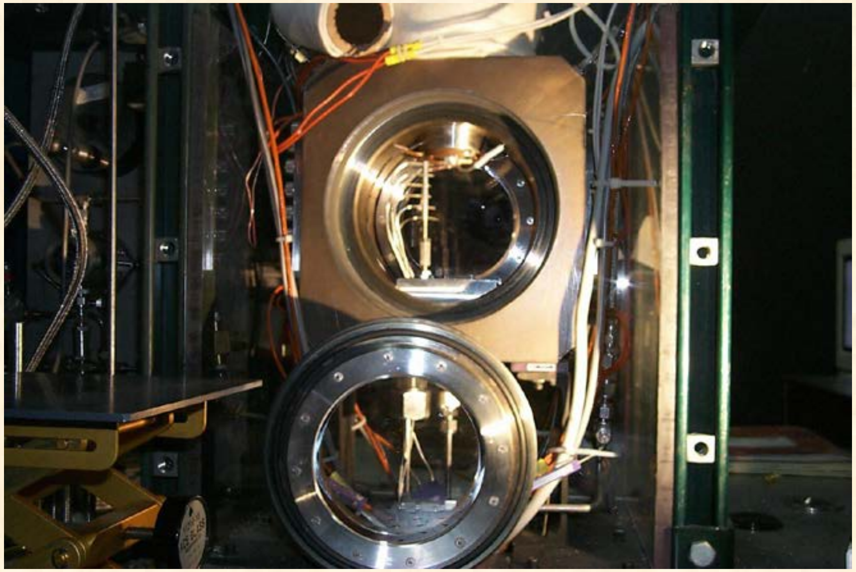

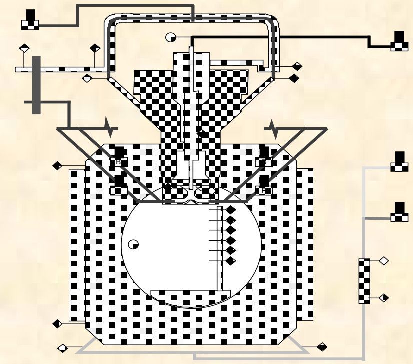

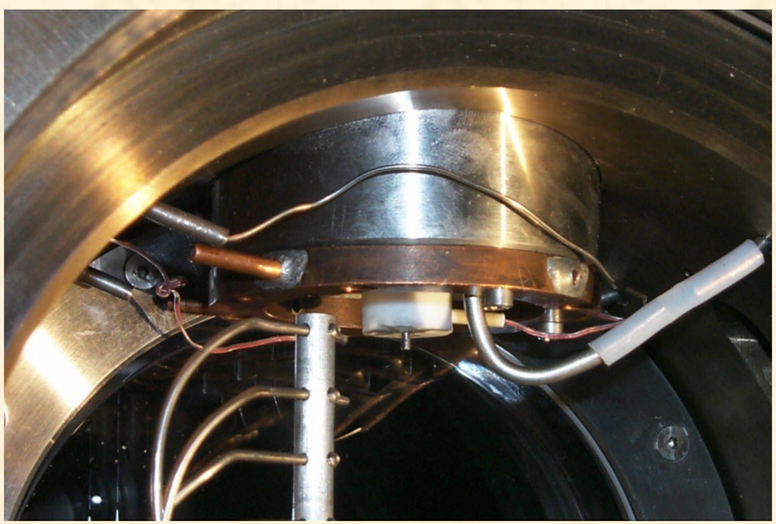

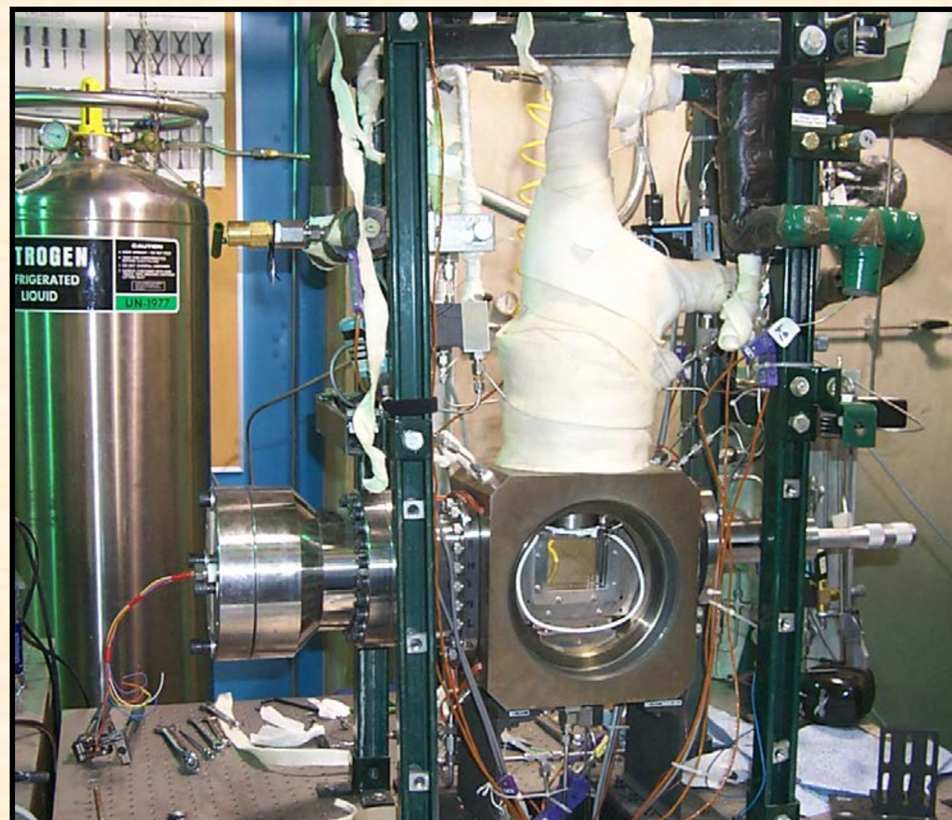

Single Jet
(no acoustic interaction)

ATC
Advanced Technology Consultants
www.advtechconsultants.com

AFRL
THE AIR FORCE RESEARCH LABORATORY
LEAD | DISCOVER | DEVELOP | DELIVER

What Do You See?

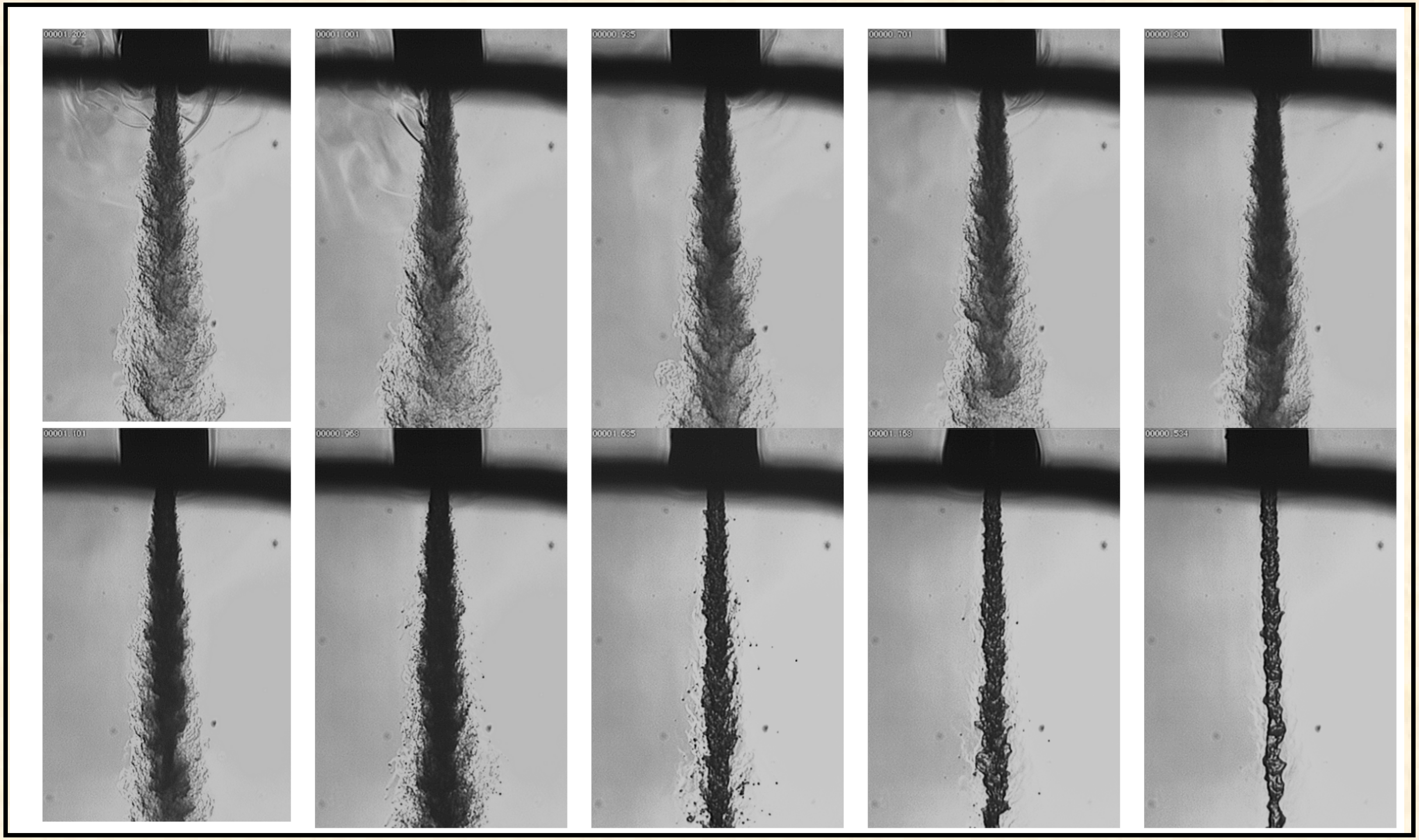

Chehroudi, et al., 2002. Visual Characteristics and Initial Growth Rates of Round cryogenic Jets at Subcritical and Supercritical Pressures, *Physics of Fluids,* Vol. 14, No. 2, February.

www.advtechconsultants.com

Single Jet At Sub- And Supercritical Conditions

Images of liquid N_2 injected into Gaseous N_2 at a fixed chamber temperature of 300K but varying sub- to supercritical pressures ($P_r=P_{ch}/P_{critical}$).Re= 25-75 x 10^3. Inj. velocity: 10-15 m/s.Froud number: 40 to 110 x 10^3. Injectant temperature: 99 to 120 K. (injector tube well insulated with no co-flow feature and no externally imposed acoustic field)

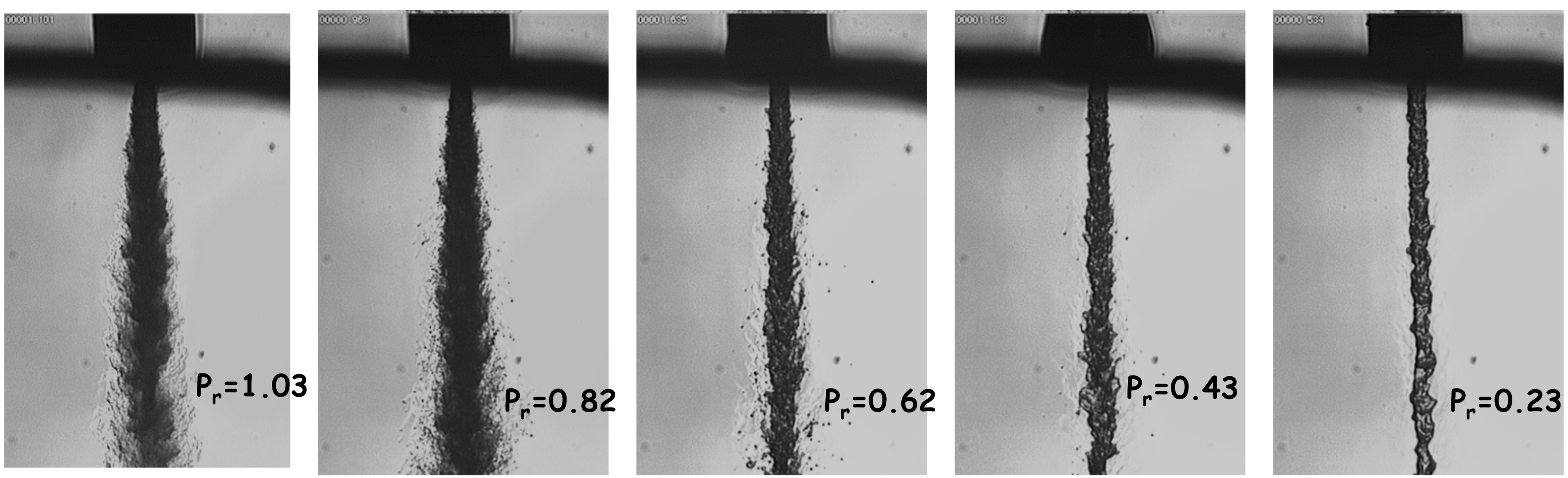

Chehroudi, B., Talley, D., and Coy, E., 2002. Visual Characteristics and Initial Growth Rates of Round cryogenic Jets at Subcritical and Supercritical Pressures, *Physics of Fluids,* Vol. 14, No. 2, February.

Single Jet At Sub- And Supercritical Conditions

ATC Advanced Technology Consultants

www.advtechconsultants.com

Images of liquid N_2 injected into Gaseous N_2 at a fixed chamber temperature of 300K but varying sub- to supercritical pressures ($P_r = P_{ch}/P_{critical}$).Re= 25-75 x 10^3. Inj. velocity: 10-15 m/s.Froud number: 40 to 110 x 10^3. Injectant temperature: 99 to 120 K. (injector tube well insulated with no co-flow feature and no externally imposed acoustic field)

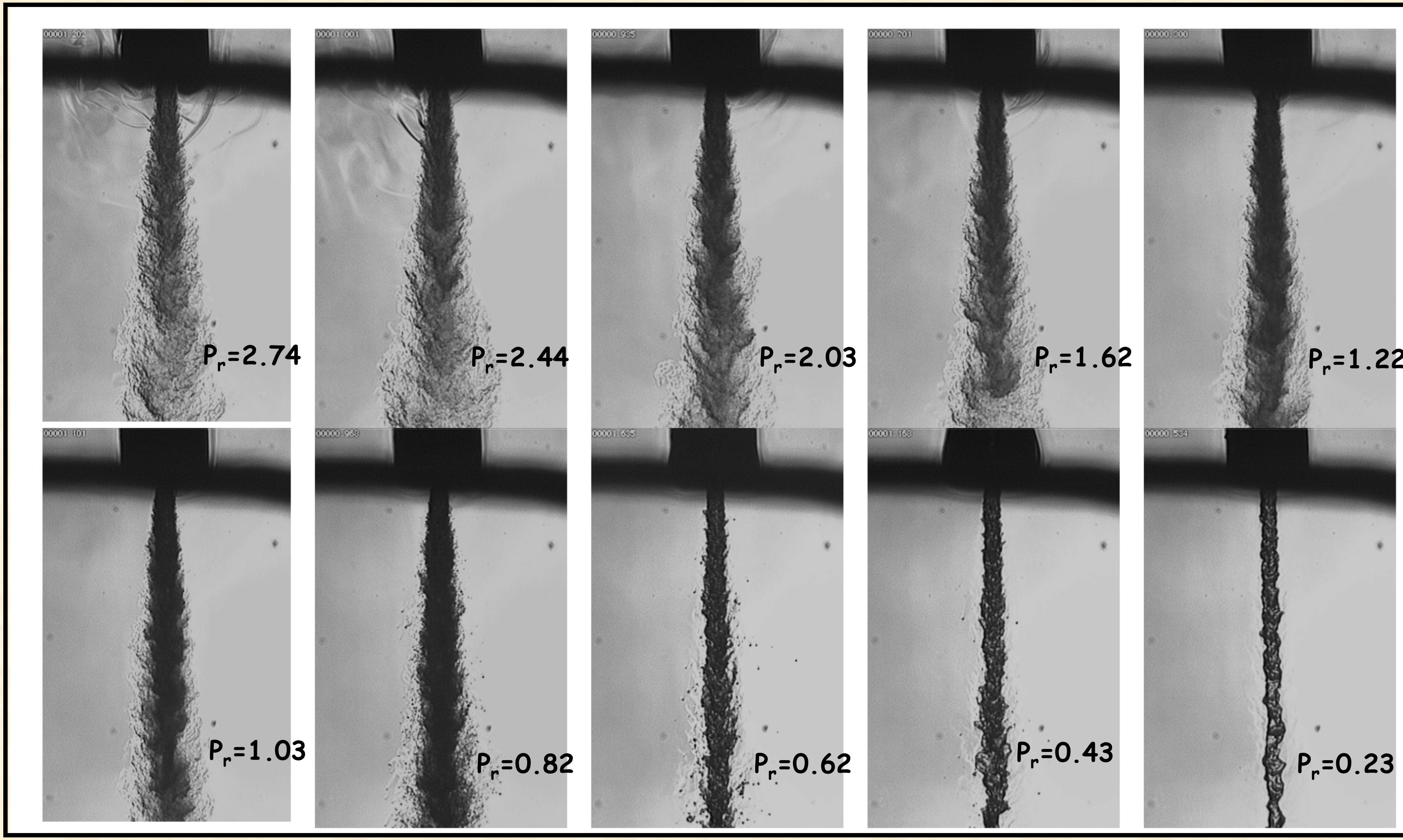

Chehroudi, et al., 2002. Visual Characteristics and Initial Growth Rates of Round cryogenic Jets at Subcritical and Supercritical Pressures, *Physics of Fluids,* Vol. 14, No. 2, February.

Single Jet At Sub- And Supercritical Conditions

Advanced Technology Consultants

www.advtechconsultants.com

Magnified images of the jet at its outer boundary showing transition to the gas-jet like appearance starting at just below the critical pressure of the injectant. Images are at fixed supercritical chamber temperature of 300 K. (injector tube well insulated with no co-flow feature and no externally imposed acoustic field)

Pch=3.13 Mpa
Reynolds=75,281
Mass flow=352 mg/s
Inj. Velocity=14.9 m/s

P_r=0.91

Appearance of conventional breakup of liquid surface indicating ligaments and drops ejecting from the mixing zone

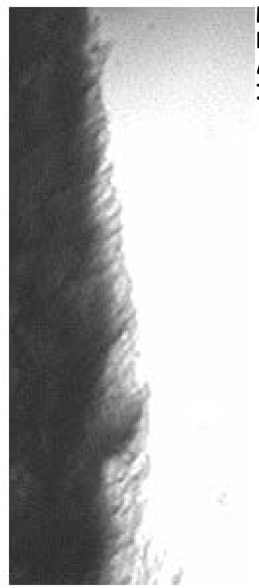

Pch=4.14 Mpa
Reynolds=66,609
Mass flow=350 mg/s
Inj. Velocity=14.1 m/s

P_r=1.22

Mixing layer affected by sub- to supercritical transition. No drops are seen. Fingure-like structures

Pch=9.19 Mpa
Reynolds=42,830
Mass flow=350 mg/s
Inj. Velocity=11.7 m/s

P_r=2.71

Appearance of Gas/gas mixing layer

Chehroudi, et al., 2002. Visual Characteristics and Initial Growth Rates of Round cryogenic Jets at Subcritical and Supercritical Pressures, *Physics of Fluids,* Vol. 14, No. 2, February.

Taylor and Hoyt, 1977 (Wind-induced Breakup Regime)

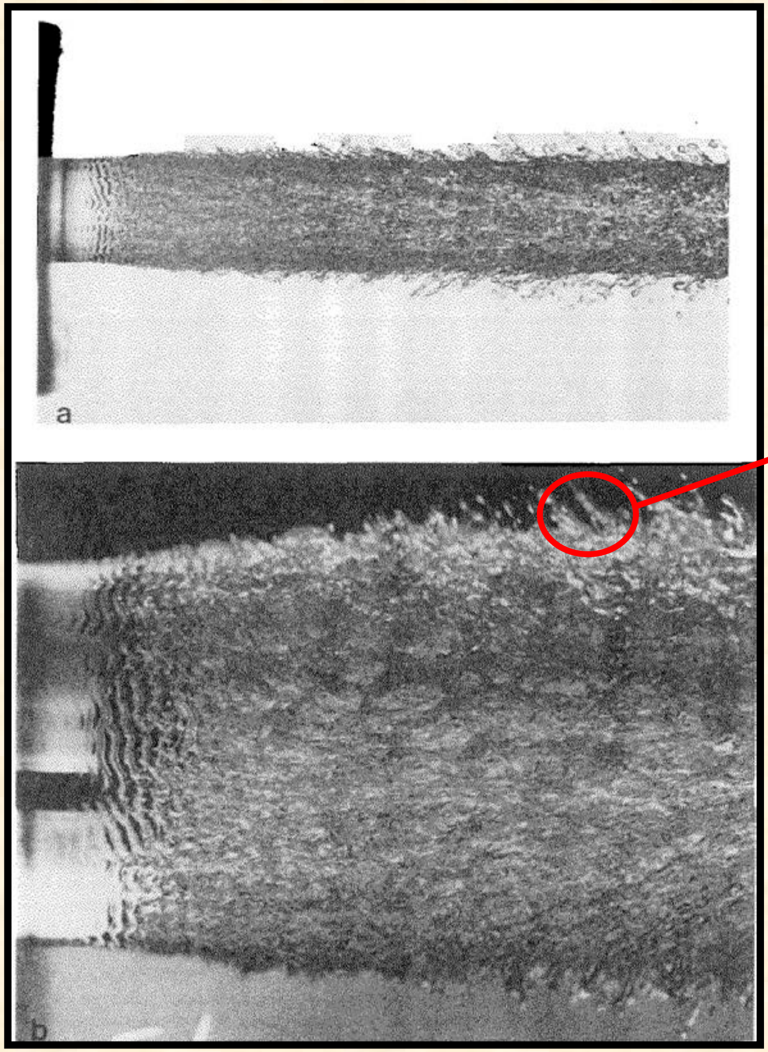

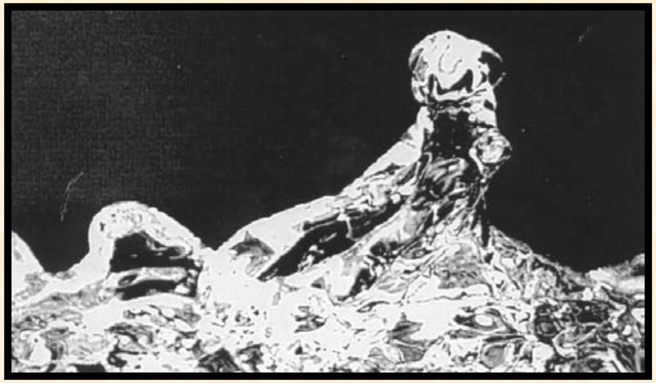

- HIGH SPEED PHOTOGRAPH OF WATER JET CLOSE TO THE NOZZLE EXIT SHOWING WAVE INSTABILITIES AND BREAKUP
- SECOND WIND-INDUCED BREAKUP REGIEM

Jet or Spray or Mixing Layer Divergence Angle vs Chamber-to-Injectant Density Ratio

www.advtechconsultants.com

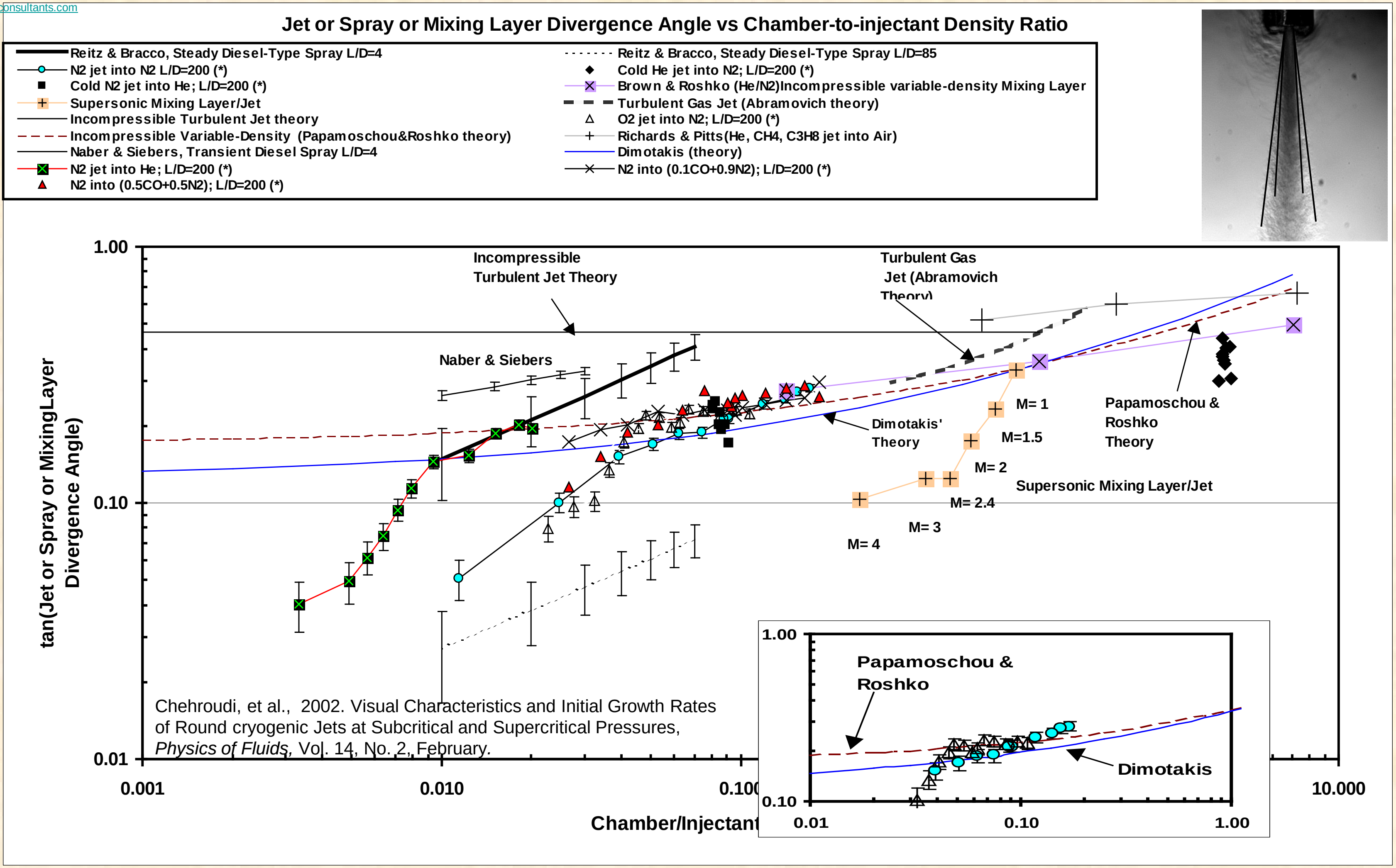

- A unique & nonexistent plot, covering 4 orders of magnitude in density ratio for mixing layer, liquid sprays (Diesel), turbulent jets (compressible & incompressive), supersonic jets, and theory
- For the first time, a *quantitative proof* that supercritical jets grow similar to variable-density incompressible jets

Growth (or Spreading) Rate for Turbulent Incompressible Round Jet
(*Abramovich)*

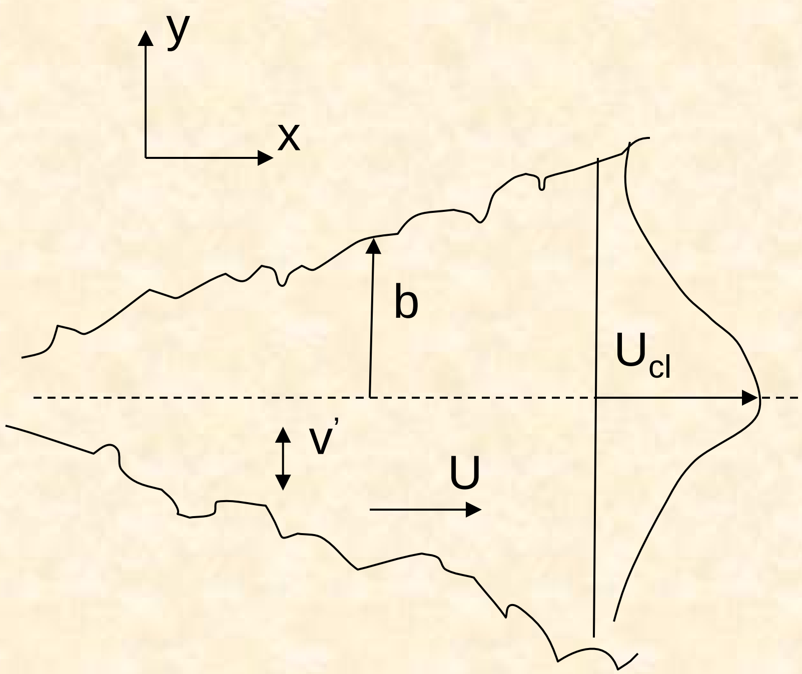

$$\frac{Db}{Dt} \propto v' \propto -\ell \frac{\partial \overline{U}}{\partial y} \propto -\ell \frac{U_{cl}}{b} \propto U_{cl} \qquad (1)$$

and since

$$\frac{Db}{Dt} = \frac{db}{dx}\frac{dx}{dt} \propto U_{cl} \frac{db}{dx} \qquad (2)$$

from the above two:

$$\frac{db}{dx} = \text{constant} \Rightarrow b = (\text{constant})x \Rightarrow$$

$$\ell = (\text{constant})\, x \qquad (3)$$

2b is defined as the thickness of the velocity profile, Db/Dt is the total derivative, ℓ is mixing length, v' is the transverse velocity fluctuations, and U_{cl} is the centerline maximum value of the time-averaged streamwise velocity profile.

Chehroudi, et al., 2002. Visual Characteristics and Initial Growth Rates of Round cryogenic Jets at Subcritical and Supercritical Pressures, *Physics of Fluids,* Vol. 14, No. 2, February.

Semi-Empirical Theory for the Jet Spreading Considering Compressibility (*Abramovich)*

$\frac{db}{dx} \propto \frac{U_1 - U_2}{U_{char}}$; where U_1 and U_2 are streamwise velocities at the boundaries of the mixing zone, U_{char} a characteristic velocity in the zone, and x is in streamwise direction.

For incompressible flow: $U_{char} = \frac{U_1 + U_2}{2}$ (4)

For compressible flow: $U_{char} = \frac{\rho_1 U_1 + \rho_2 U_2}{\rho_1 + \rho_2}$ (5)

From above equations for compressible flow:

$\frac{db}{dx} = C \frac{1+\rho_r}{2} \frac{1-U_r}{1+\rho_r U_r}$; where

$U_r = \frac{U_2}{U_1}$ and $\rho_r = \frac{\rho_2}{\rho_1}$.

In the main region of the jet:

$U_r = \frac{U_{ambient}}{U_{cl}}$;

$\rho_r = \frac{\rho_{ambient}}{\rho_{cl}}$; $U_{cl} = U_{cl}(x)$; $\rho_{cl} = \rho_{cl}(x)$

If U_r and ρ_r do not depend on x (i.e. initial region) then from above:

$$\frac{b}{x} = C \frac{1+\rho_r}{2} \frac{1-U_r}{1+\rho_r U_r} \quad (6).$$

From experiments in the initial region of the submerged jet (i.e. $U_r = 0$) of an incompressible fluid ($\rho_r = 1$) $C = 0.27$ is proposed. However, various experiments in hot jets, high-velocity jets, and supersonic jets under off-design discharge suggest a value of $C = 0.22$.

Chehroudi, et al., 2002. Visual Characteristics and Initial Growth Rates of Round cryogenic Jets at Subcritical and Supercritical Pressures, *Physics of Fluids,* Vol. 14, No. 2, February.

ATC Advanced Technology Consultants

www.advtechconsultants.com

Theoretical Growth (or Spreading) Rate for Incompressible Variable-density Mixing Layer

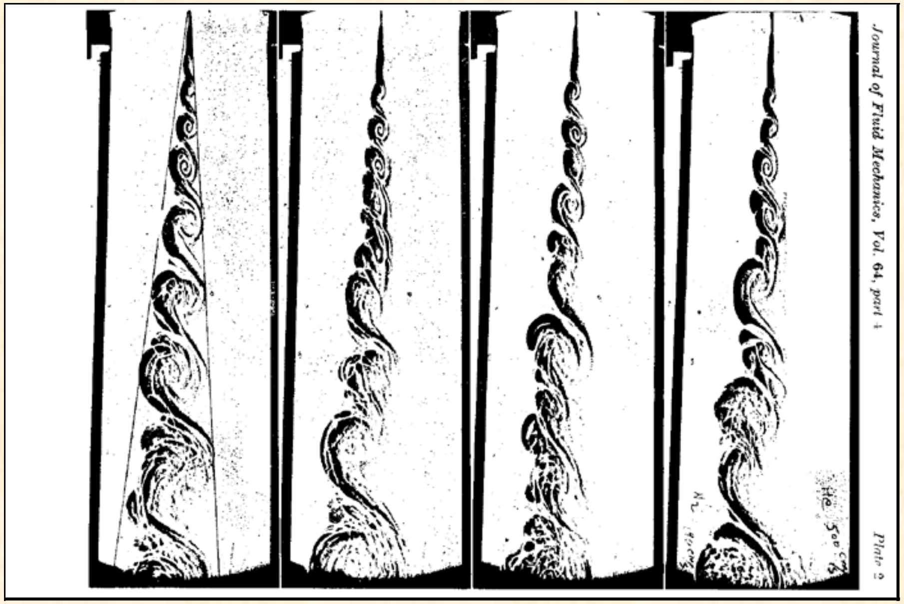

Visual Thickness

Brown/Papamoschou- Roshko

(CalTech)

$$(M_c = (U - U_c)/a;\ \text{a is speed of sound})$$

$$U_c = (U_1\sqrt{\rho_1} + U_2\sqrt{\rho_2})/(\sqrt{\rho_1} + \sqrt{\rho_2})$$

$$\delta'_{vis} = 0.17(\Delta U/U_c) =$$

$$= 0.17(1 - U_2/U_1)[1 + (\rho_2/\rho_1)^{1/2}]/[1 + (U_2/U_1)(\rho_2/\rho_1)^{1/2}]$$

Vorticity Thickness

Dimotakis (CalTech)

$$\delta'_{\omega} = \varepsilon\{(1 - U_2/U_1)/[1 + (\rho_2/\rho_1)^{1/2}(U_2/U_1)]\}\{1 + (\rho_2/\rho_1)^{1/2} - [1 - (\rho_2/\rho_1)^{1/2}]/[1 + 2.9(1 + U_2/U_1)/(1 - U_2/U_1)]\}$$

- Chehroudi, et al., 2002. Visual Characteristics and Initial Growth Rates of Round cryogenic Jets at Subcritical and Supercritical Pressures, *Physics of Fluids,* Vol. 14, No. 2, February.
- *Papamoschou, D. and Roshko, A.. "The compressible turbulent shear layer: an experimental study," J. Fluid Mech., vol. 197, 1988, pp. 453-477.*
- *Brown, G. "The Entrainment and Large Structure in Turbulent Mixing Layers," 5th Australian Conf. on Hydraulics and Fluid Mech., 1974, pp. 352-359.*
- *Dimotakis, P. E. "Two-dimensional shear-layer entrainment," AIAA Journal, 21, No. 11, 1986, pp. 1791-1796.*

Characteristic Time Analysis

- **Characteristic bulge formation time (τ_b) at the jet interface (*Tseng et al*.): $(\rho_l L^3 / s)^{1/2}$; ρ_l , L, s are liquid density, characteristic dimension of turbulent eddy, and surface tension, respectively.**
- **Characteristic time for gasification (τ_g) (D-square law): D^2/K; D and K are drop diameter and vaporization constant.**

- **<u>A Hypothesis</u>: If these two characteristic times (calculated for appropriate length scales) are comparable, then an interface bulge may not be separated as an unattached entity because it is gasified as fast as it desires to be detached (*onset of the gas-jet behavior*)**

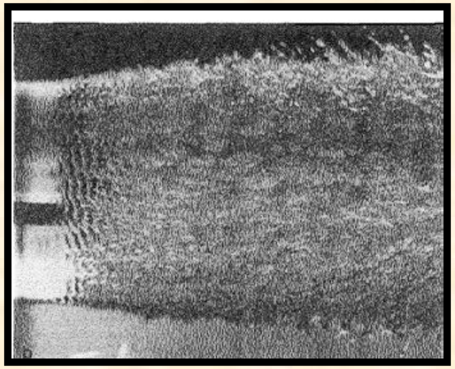

Chehroudi, et al., 2002. Visual Characteristics and Initial Growth Rates of Round cryogenic Jets at Subcritical and Supercritical Pressures, *Physics of Fluids,* Vol. 14, No. 2, February.

ATC
Advanced Technology Consultants
www.advtechconsultants.com

Remarkably Similar Equation Format for Different Cases

- **Theoretical isothermal liquid spray growth rate (θ_s) based on Orr-Sommerfeld equation and stability analysis to find the wavelength of the most unstable interface wave:**

$$\theta_s \cong 0.270\ [\ 0 + (\rho_g/\rho_l)^{0.5}]$$

- **Brown/Papamoschou-Rashko theory for incompressible variable-density gaseous mixing layer/jet:**

$$\theta_{P/R} \cong 0.212\ [\ 1 + (\rho_g/\rho_l)^{0.5}]$$

- **Dimotakis theory for incompressible variable-density gaseous mixing layer/jet:**

$$\theta_D \cong 0.265\ [0.59 + (\rho_g/\rho_l)^{0.5}]$$

- **ALL HAVE THE SQUARE ROOT OF DENSITY RATIO AND REMARKABLY THE SAME EQUATION FORMAT**

Chehroudi, et al., 2002. Visual Characteristics and Initial Growth Rates of Round cryogenic Jets at Subcritical and Supercritical Pressures, *Physics of Fluids,* Vol. 14, No. 2, February.

A Proposed Model Equation

- Based on the information from previous slide, the following "intuitive" equation is proposed for both sub- and supercritical (measured) growth rates:

$$\theta_{Ch} \cong 0.27 \left[(\tau_b/(\tau_b + \tau_g)) + (\rho_g/\rho_l)^{0.5} \right]$$

- For isothermal liquid case: $\tau_g >> \tau_b$ and $\tau_g \to \infty$. It then collapses to the isothermal spray case.
- For subcritical the $(\tau_b/(\tau_b + \tau_g))$ is calculated until it reaches 0.5. After that it is maintained constant at 0.5 for supercritical gas-like jet.
  - The transition point (between subcritical & supercritical behaviors) is found to be approximately when

    $(\tau_b/(\tau_b + \tau_g)) \cong 0.5$, that is:

    $\tau_g \cong \tau_b$, which means that it vaporizes as fast as it forms the bulge

Chehroudi, et al., 2002. Visual Characteristics and Initial Growth Rates of Round cryogenic Jets at Subcritical and Supercritical Pressures, *Physics of Fluids,* Vol. 14, No. 2, February.

ATC Advanced Technology Consultants

www.advtechconsultants.com

A Proposed Model Equation (cont.)

- $(\tau_b / (\tau_b + \tau_g))$ is assumed to be a dominant function of the density ratio (ρ_g/ρ_l); i.e. $\tau_b / (\tau_b + \tau_g)) = F(\rho_g / \rho_l)$.

- The function F is only calculated for the N2-into-N2 case and is taken to be the same for other (N_2-into-He and N_2-into-Ar) cases. For example, for N_2-into-He :

$$\theta_{Ch} \cong 0.27 \, [\, G(\rho_g / \rho_l) + (\rho_g / \rho_l)^{0.5}] \quad \text{where} \quad G(\rho_R) = F(\rho_R')$$

$\rho_R = (\rho_g / \rho_l)$; $\rho_R' = \rho_R - (1\text{-}X)\, \rho_R = X\rho_R$

$X = 1.0$ for N_2-into-N_2; $X = 0.2$ for N_2-into-He ; $X = 1.2$ for N_2-into-Ar.

Chehroudi, et al., 2002. Visual Characteristics and Initial Growth Rates of Round cryogenic Jets at Subcritical and Supercritical Pressures, *Physics of Fluids,* Vol. 14, No. 2, February.

ATC Advanced Technology Consultants

www.advtechconsultants.com

Comparison of the Proposed Model (solid red line) with Experimental Data

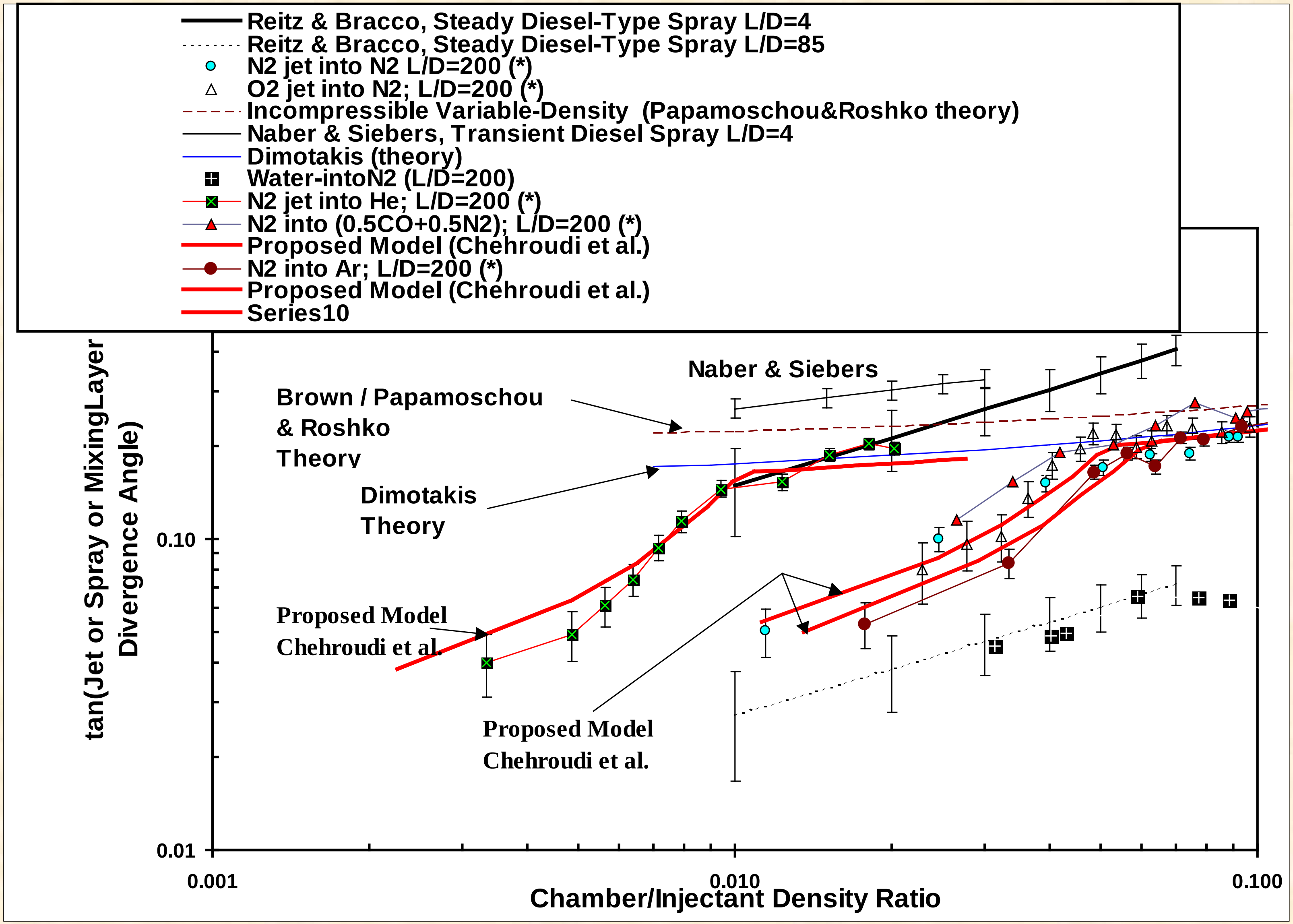

Chehroudi, et al., 2002. Visual Characteristics and Initial Growth Rates of Round cryogenic Jets at Subcritical and Supercritical Pressures, *Physics of Fluids,* Vol. 14, No. 2, February.

Fractal Dimension

ATC Advanced Technology Consultants

www.advtechconsultants.com

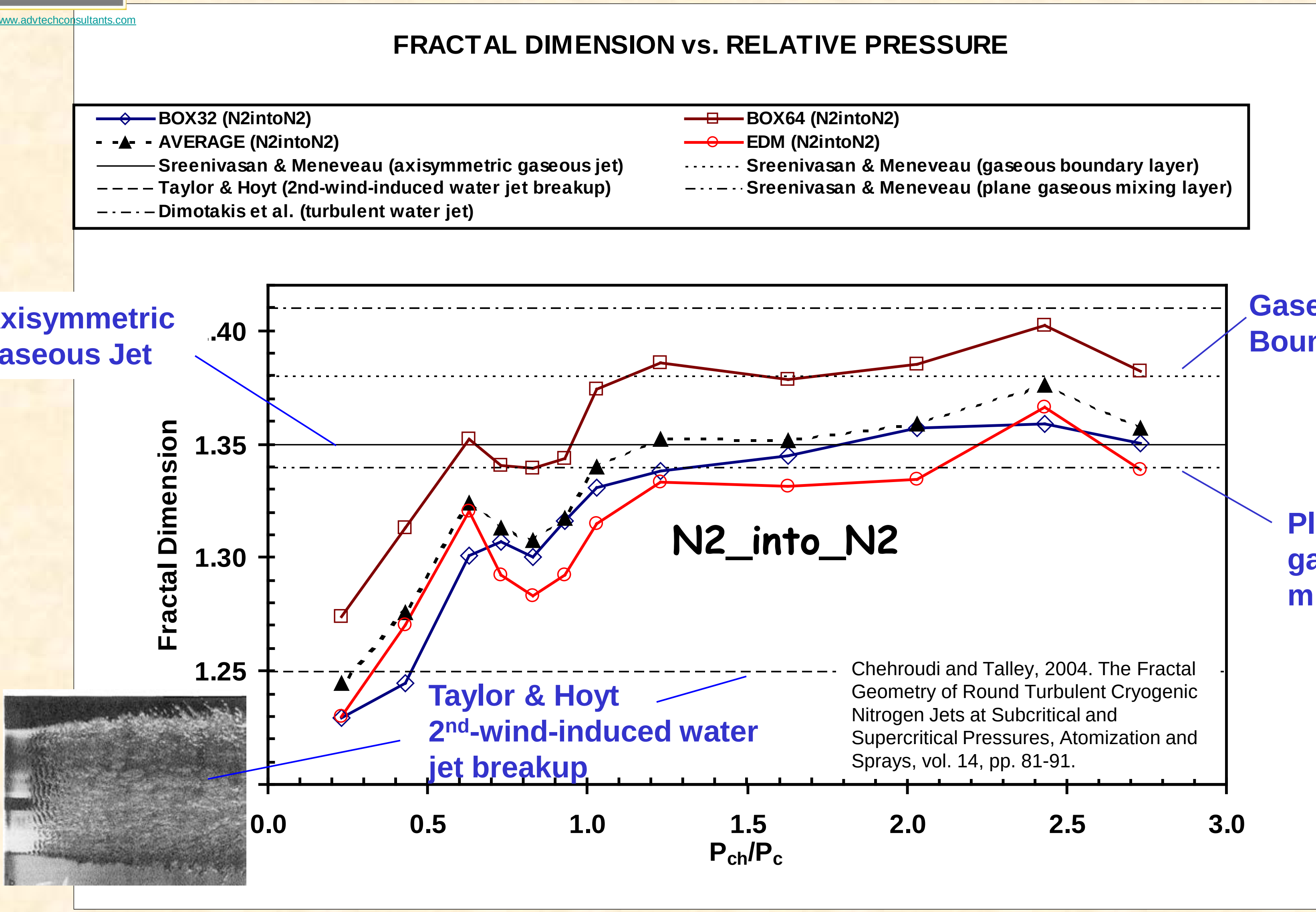

Box-counting and Minkowski (EDM algorithm) fractal dimensions of the visual boundary of the jet as a function of the relative chamber pressure for N_2-into-N_2 injection.

ATC
Advanced Technology Consultants
www.advtechconsultants.com

Raman Scattering Approach

- Nd-Yag laser in 2nd harmonic at 532 nm
- Raman signal at 607 nm
- Double loop optical delay to extend pulse width from 10 ns to 30 ns.
- Notch filter at 532 nm; band pass and hi-pass filter to isolate Raman signal.
- Princeton Instruments N_2 cooled ICCD camera
- Sheet forming optics to various sheet widths.

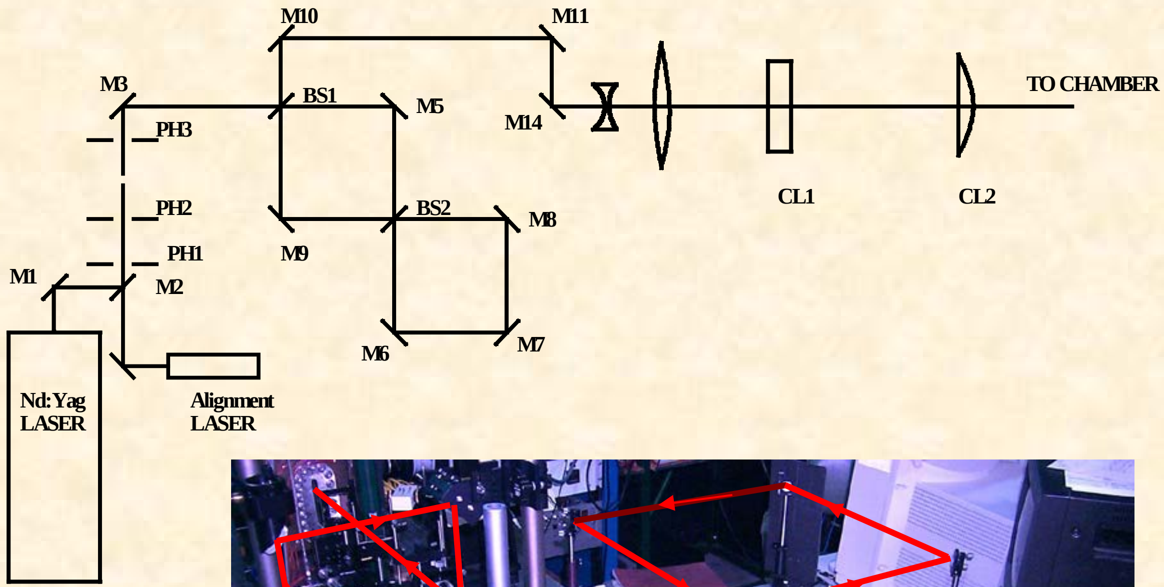

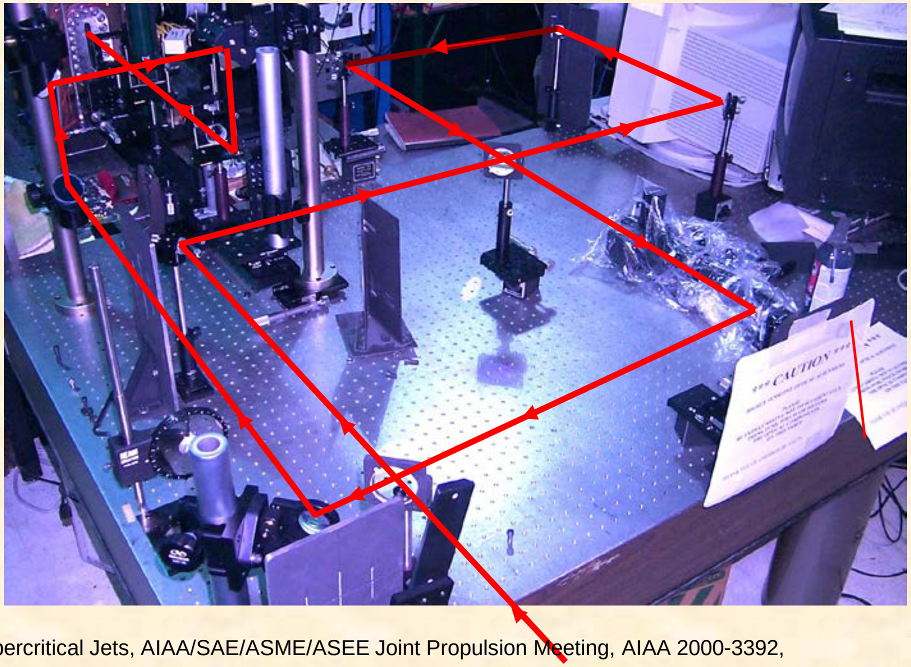

Chehroudi, et al., 2000. Raman Scattering Measurements in the Initial Region of Sub- and Supercritical Jets, AIAA/SAE/ASME/ASEE Joint Propulsion Meeting, AIAA 2000-3392, Huntsville, AL, 17-19 July.

Self-similarity Plot Supercritical Regime(3)

www.advtechconsultants.com

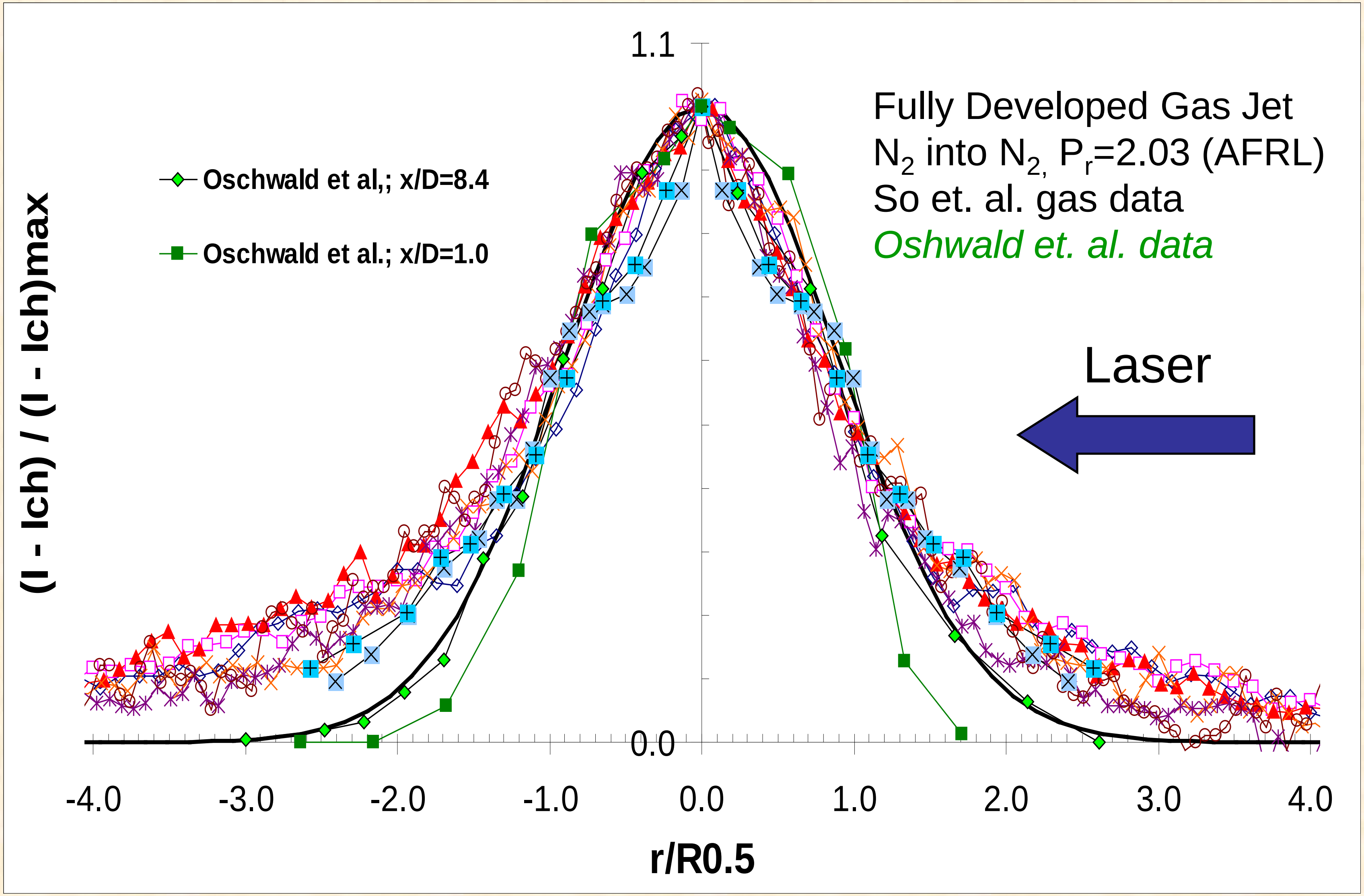

Chehroudi, et al., 2000. Raman Scattering Measurements in the Initial Region of Sub- and Supercritical Jets, AIAA/SAE/ASME/ASEE Joint Propulsion Meeting, AIAA 2000-3392, Huntsville, AL, 17-19 July.

www.advtechconsultants.com

Growth (or Spreading) Rates

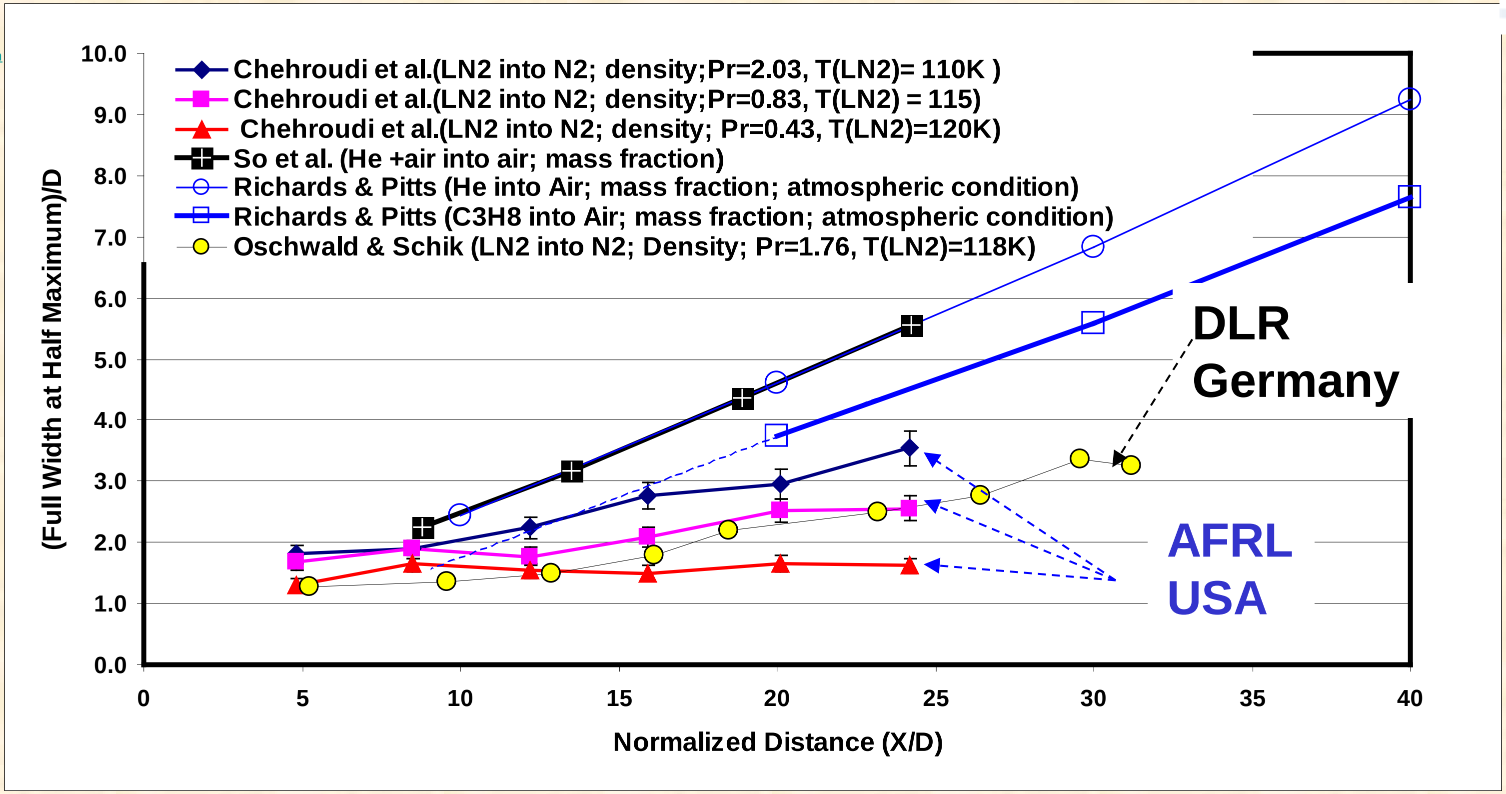

Normalized FWHM of the density surplus radial profiles as a function of the normalized distance from the injector.

	Fluid Inj/Cham	Tinj K	Pch MPa	Tch K	Reduced Pressure Pr	Inj/Chamb Density Ratio	Diameter D mm	L/D	x/D	Raynolds number Re	Profile used to measure FWHM	
Oschwald et al	N2/N2	118	4	298	1.17	3.34	1.9	11.5	8.42	1.2E+05	Density	in Figs. 7, 8
Oschwald et al	N2/N2	140	4	298	1.17	12.5	1.9	11.5	1.05	1.3E+05	Density	in Figs. 8
Chehroudi et al	N2/N2	95	6.9	295	2.03	7.1	0.505	100	4.8 to 24.4	3.5E+04	Density	in Figs. 8,10,11
Chehroudi et al	N2/N2	110	1.5	295	0.43	40.6	0.505	100	4.8 to 24.5	1.2E+04	Density	in Figs.10,11
So et. al.	(He+Air)/Air	275	0.1	275	0.08	0.64	9.5		5.1	5.0E+03	Concentration&Density	in Figs. 8, 11
So et. al.	(He+Air)/Air	275	0.1	275	0.08	0.64	9.5		6.4	5.0E+03	Concentration&Density	in Figs. 8, 11
Richards & Pitts	He into Air	275	0.1	275	0.44	0.138	6.35	~50	20-80	4.0E+03	Mass fraction	in Fig. 11
Richards & Pitts	C3H8 into Air	275	0.1	275	0.02	1.56	6.35	~50	40-120	2.5E+04	Mass fraction	in Fig. 11

Chehroudi, et al., 2000. Raman Scattering Measurements in the Initial Region of Sub- and Supercritical Jets, AIAA/SAE/ASME/ASEE Joint Propulsion Meeting, AIAA 2000-3392, Huntsville, AL, 17-19 July.

ATC Advanced Technology Consultants

www.advtechconsultants.com

Comparison of Shadowgraph Measurements with Raman Measurements

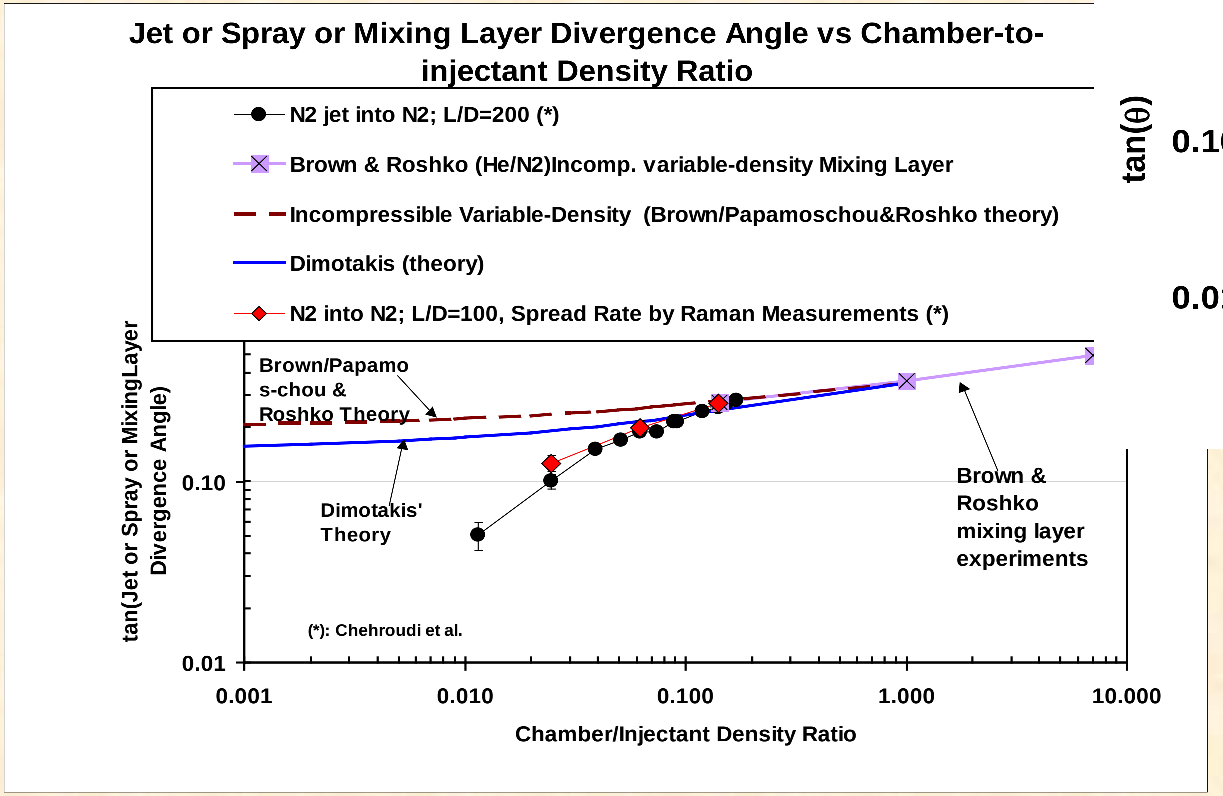

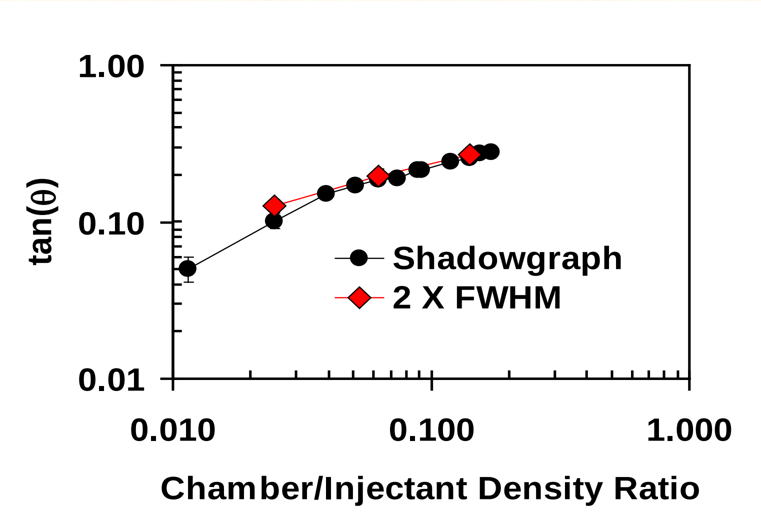

- 2 (FWHM) for Raman = Shadowgraph
- **Good Agreement: Indicating Consistency & integrity of two sets of data**

Chehroudi, et al., 2002. Cryogenic Shear Layers: Experiments and Phenomenological Modeling of the Initial Growth Rate Under Subcritical and Supercritical Conditions, *Invited Paper, International Journal of Heat and Fluid Flow*, 23, pp. 554-563.

Large Eddy Simulation based model Validates AFRL experimental results

ATC Advanced Technology Consultants

www.advtechconsultants.com

UNDER SUPERCRITICAL CONDITIONS: Casiano/MSFC (Sackheim), Yang/Penn State

➢ effects of momentum flux and chamber operating conditions investigated using LES

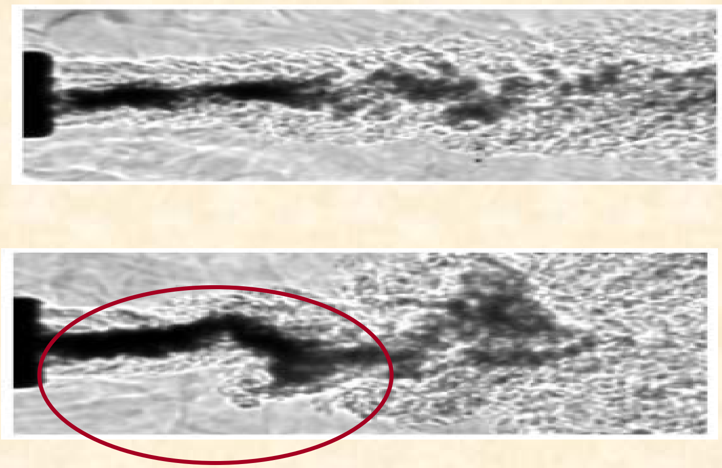

shadowgraph images, AFRL

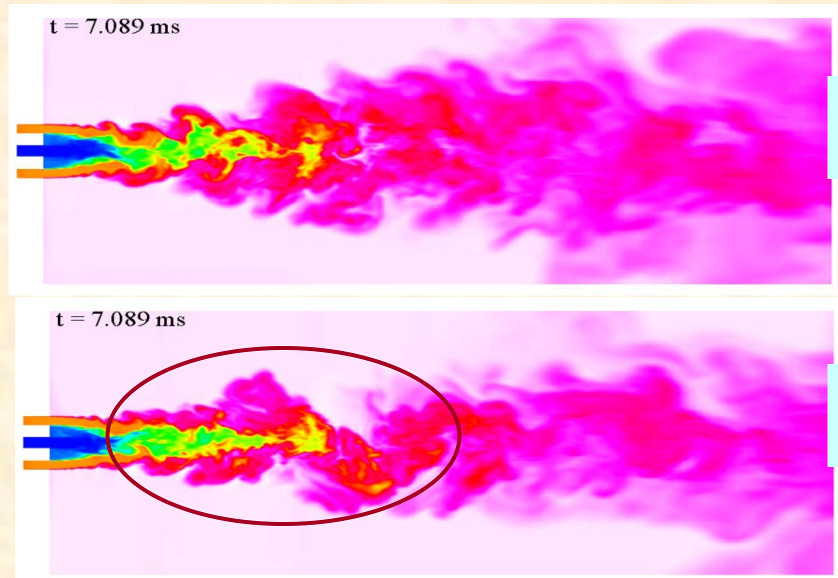

without acoustic

with acoustic

three-dimensional LES, Penn State

PENNSTATE

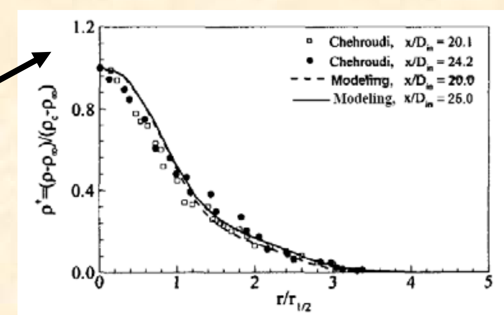

Fig.3 Comparison of computational and experimental density profiles at different axial locations.

- Quantitative agreement between computation and AFRL experimental data (no acoustic)
- Qualitative agreement of preliminary computational results under external transverse acoustic field

Single Jet
(acoustic interaction)

High-Chamber-Pressure Test Rig

ATC
Advanced Technology Consultants
www.advtechconsultants.com

AFRL
THE AIR FORCE RESEARCH LABORATORY
LEAD | DISCOVER | DEVELOP | DELIVER

Housing for the PiezoSiren and the Waveguide flanged to the high-pressure chamber

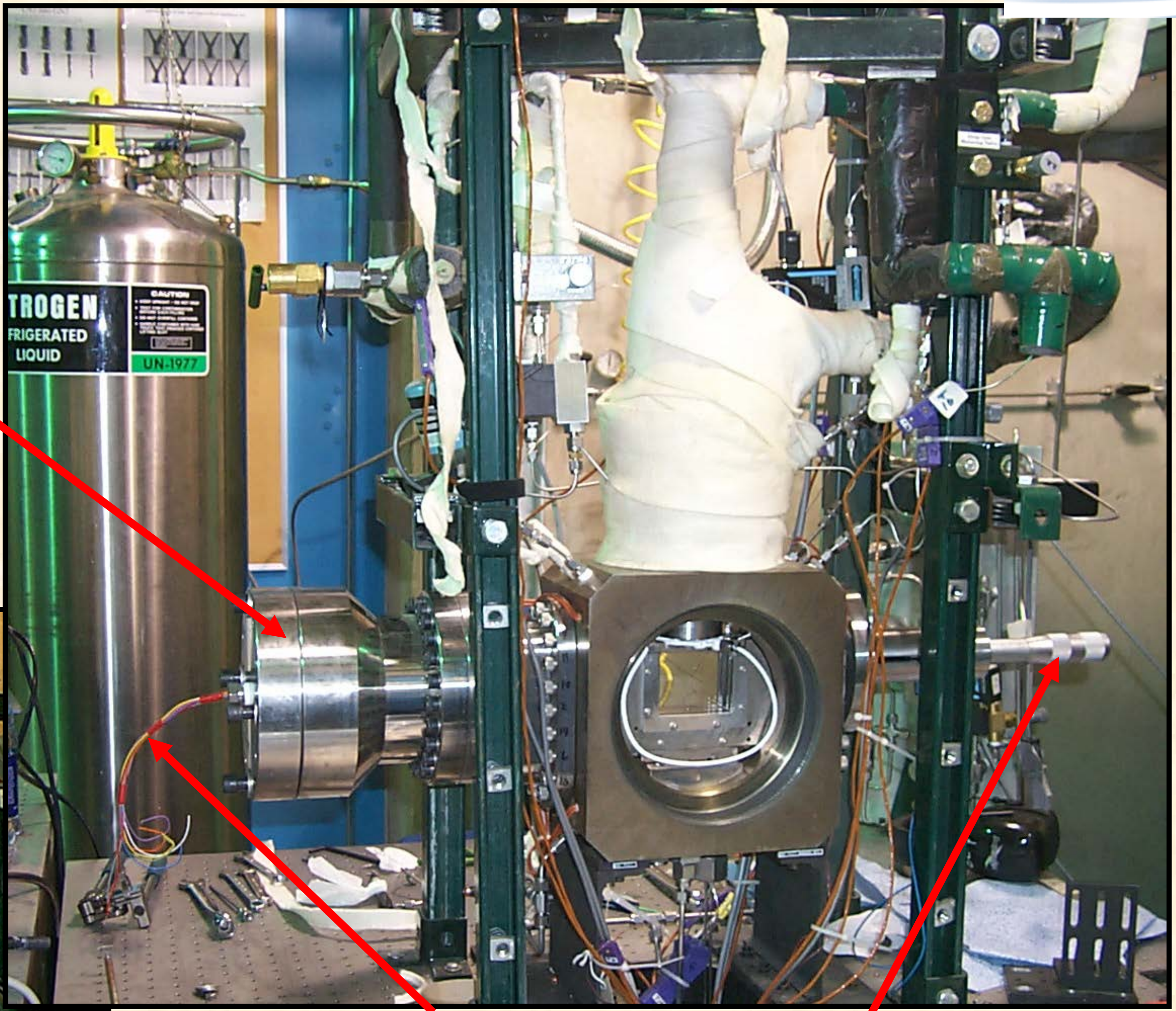

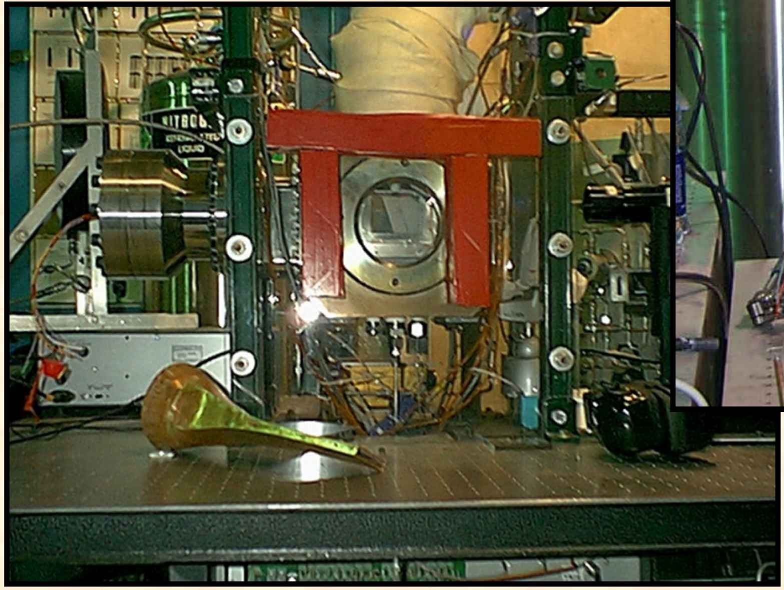

Wires from the PiezoSiren to wide-band amplifier

Pressure transducer traversing micrometer

www.advtechconsultants.com

PiezoSiren for Acoustic Field Generation

Circular-to-Rectangle Waveguide

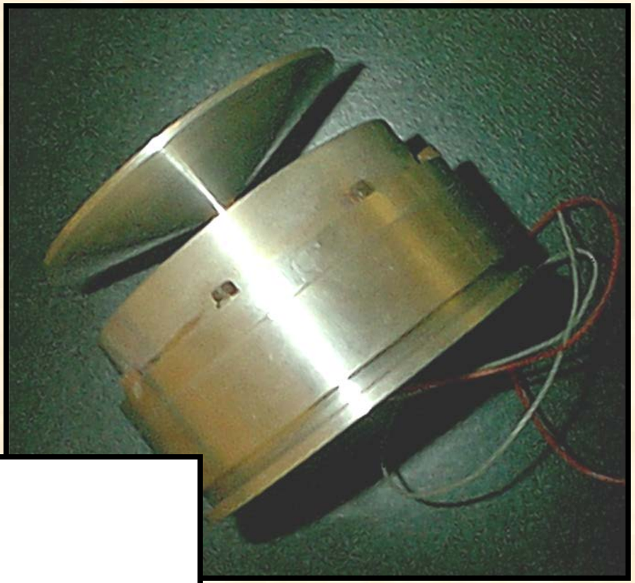

PiezoSiren

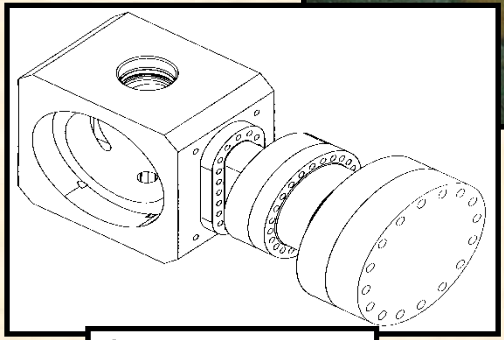

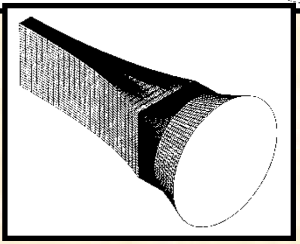

- PiezoSiren generates up to 180 dB SPL
- Designed to operate under high pressure
- Several resonance frequencies
- Most dominant are at ~ 2700 and ~4800 Hz
- The acoustic waves are channeled through a specially designed waveguide

ATC
Advanced Technology Consultants
www.advtechconsultants.com

Mapping Of The Acoustic Field

AFRL
THE AIR FORCE RESEARCH LABORATORY
LEAD | DISCOVER | DEVELOP | DELIVER

OFF

OFF

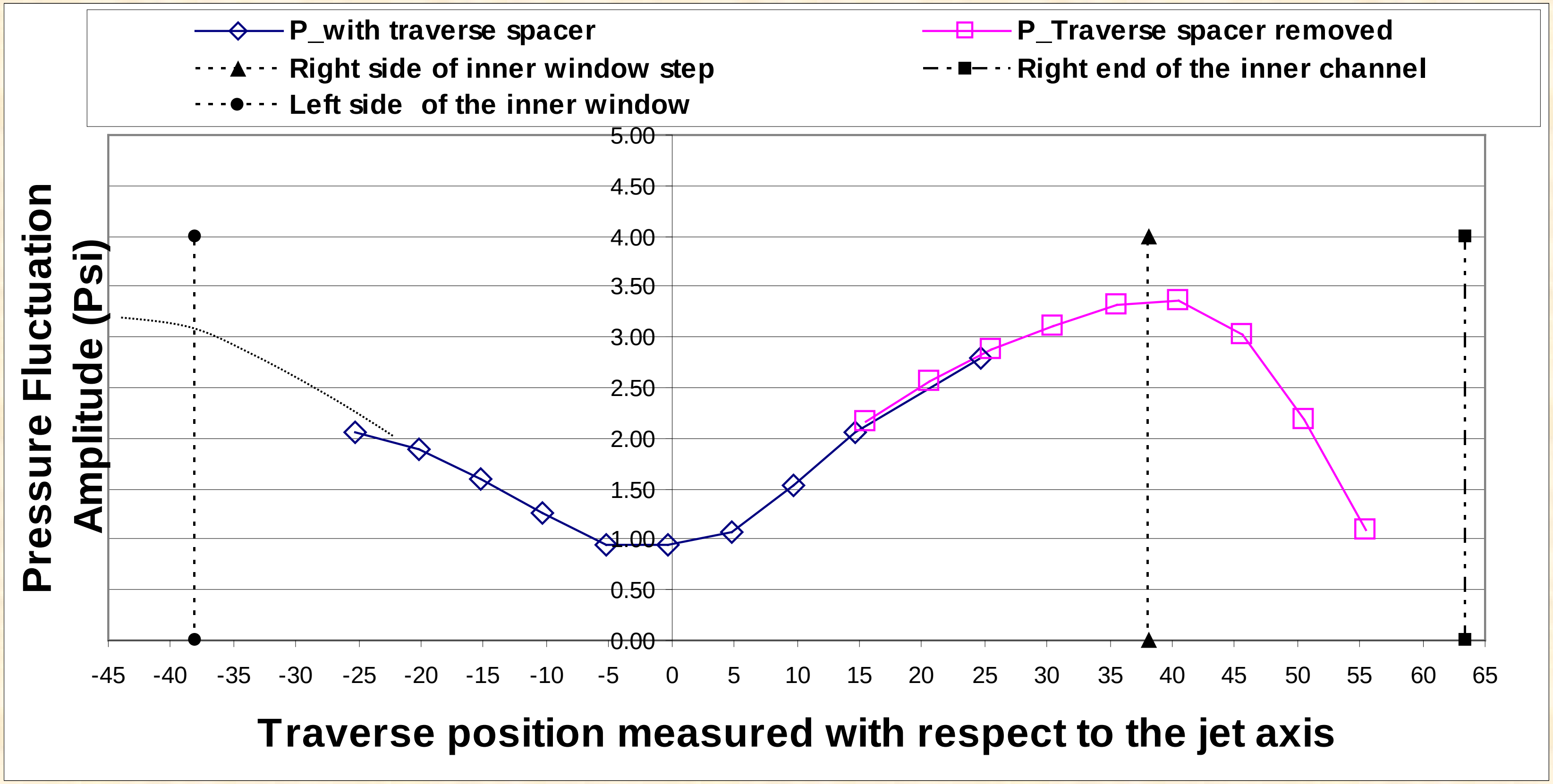

ON

Pch = 2.48 MPa, Frequency= 2700 Hz

ATC
Advanced Technology Consultants
www.advtechconsultants.com

Interaction of Acoustic Waves with a Cryogenic Nitrogen Single Jet at Subcritical Pch

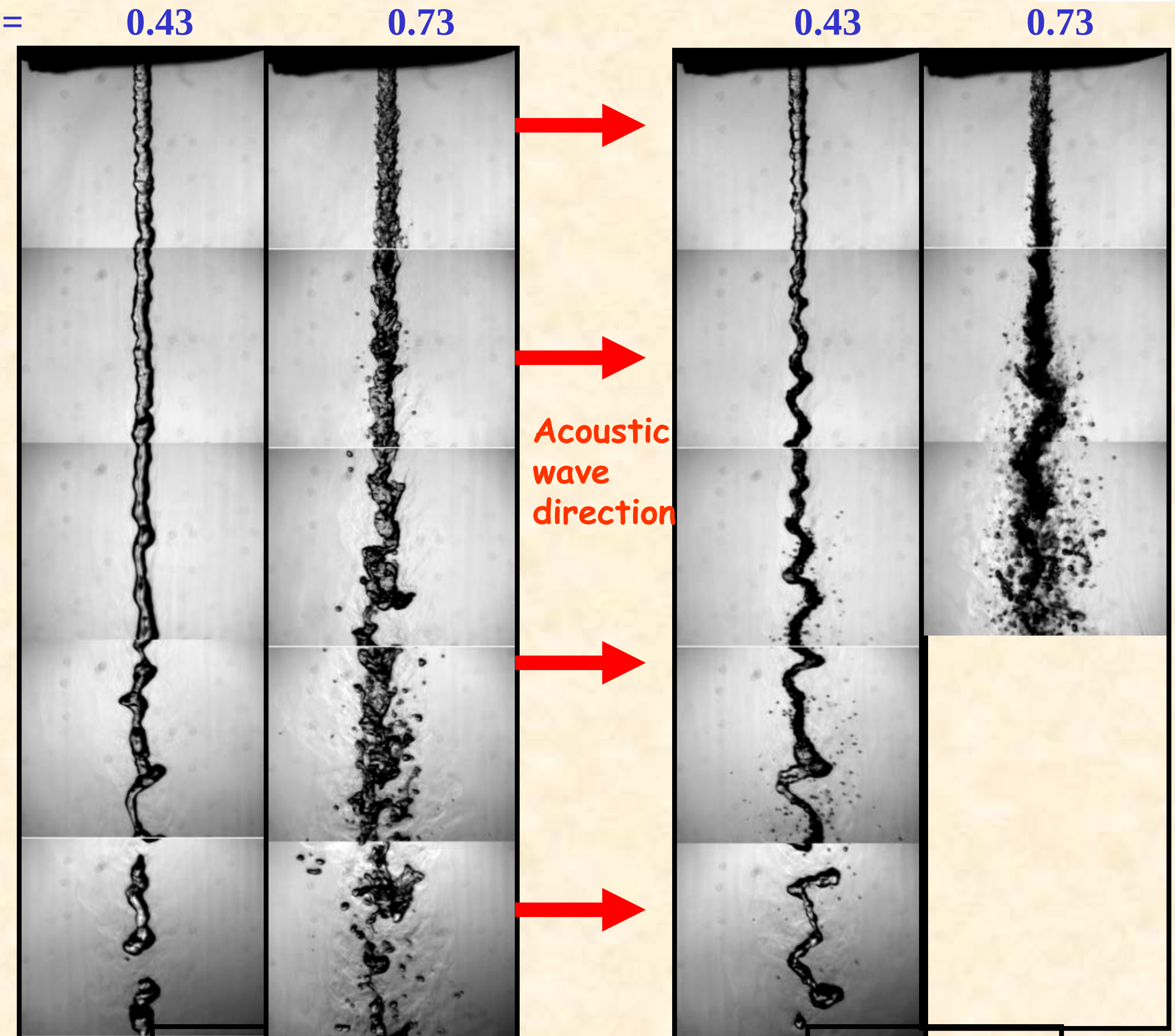

Subcritical

Frequency: 2700 Hz
Flow rate: 150mg/s
Chamber temperature: 300 K

- **Acoustic waves amplify the instabilities**
- **Accelerates liquid breakup**
- **Generates small satellite droplets**
- **Constricts the jet diameter in the wave direction**

Single jet
View: perpendicular to acoustic direction

Chehroudi, B., et al., 2002. Interaction of Acoustic Waves with a Cryogenic Nitrogen Jet at Sub- and Supercritical Pressures, 40th AIAA Aerospace Sciences Meeting & Exhibit, AIAA Paper 2002-0342, Reno, Nevada, January 14-17.

ATC Advanced Technology Consultants

www.advtechconsultants.com

Interaction of Acoustic Waves with a Cryogenic Nitrogen Single Jet at Supercritical Pch

Supercritical

Frequency: 2700 Hz
Flow rate: 150mg/s
Chamber temperature: 300 K

- **Shorter dark core**
- **Comparable jet thickness**
- **Comparable growth rate**
- **Not as dramatic as subcritical**

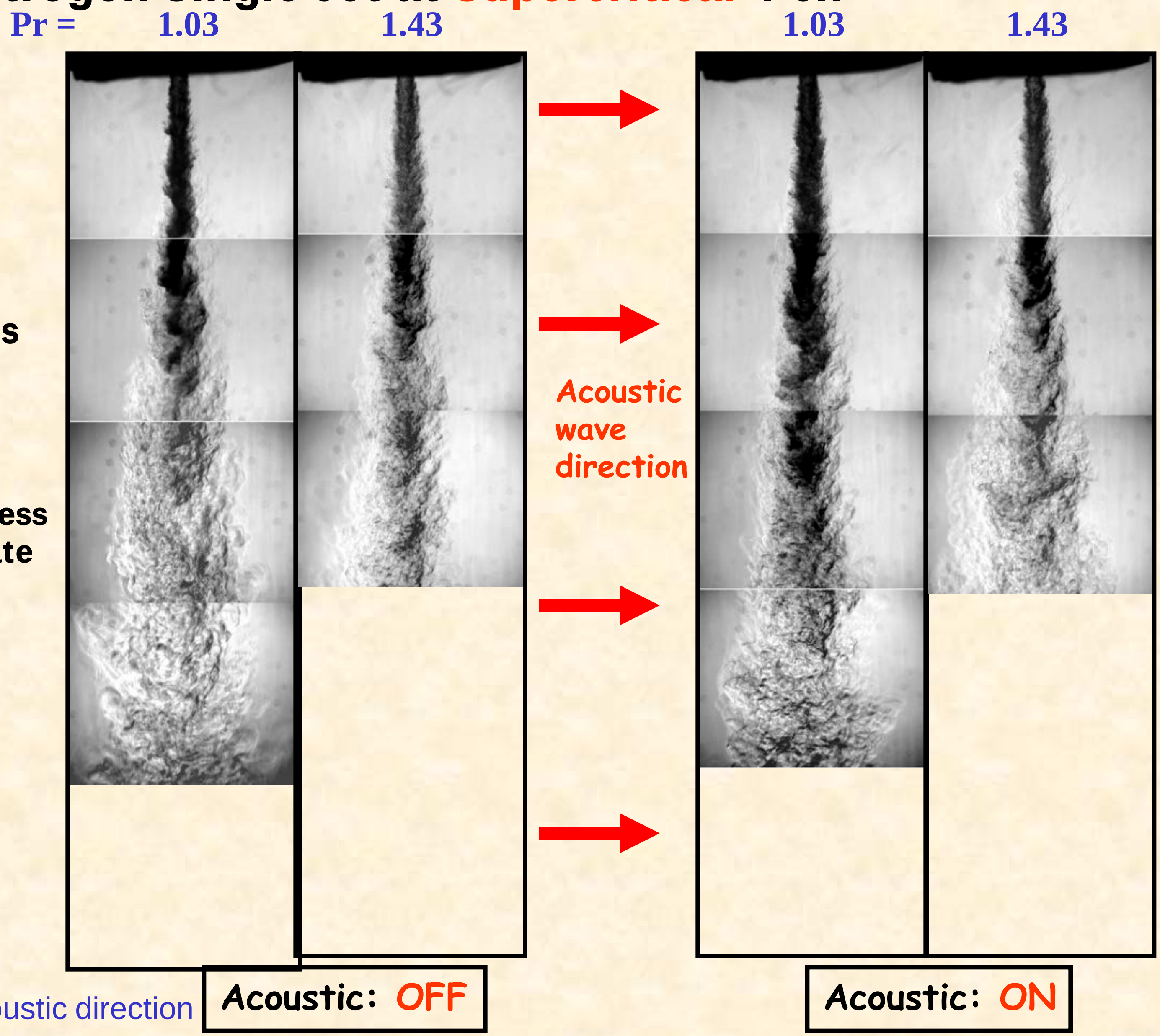

Single jet

View: perpendicular to acoustic direction

Chehroudi, B., et al., 2002. Interaction of Acoustic Waves with a Cryogenic Nitrogen Jet at Sub- and Supercritical Pressures, 40th AIAA Aerospace Sciences Meeting & Exhibit, AIAA Paper 2002-0342, Reno, Nevada, January 14-17.

Interaction of Acoustic Waves with a Cryogenic Nitrogen Single Jet at Subcritical Pch

ATC Advanced Technology Consultants

www.advtechconsultants.com

Subcritical

Frequency: 2700 Hz
Flow rate: 150mg/s
Chamber temperature: 300 K

- **Acoustic waves amplify the instabilities**
- **Accelerates liquid breakup**
- **Generates small satellite droplets**
- **Widens the jet diameter in the normal to wave direction**

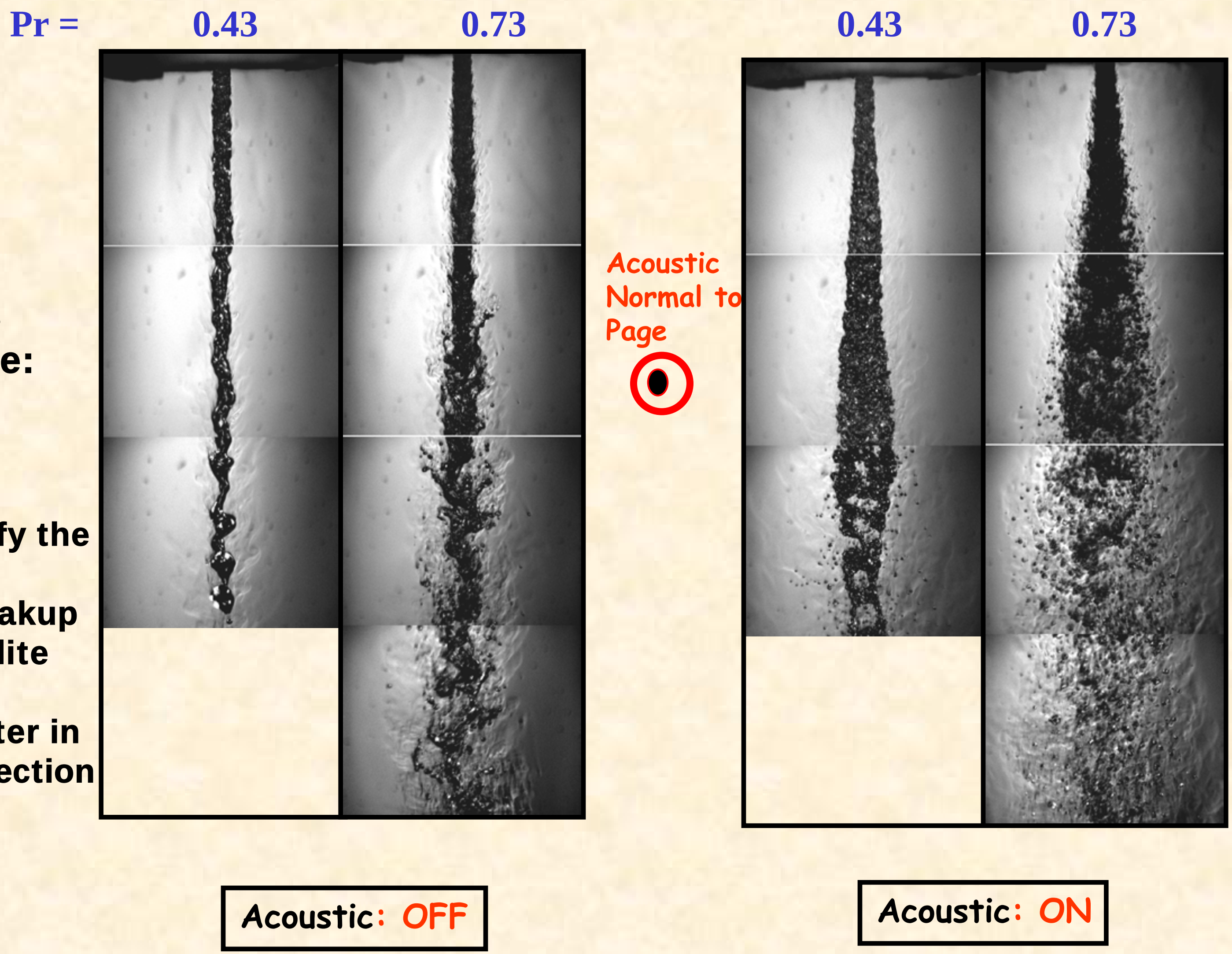

Single jet

View: in the acoustic direction

Chehroudi, B., et al., 2002. Interaction of Acoustic Waves with a Cryogenic Nitrogen Jet at Sub- and Supercritical Pressures, 40th AIAA Aerospace Sciences Meeting & Exhibit, AIAA Paper 2002-0342, Reno, Nevada, January 14-17.

ATC
Advanced Technology Consultants
www.advtechconsultants.com

Interaction of Acoustic Waves with a Cryogenic Nitrogen Single Jet at Supercritical Pch

Pr = 1.03 1.43 1.03 1.43

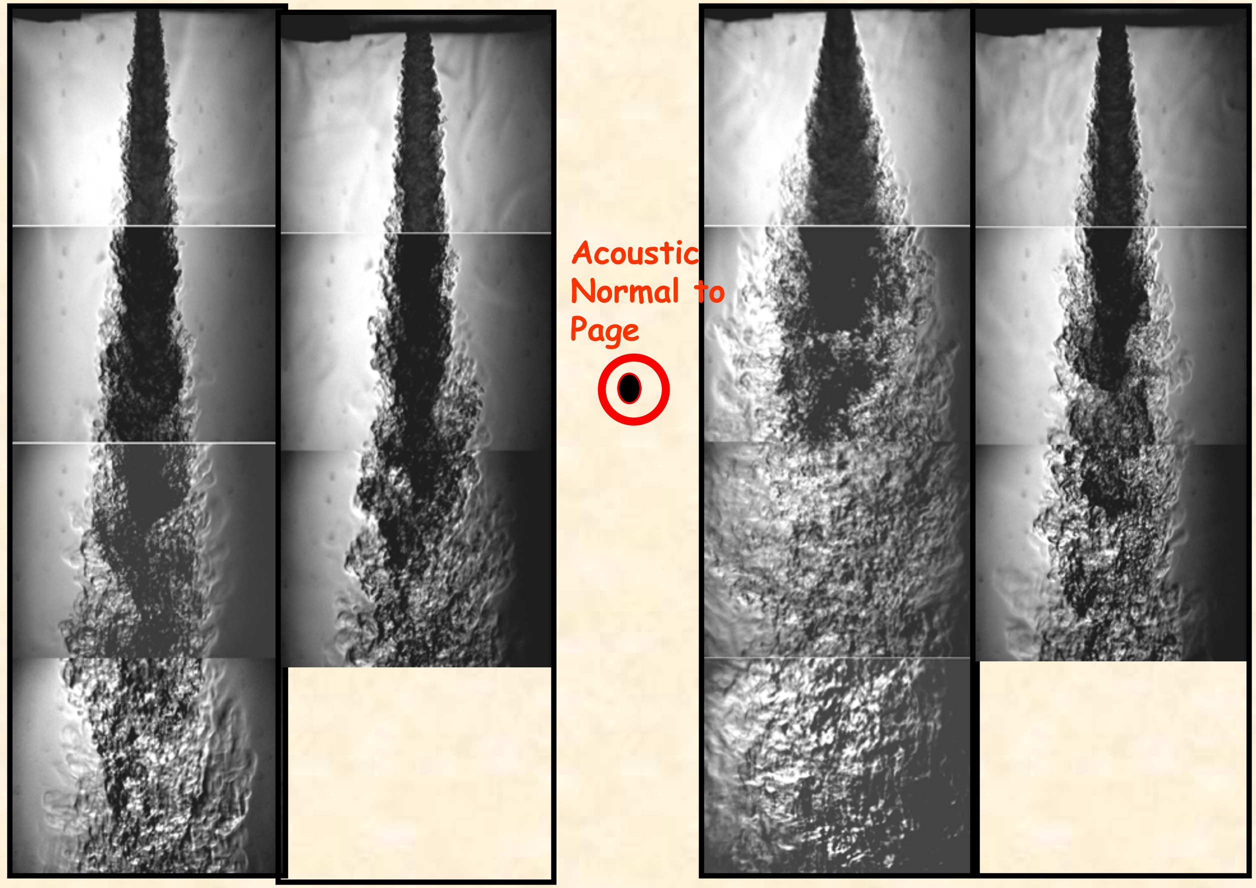

Acoustic: OFF

Acoustic: ON

Supercritical

Frequency: 2700 Hz
Flow rate: 150mg/s
Chamber temperature: 300 K

- Shorter dark core
- Wider jet thickness
- Faster growth rate

Single jet

View: in the acoustic direction

Chehroudi, B., et al., 2002. Interaction of Acoustic Waves with a Cryogenic Nitrogen Jet at Sub- and Supercritical Pressures, 40th AIAA Aerospace Sciences Meeting & Exhibit, AIAA Paper 2002-0342, Reno, Nevada, January 14-17.

ATC Advanced Technology Consultants
www.advtechconsultants.com

Spreading Angle at Sub- and Supercritical Conditions

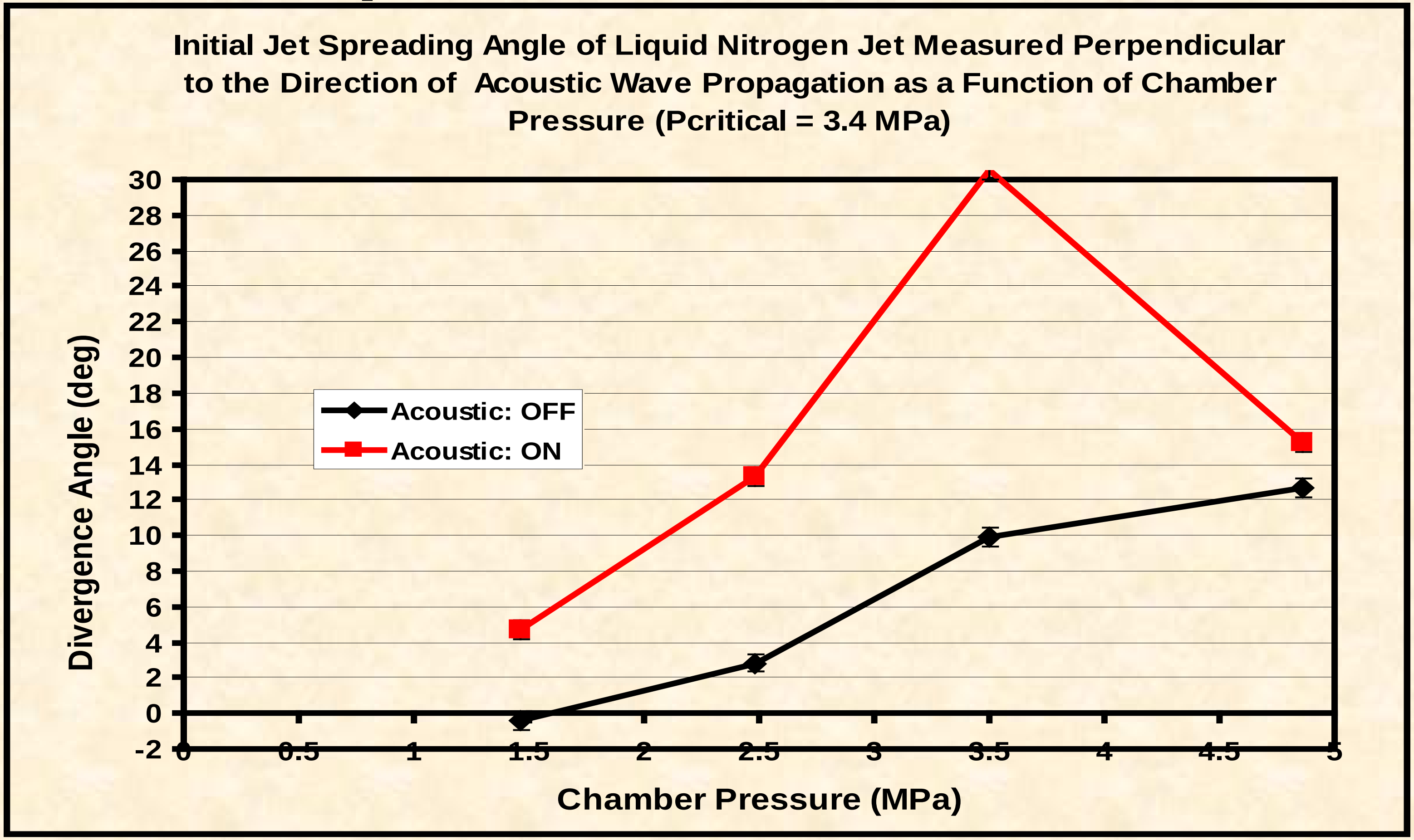

Single jet

- A significant widening of the jet perpendicular to the acoustic wave direction
- Largest effect is observed near the critical point

Chehroudi, B., et al., 2002. Interaction of Acoustic Waves with a Cryogenic Nitrogen Jet at Sub- and Supercritical Pressures, 40th AIAA Aerospace Sciences Meeting & Exhibit, AIAA Paper 2002-0342, Reno, Nevada, January 14-17.

Dark Core Length at Sub- and Supercritical Conditions

Single jet

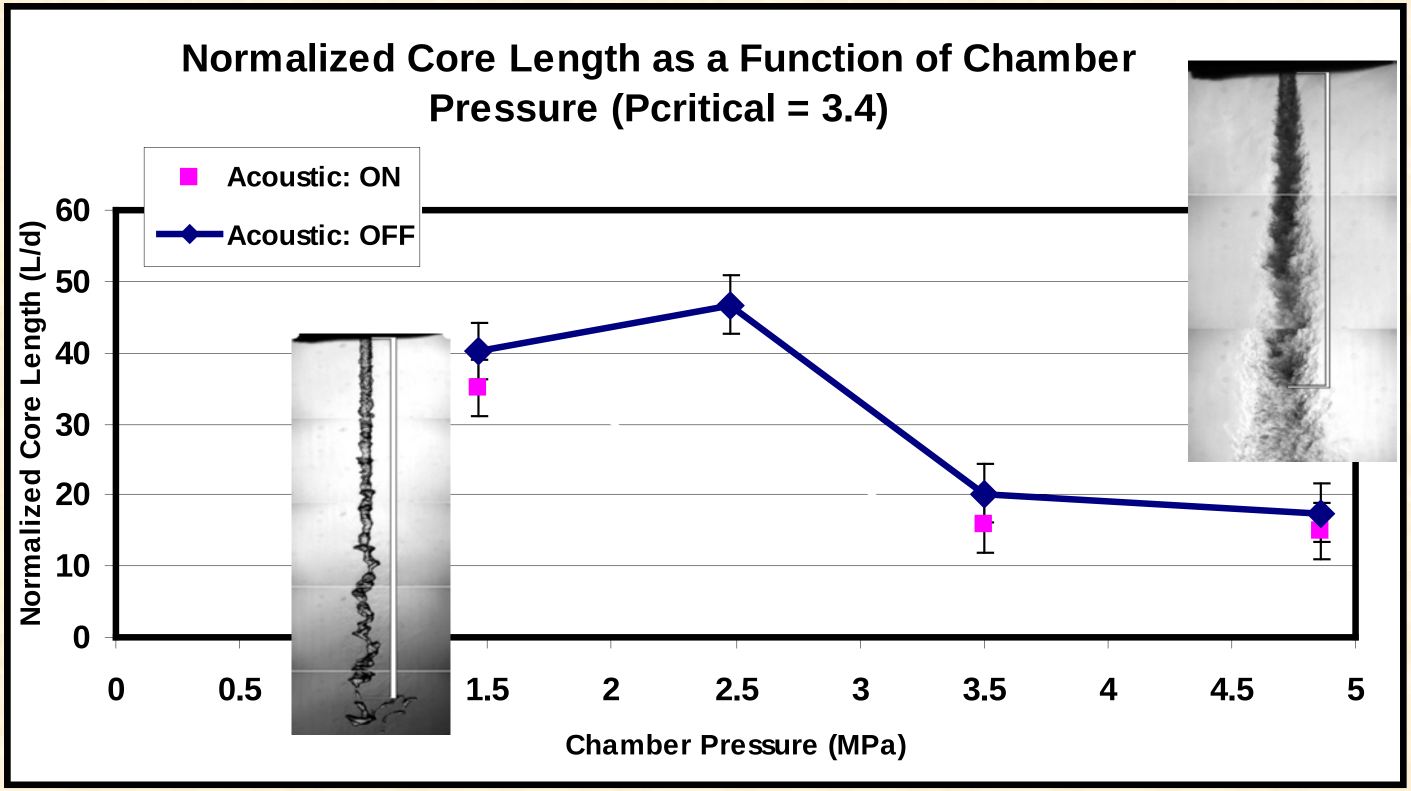

- Effects of acoustic wave on the intact-core (subcritical) or dark-core (Supercritical) length
- Acoustic waves shortens these lengths

Chehroudi, B., et al., 2002. Interaction of Acoustic Waves with a Cryogenic Nitrogen Jet at Sub- and Supercritical Pressures, 40th AIAA Aerospace Sciences Meeting & Exhibit, AIAA Paper 2002-0342, Reno, Nevada, January 14-17.

ATC Advanced Technology Consultants
www.advtechconsultants.com

Interaction of Acoustic Waves with a Cryogenic Nitrogen Jet at Sub- and Supercritical Conditions

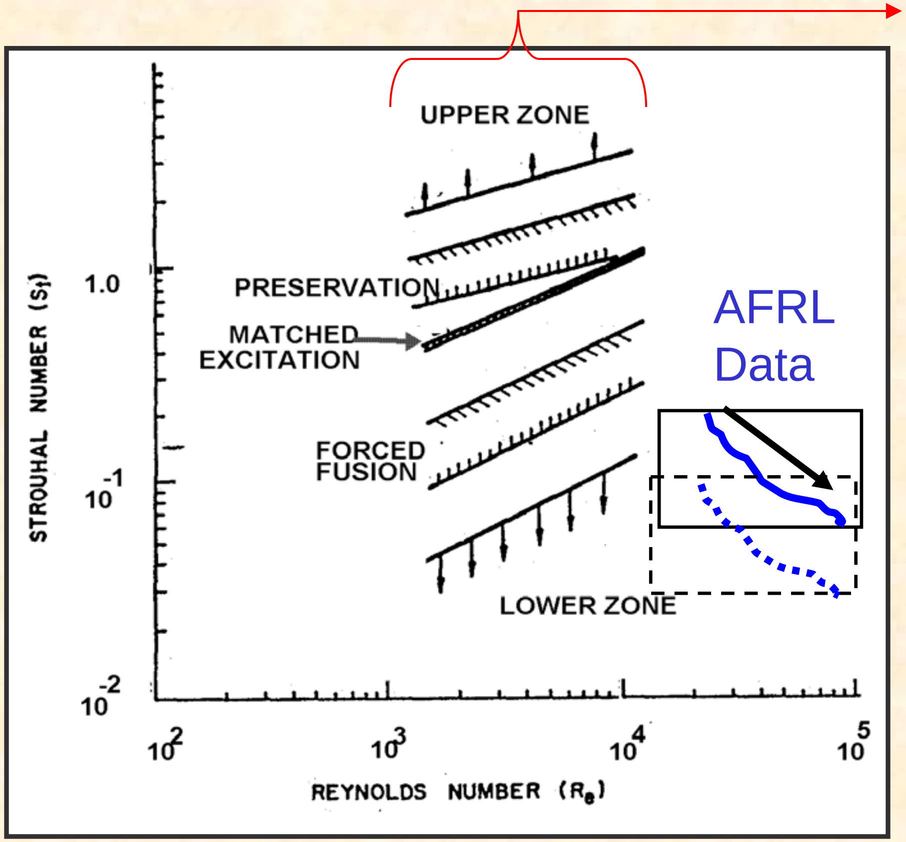

Single jet

What we know about gaseous jets:

- **Upper zone regime**: No effects were observed
- **Preservation regime:** The core flow of the jet tended to be preserved followed by the induction of smaller vortices, the time-averaged velocity profile was narrowed, and the longitudinal turbulence was decreased (relative to undisturbed case)
- **Matched:** When the excitation frequency was matched with the natural breakdown frequency, the effect was to accelerate the process of vortex formation and growth relative to the undisturbed case
- **Forced fusion regime:** The natural breakdown vortices were forced to fuse early as a result of the formation of large-diameter applied disturbance vortices.
- **Lower zone regime:** The vortex growth was unaffected in their formation region

Chehroudi, et al., 2002. Interaction of Acoustic Waves with a Cryogenic Nitrogen Jet at Sub- and Supercritical Pressures, 40th AIAA Aerospace Sciences Meeting & Exhibit, AIAA Paper 2002-0342, Reno, Nevada, January 14-17.

Rockwell, D. O.," External Excitation of Planar Jets," *Journal of Applied Mechanics*, pp. 883-891, December 1972.

ATC
Advanced Technology Consultants

www.advtechconsultants.com

Coaxial Jet
(No acoustic interaction)

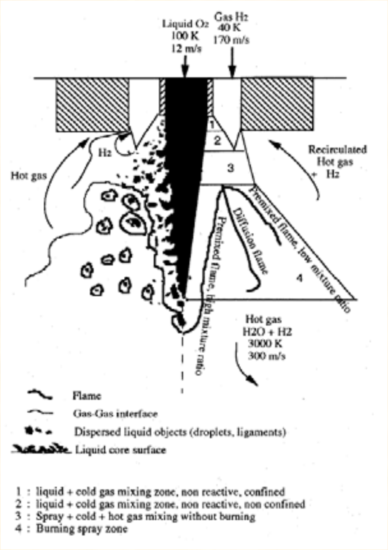

B. Chehroudi, PhD

ATC Advanced Technology Consultants

www.advtechconsultants.com

Coaxial Jets Injector

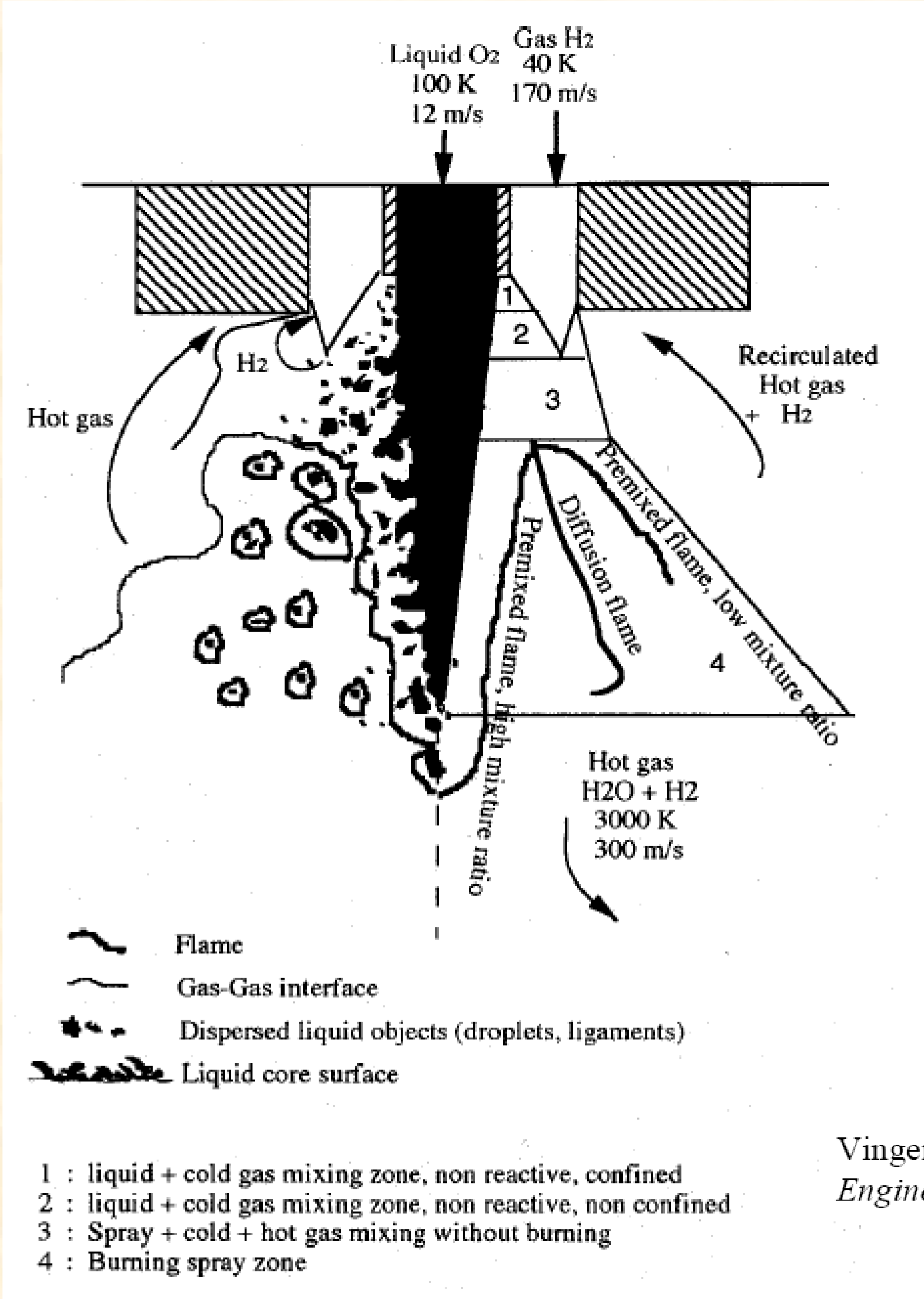

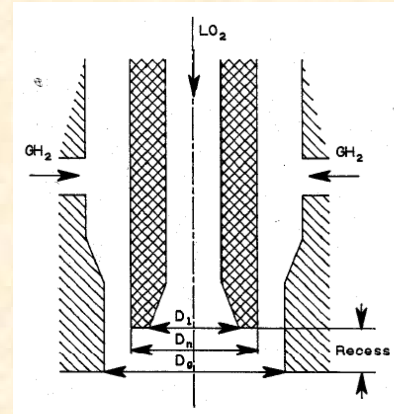

Prof. Fred Culick (Caltech):
ONERA Lectures on
Combustion Instability

Vingert et al., (1993) PSU Symposium, *Liquid Rocket Engine Combustion Instability*, (pp. 145–189).

ATC
Advanced Technology Consultants

www.advtechconsultants.com

Coaxial Injector

Manifold for gaseous co-flow distribution

Injector tip

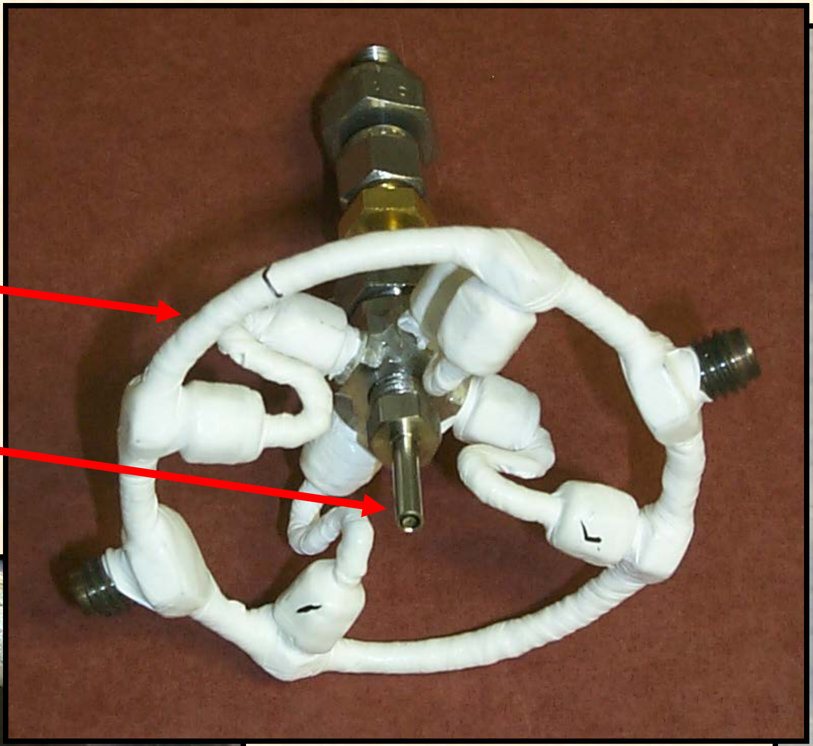

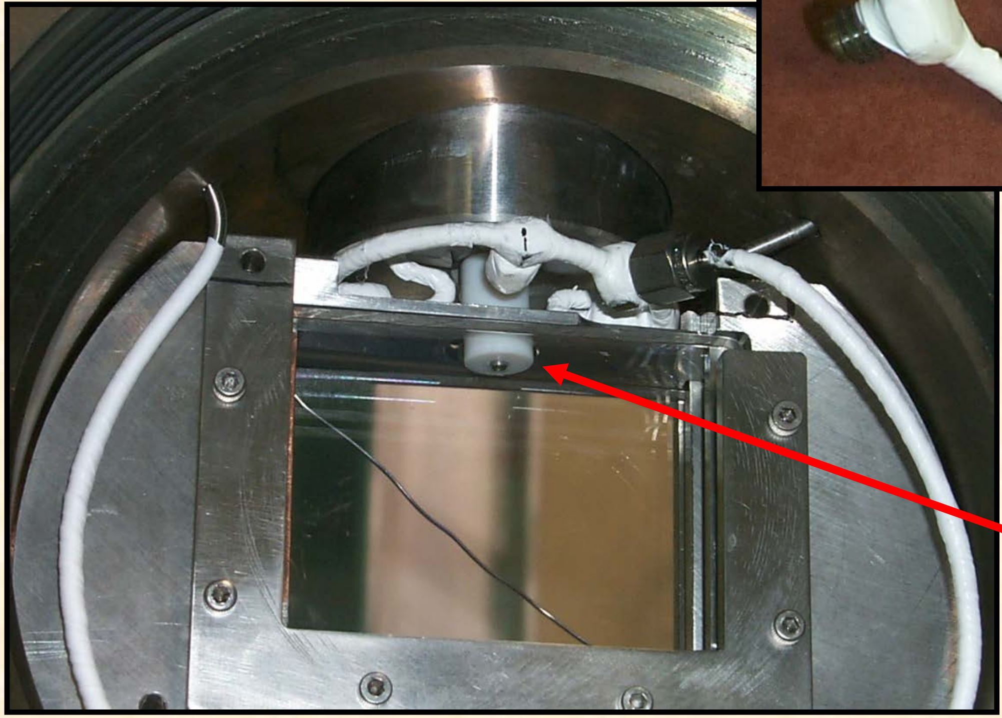

Injector and its holder inside the chamber

ATC
Advanced Technology Consultants
www.advtechconsultants.com

AFRL
THE AIR FORCE RESEARCH LABORATORY
LEAD | DISCOVER | DEVELOP | DELIVER

Supercritical Facility

BEFORE UPGRADES

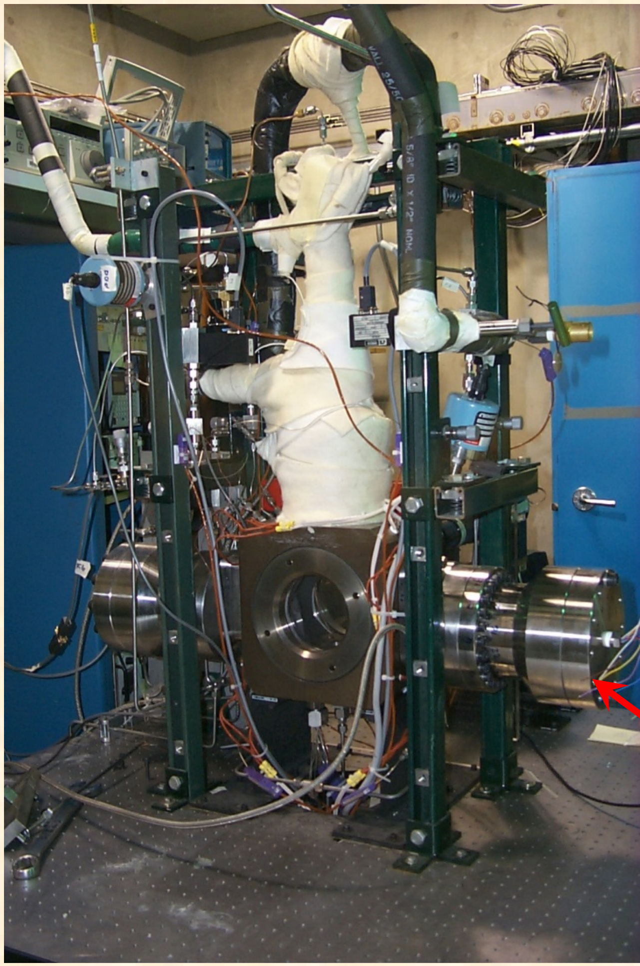

AFTER UPGRADES

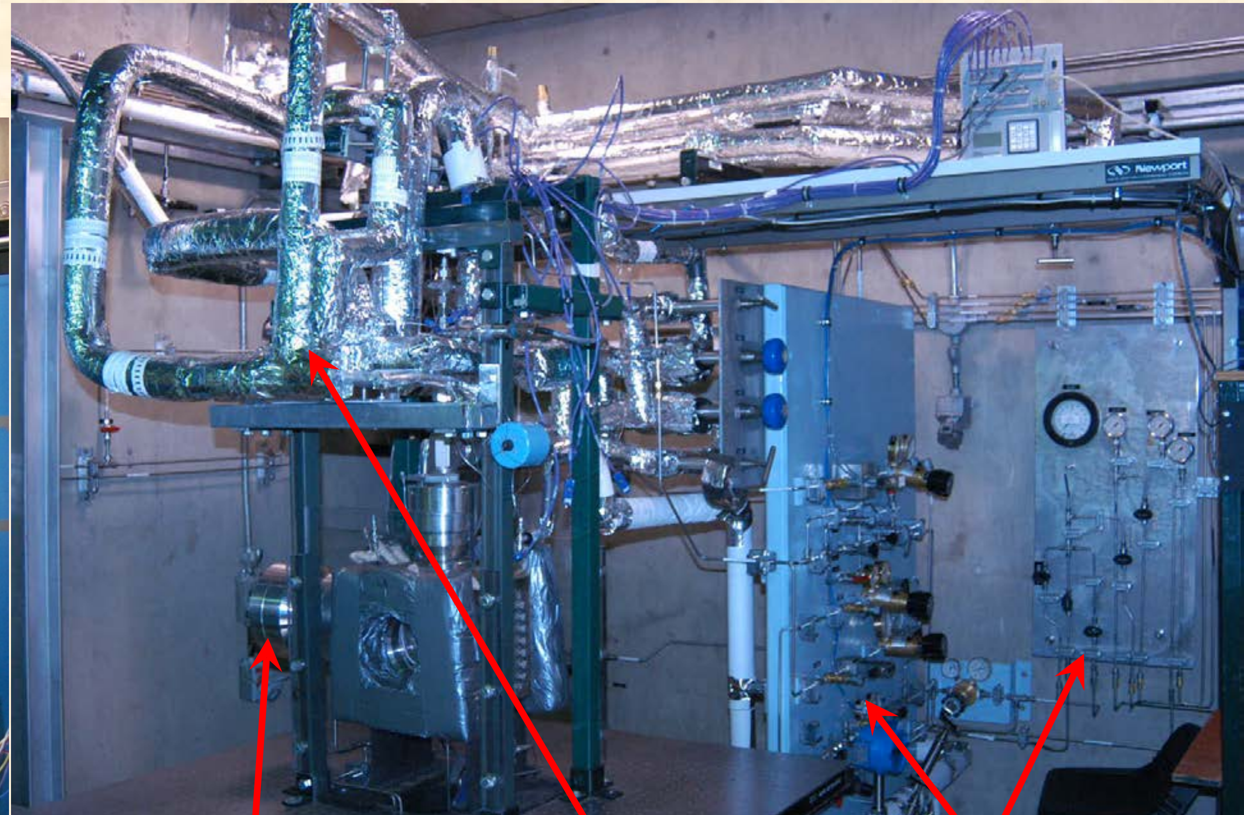

Acoustic Driver

New Coax HX

New Control Panels

Jet Exit Plane Temperature Measurement

ATC Advanced Technology Consultants

www.advtechconsultants.com

- Axial Location of TC ~0.28D_i down of injector Exit Plane
- Traverse through jet measure radial profile
- Each individual TC calibrated with precision RTD
- Accuracy of temperature measurement critical for computed properties

PENNSTATE 1855 COAXIAL INJECTOR

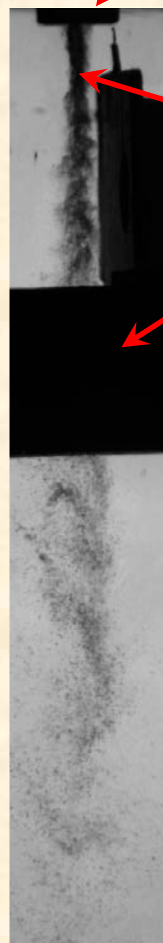

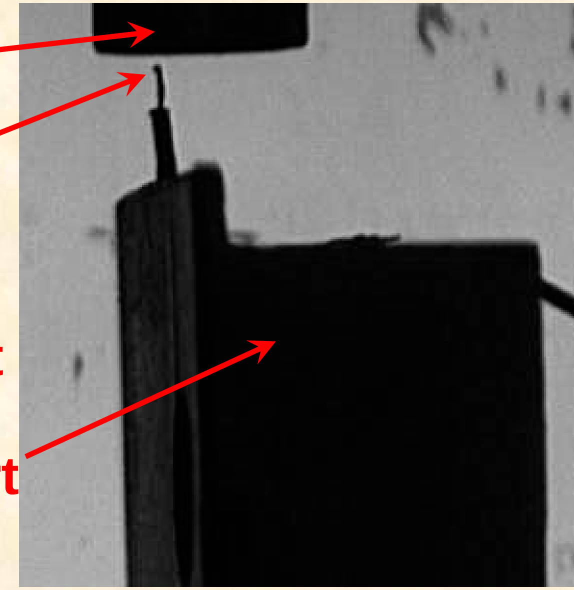

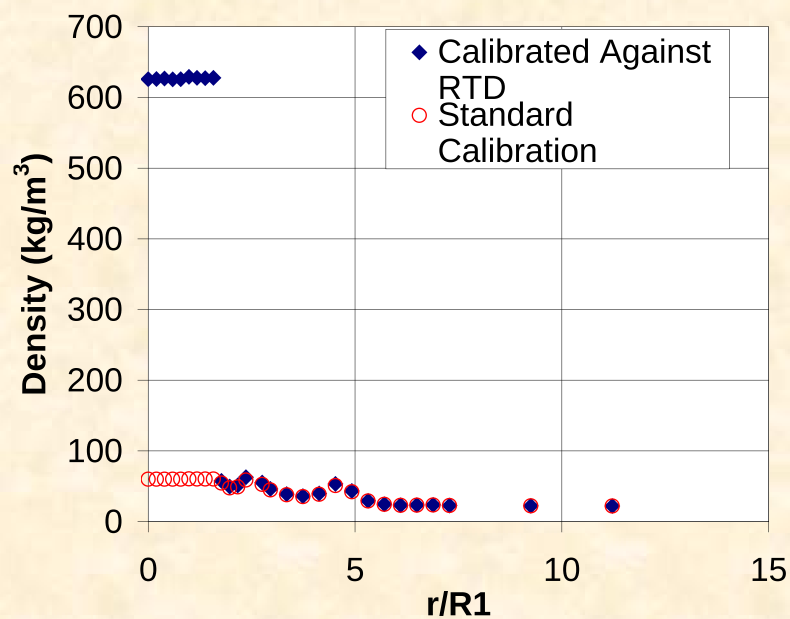

Davis, D., Chehroudi, B., and Sorensen, I., 2005. Measurements in an Acoustically-Driven Coaxial Jet under Supercritical Conditions, 43ed AIAA Aerospace Sciences Meeting and Exhibit, Paper No. AIAA-2005-0736, Reno, Nevada, January 10-13.

ATC Advanced Technology Consultants

www.advtechconsultants.com

Exit Plane Temperature Profiles

AFRL THE AIR FORCE RESEARCH LABORATORY LEAD | DISCOVER | DEVELOP | DELIVER

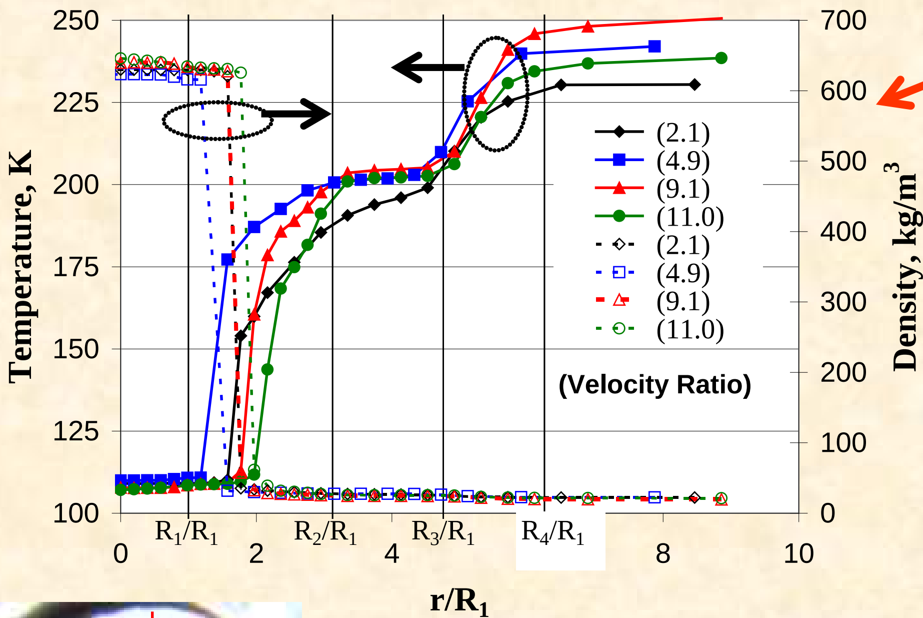

- **Subcritical *P* = 1.5 MPa**
- **Steep transition from gas to liquid**
- **Core "top-hat" shape**
- **The width of the core changes with VR**

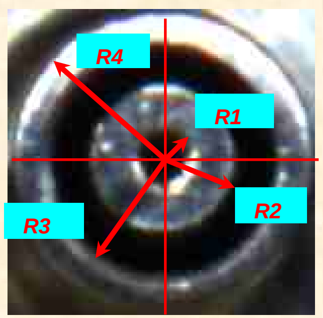

COAXIAL INJECTOR

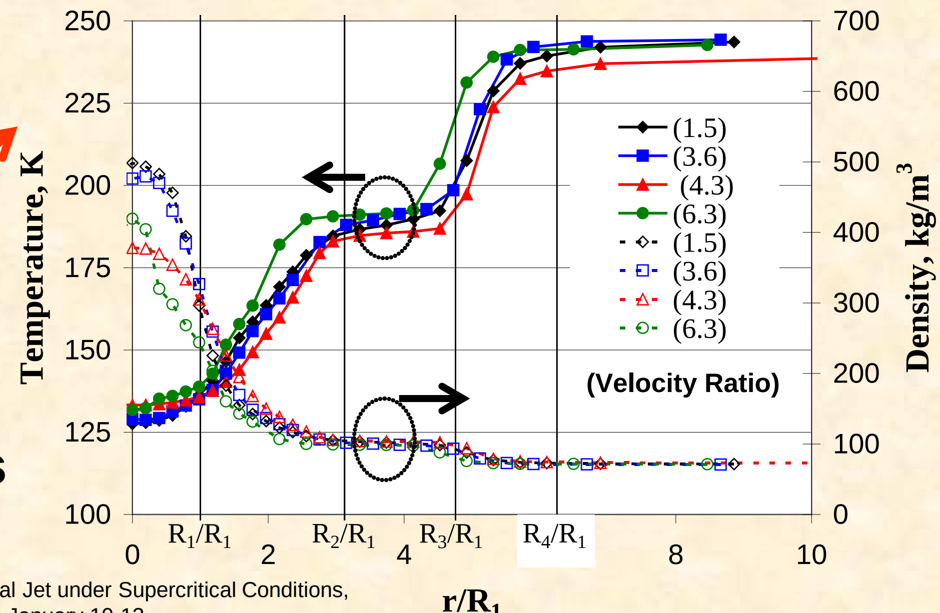

- **Supercritical *P* = 4.9 MPa**
- **Gradual transition from gas to liquid**

Davis, D., Chehroudi, B., and Sorensen, I., 2005. Measurements in an Acoustically-Driven Coaxial Jet under Supercritical Conditions, 43ed AIAA Aerospace Sciences Meeting and Exhibit, Paper No. AIAA-2005-0736, Reno, Nevada, January 10-13.

Automated Dark-Core Length Measurement

- **Threshold Images based on Image Histogram**
- **Accounts for variability from image to image**

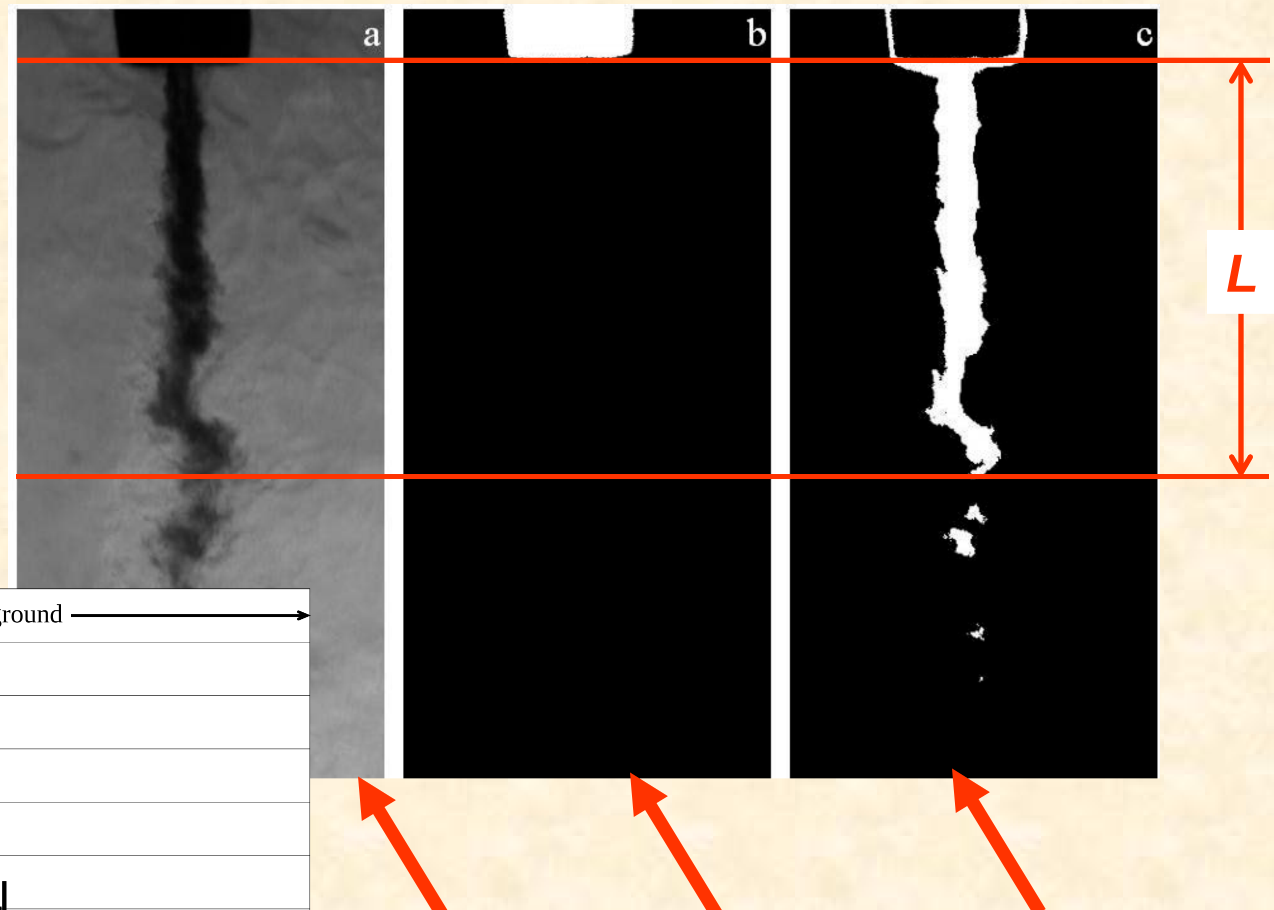

Untouched Original **Injector Threshold** **Dark Core Threshold**

Image Histogram

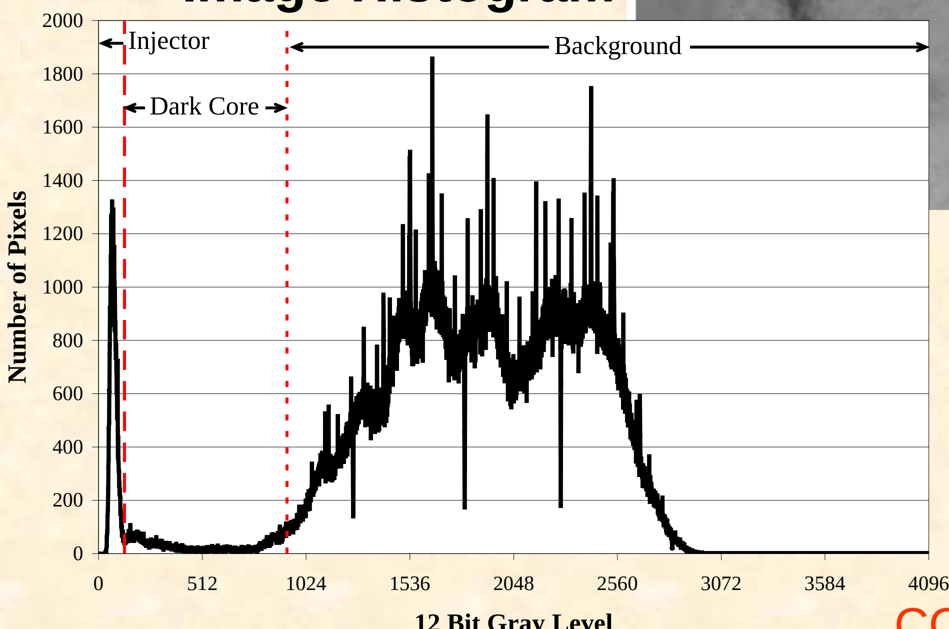

COAXIAL INJECTOR

Mean Dark Core Length vs. Momentum Flux Ratio

ATC Advanced Technology Consultants
www.advtechconsultants.com

AFRL THE AIR FORCE RESEARCH LABORATORY LEAD | DISCOVER | DEVELOP | DELIVER

- "Two-Phase" Subcritical *P* jet's core length longer than near- or supercritical
- "Single-Phase" Near- and Supercritical *P* core length scales with $M^{-0.5}$
- *(M is outer-to-inner jet momentum flux ratio)*

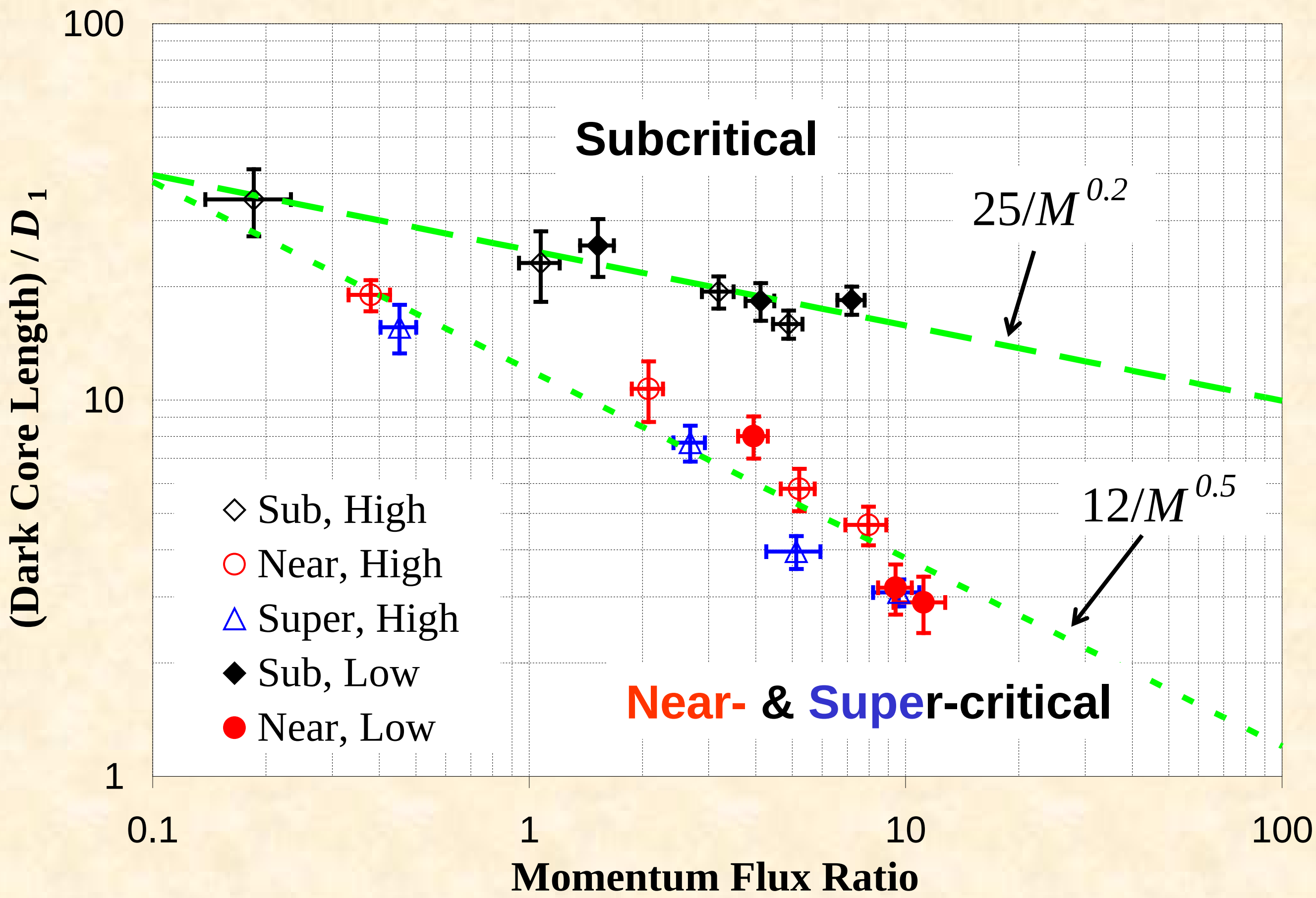

PENNSTATE 1855

Davis, D. W. and Chehroudi, B., 2006. Measurements in an Acoustically-Driven Coaxial Jet under Supercritical Conditions, *AIAA J. of Propulsion and Power*, Vol. 23, No. 2, March-April, pp. 364-374.

COAXIAL INJECTOR

www.advtechconsultants.com

Literature Reporting Core-Length of Shear-Coaxial Jets

Author	Date	Fluid Inner Jet	Fluid Outer Jet	Fluid Ambient	D1 (mm)	D2 (mm)	D3 (mm)	(D3-D2)/2 (mm)	Area Ratio	Post Recess (mm)	Injector Lpost/D1
Forstall & Shapiro	1950	Air+10%He	Air	Air	6.4, 25	NR	102	NR	NR	NR	NR
Chigier & Beer	1964	Air	Air	Air	25	64	97	16.5	8.50	0*	NR
Champage&Wygnanski	1971	Air	Air	Air	25	NR	NR	NR	1.28, 2.94	0*	NR
Au and Ko	1987	Air	Air	Air*	2	2.2	4	0.9	2.79	0*	NR
Eroglu et al.	1991	Water	Air	Air	0.971	1.262	10.36	4.549	112.15	-0.6	57
Woodward	1993	KI (aq.)	N2, He	N2, He	4.76	6.35	9.86	1.76	2.51	0.0	85
Villermaux et al.[g]	1994	Water	Water	Water	40	51	55	0.2	0.27	0*	"long"
Englebert et al.	1995	Water	Air	Air	2.3	2.95	14.95	6.00	40.60	0.0	22
Carreau et al.	1997	LOX	He, N2, Ar	NC[c]	5[d]	5.57[d]	16[d]	5.2[d]	9	0.0	NR
Rehab et al.[g]	1997	Water	Water	Water	NR	NR	NR	NR	1.82, 1.87, 5.24[e]	0*	NR
Rehab et al.[g]	1997	Water	Water	Water	20	21	27	3	1.82	0	NR
Villermaux [g,h]	1998	Water	Water	Water	NR	NR	NR	NR	NR	NR	NR
Lasheras et al.[g]	1998	Water	Air	Air	3.8	4.2	5.6	0.7	0.95	0	29
Lasheras&Hopfinger [g,i]	2000	NR	NR	NR	NR	NR	NR	NR	NR	NR	NR
Favre-Marinet&Schettini	2001	Air, SF6	Air,He	Air, He	20	20.4	27	3.3	0.78	0.0	6.75
Porcheron et al.	2002	LOX, Water	He, N2, Ar, Air	Air	5, 2.1	5.57, 2.5	16, 7	2.25	9, 9.69	0*	NR
Davis	2005	N2	N2	N2	0.51	1.59	2.42	0.415	12.80	0.25	100

Author	Date	Pressure (MPa)	Ti (K)	To (K)	Too (K)	Density Ratio Outer/Inner	Velocity Ratio Outer/Inner	*M* Outer/Inner	Re Inner (10^4)	Re Outer (10^4)	We
Forstall & Shapiro	1950	0.1*	Ambient [a]	Ambient	Ambient	1.09	0.2 - 0.75	0.04 - 0.61	NR	NR	NA
Chigier & Beer	1964	0.1*	Ambient	Ambient	Ambient	1*	0.024 - 2.35	5.8e-4 - 5.52	~10 [b]	~10 [b]	NA
Champage&Wygnanski	1971	0.1	Ambient	Ambient	Ambient	1*	0 - 10	0 - 100	1.01 - 10.15	0 - 9.6	NA
Au and Ko	1987	0.1*	Ambient	Ambient	Ambient	1*	1.25 - 6.67	1.5 - 44	NR	NR	NA
Eroglu et al.	1991	0.1*	Ambient	Ambient	Ambient	0.001	4.5 - 131.2	0.02 - 17.2	0.15 - 0.93	2.0 -11.6	15 - 530
Woodward	1993	0.1 - 2.17	Ambient	Ambient	Ambient	0.0006 -0.018	0 - 30	0 - 1.7	7.86 - 18.9	NR	12 - 3600
Villermaux et al.[g]	1994	0.1*	Ambient	Ambient	Ambient	1	1 - 6	1 - 36	>5000	>5000	NA
Englebert et al.	1995	0.1	293	293 - 636	293	0.0008 - 0.0012	10.25 - 66.75	0.12 - 4.3	0.54 - 3.4	4.8 - 16.5	76 - 2610
Carreau et al.	1997	0.1	82[d]	245 - 272[d]	NC	NR	NR	3 - 21.5	5.32 - 8.11	NR	0.919e4 - 3.48e4
Rehab et al.[g]	1997	0.1*	Ambient	Ambient	Ambient	1	2.2 - 5.6	4.9 - 31	1 - 10	1 - 10	NA
Rehab et al.[g]	1997	0.1*	Ambient	Ambient	Ambient	1	2 - 5	4 - 25	NR[f]	NR[f]	NA
Villermaux [g,h]	1998	NR	NR	NR	NR	1*	NR	NR	NR	NR	NR
Lasheras et al.[g]	1998	0.1	Ambient	Ambient	Ambient	0.001	NR	NR	NR	NR	NR
Lasheras&Hopfinger [g,i]	2000	NR	NR	NR	NR	NR	NR	NR	NR	NR	NR
Favre-Marinet&Schettini	2001	0.1	Ambient	Ambient	Ambient	0.028 - 1	3.0 - 70	1 - 200	NR	3200, 11000	NA
Porcheron et al.	2002	0.1	82, 293	245 - 293	293	1.6e-4 - 2.3e-3	NR	2 - 21.6	NR	NR	0 - 14000
Davis	2005	1.4 - 49	108 - 133	132 - 204	197 - 249	0.04 - 0.56	1.2 - 11.1	0.19 - 11.2	1.2 - 3.2	0.8 - 19	32 - oo

Davis, D. W. and Chehroudi, B., 2006. Measurements in an Acoustically-Driven Coaxial Jet under Supercritical Conditions, *AIAA J. of Propulsion and Power*, Vol. 23, No. 2, March-April, pp. 364-374.

Literature Reporting Core-Length of Shear-Coaxial Jets Correlations

Table 1. Summary of published operating conditions, geometries, measurement techniques, and proposed equations from the literature, measuring or correlating core length for shear-coaxial jets. (continued)

REF	Author	Diagnostic	Quantity Measured	Equation
6	Forstall & Shapiro	Pitot tube, Sampling Tube	Potential Core	$L/D_1 = 4+12V_r$
7	Chigier & Beer	Pitot tube	Potential Core	NR
8	Champagne & Wygnanski	Hot wire anemo-meter	Inner Core	NR
9	Au and Ko	Hot wire anemo-meter	Potential Core	$L/D_1 = 9.9/V_r$
10	Eroglu et al.	Back-lit still	Liquid Intact Length	$L/D_1 = 0.66\,We^{-0.4}\,Re^{0.6}$
11	Woodward	x-ray Radio-graphy	Intact Liquid Core Length	$L/D_1 = 0.0095\left(\frac{\rho_o}{\rho_i}\right)^{\frac{-0.36}{H}} We^{-0.22/H}\,Re^{0.68}$
15	Villermaux et al. [g]	Hot film anemo-meter	Potential Core / Cone	$L/D_1 = 7/V_r$
12	Englebert et al.	Back-lit high-speed 16mm film	Breakup Length	$L/D_1 = 40\,We^{-0.27}$ $\frac{2L}{D_3 - D_2} = 10.6M_R^{-0.3} = 13.7E_R^{-0.2}$
13	Carreau et al.	Fiber optic Probe	Breakup Length, Potential Cone Length	$L/D_1 = 0.0012\left(\frac{\rho_o}{\rho_i}\right)^{-0.32} We^{-0.33}\,Re^{0.55}$
16	Rehab et al. [g]	Hot film anemo-meter, Pitot tube, LIF image	Potential Core	$L/D_1 = 6/V_r;\ L/D_1 = 8/V$ $L/D_1 = 0.5\left(\frac{1}{(C\alpha V_r)^2} - 1\right)^{1/2} \approx \frac{1}{2C\alpha V_r}$
17	Rehab et al. [g]	Hot-film anemo-meter	Potential Cone	$L/D_1 = c/V_r;\ 6 < c < 8$
18	Villermaux [g,h]	h	Potential Cone, Liquid intact length	$L/D_1 = 6/M^{1/2}$

Table 1. Summary of published operating conditions, geometries, measurement techniques, and proposed equations from the literature, measuring or correlating core length for shear-coaxial jets. (continued)

REF	Author	Diagnostic	Quantity Measured	Equation
19	Lasheras et al. [g]	Photo-graph	Liquid intact length	$L/D_1 = \left(\frac{1}{4(C\alpha)^2 M} - \frac{1}{4}\right)^{1/2} \approx \frac{6}{M^{1/2}}$
20	Lasheras & Hopfinger [g,i]	i	i	$L/D_1 = \frac{1}{2cM^{2/3}}\left(\frac{\sigma}{\propto_i U_i}\right)^{1/3}$ $L/D_1 \approx \frac{6}{M^{1/2}}\left(\left\|1 - \frac{U_i}{U_o}\right\|\right)^{-1}$ $L/D_1 \approx \frac{6}{M^{1/2}} \frac{1}{\left(1 - \frac{B\sigma}{\propto_o U_o}\right)^{0.5}}$
21	Favre-Marinet & Schettini	Aspirating Probe w/ hot-wire	Potential Core	$L/D_1 \propto M^{-0.5}$
14	Porcheron et al.	Fiber optic Probe	Liquid Core	$L/D_1 = 2.85\left(\frac{\rho_o}{\rho_i}\right)^{-0.38} Z^{0.34} M^{-0.13}$
This work	Davis	Shadow-graph	Dark Core	$L/D_1 \approx \frac{12}{M^{1/2}}$ $L/D_1 \approx \frac{25}{M^{0.2}}$

Table 1. Notes

NR = not reported
NA = not applicable
NC = not clear from report
Amb. = ambient
* assumed from the context, but not directly reported
[a] Ambient temperature assumed from the context of discussion, but not specifically stated in report.
[b] reported as approximately 10^5
[d] The dimensions of the injector and the temperatures were not given in the paper, but were given in the paper by Porcheron et al.[14]
[e] This number is the diameter ratio squared, which is approximately the area ratio for a very thin lip injector. The only dimensional information given was the diameter ratios (1.35, 1.37, and 2.29 mm) and the lip thickness (D2-D1)/2 of 0.3 mm.
[f] A *Re* based on momentum conservation reported and defined as $Re = \rho_o U_o D_3/\propto^*(1-(D_1/D_3))^{0.5}$ ranged from $10^4 - 10^5$.
[g] These papers are from the same collaboration / research group over several years.
[h] This paper was an analysis paper that presented a different equation based on the data from the same group of researchers[16,17]
[i] This paper was a review paper encompassing the work from this same collaboration of researchers, as well as others.
[j] Unable to make measurements from images, and therefore not compared quantitatively to theory for core length.

Davis, D. W. and Chehroudi, B., 2006. Measurements in an Acoustically-Driven Coaxial Jet under Supercritical Conditions, *AIAA J. of Propulsion and Power*, Vol. 23, No. 2, March-April, pp. 364-374.

Core Length of Coaxial Jets

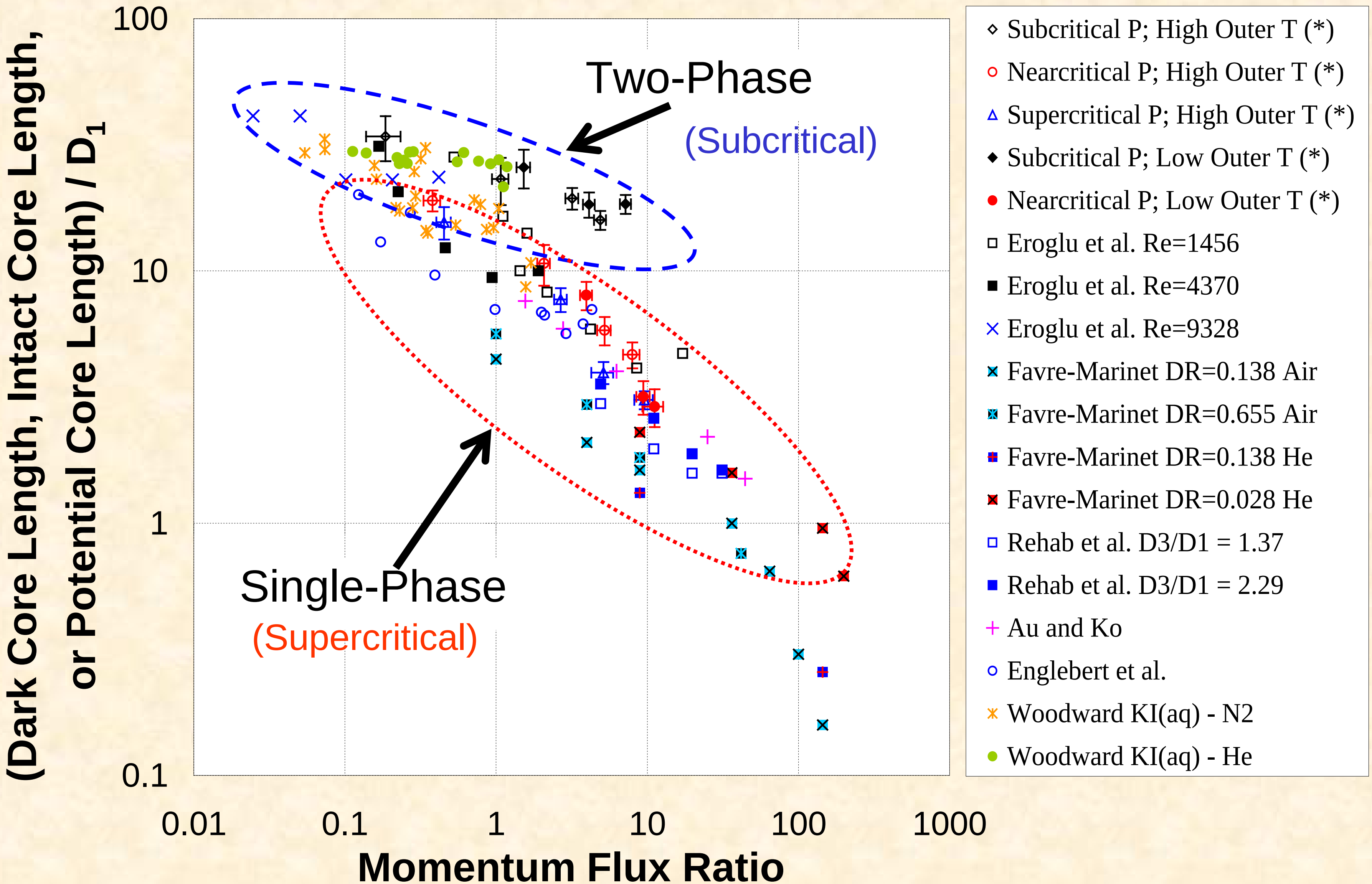

Davis, D. W. and Chehroudi, B., 2006. Measurements in an Acoustically-Driven Coaxial Jet under Supercritical Conditions, *AIAA J. of Propulsion and Power*, Vol. 23, No. 2, March-April, pp. 364-374.

Core Length of Coaxial Jets

ATC Advanced Technology Consultants
www.advtechconsultants.com

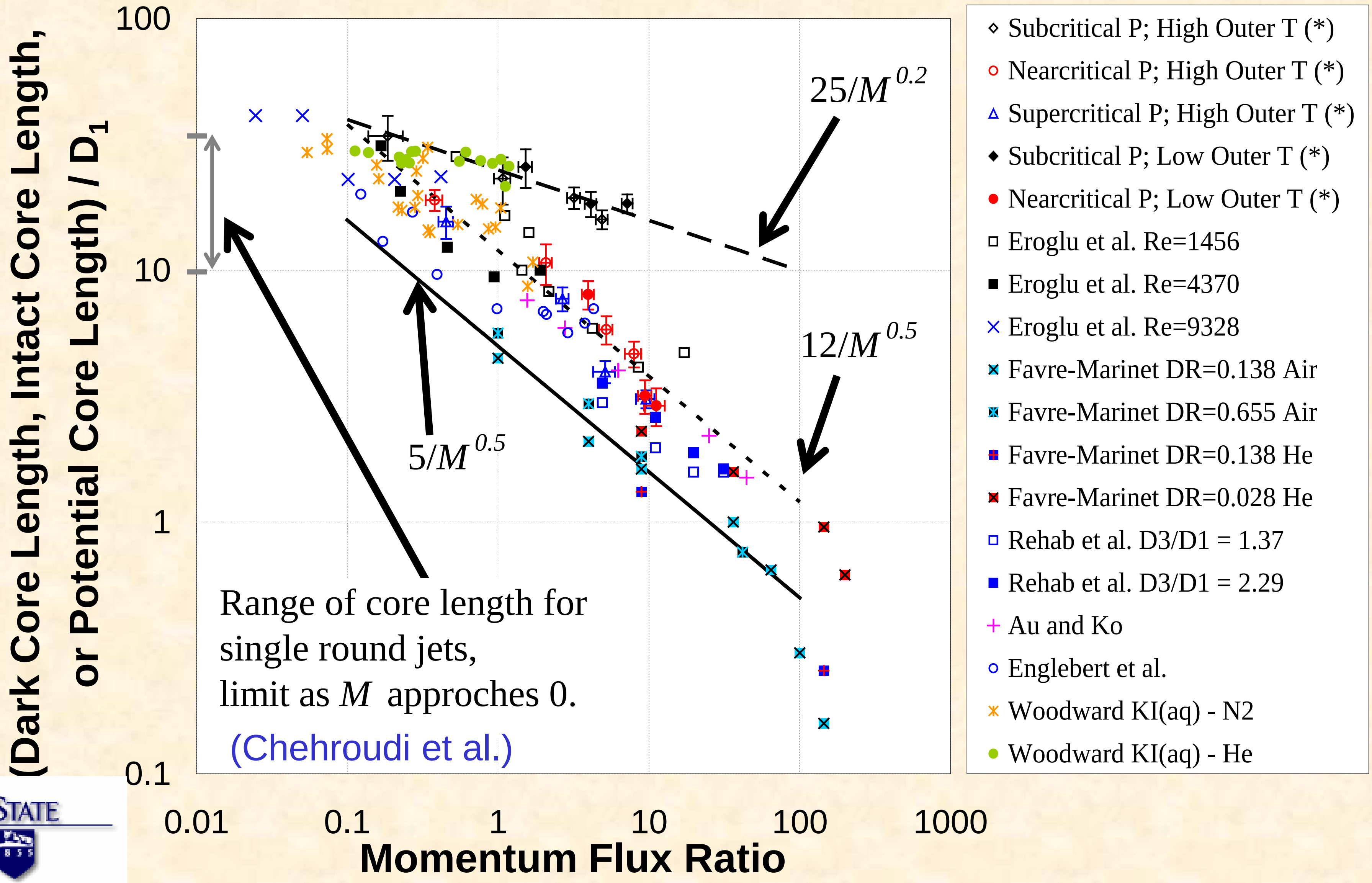

Davis, D. W. and Chehroudi, B., 2006. Measurements in an Acoustically-Driven Coaxial Jet under Supercritical Conditions, *AIAA J. of Propulsion and Power*, Vol. 23, No. 2, March-April, pp. 364-374.

ATC Advanced Technology Consultants

www.advtechconsultants.com

Core Length
Low Momentum Flux Ratio

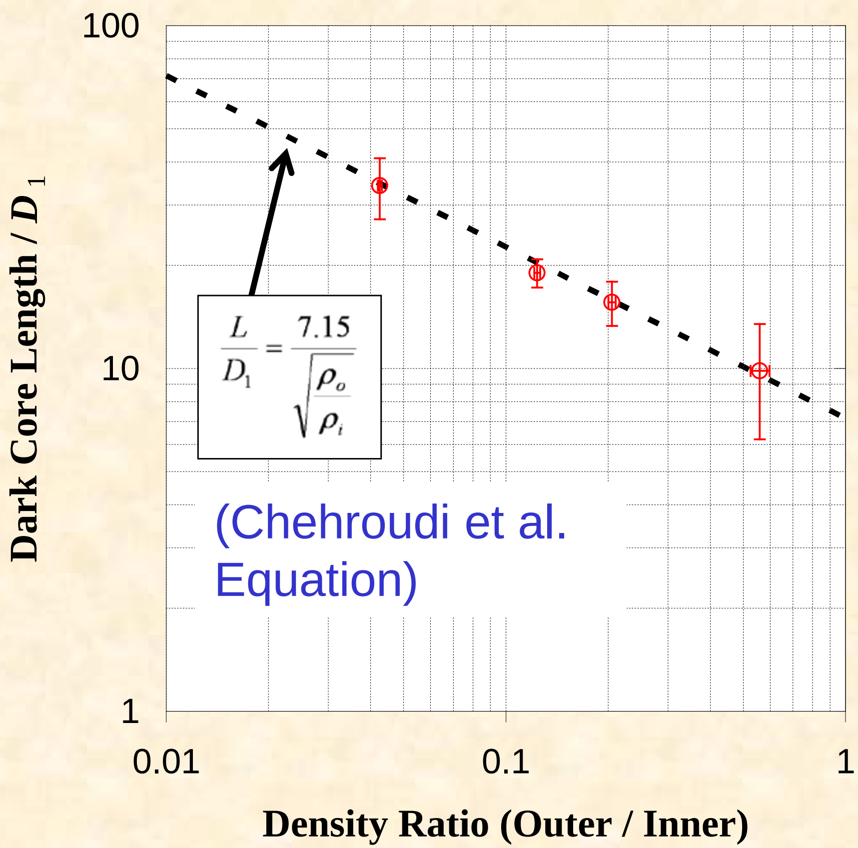

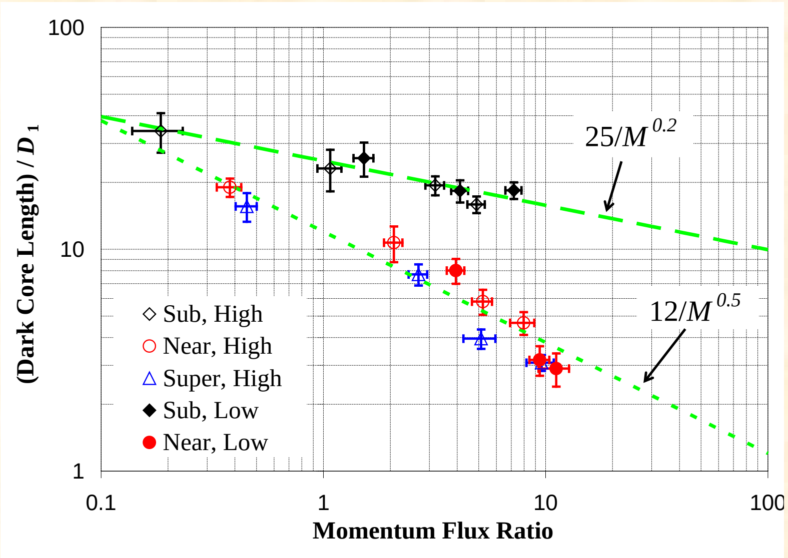

COAXIAL INJECTOR

- *M* < 1 core length of ***shear coaxial jet*** behaves like that of a ***single round jet***.
- Core length scales with the ***square root of density ratio*** according to the equation of Chehroudi and Bracco, 1985 developed for SINGLE JETS.

- Davis, D. W. and Chehroudi, B., 2006. Measurements in an Acoustically-Driven Coaxial Jet under Supercritical Conditions, *AIAA J. of Propulsion and Power*, Vol. 23, No. 2, March-April, pp. 364-374.
- Chehroudi, B., Chen, S. H., Bracco, F. V., and Onuma, Y., 1985. On the Intact Core of Full-Cone Sprays, Society of Automotive Engineers, 1985 Congress and Exposition, *SAE Transaction Paper 850126*, February 25-March 1. *Also, 1985 Arch. T. Colwell Merit Award.*

Spreading rate of the shear layer for single and coaxial jets

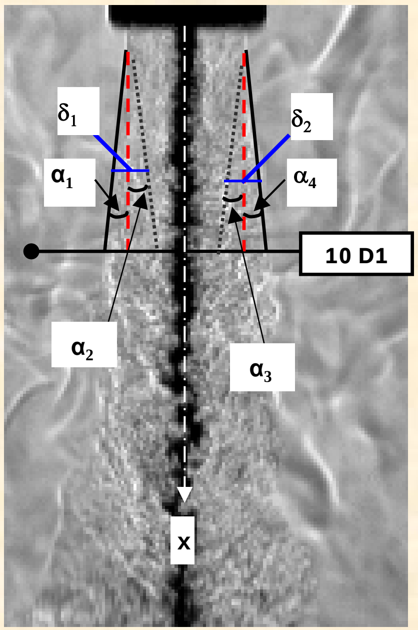

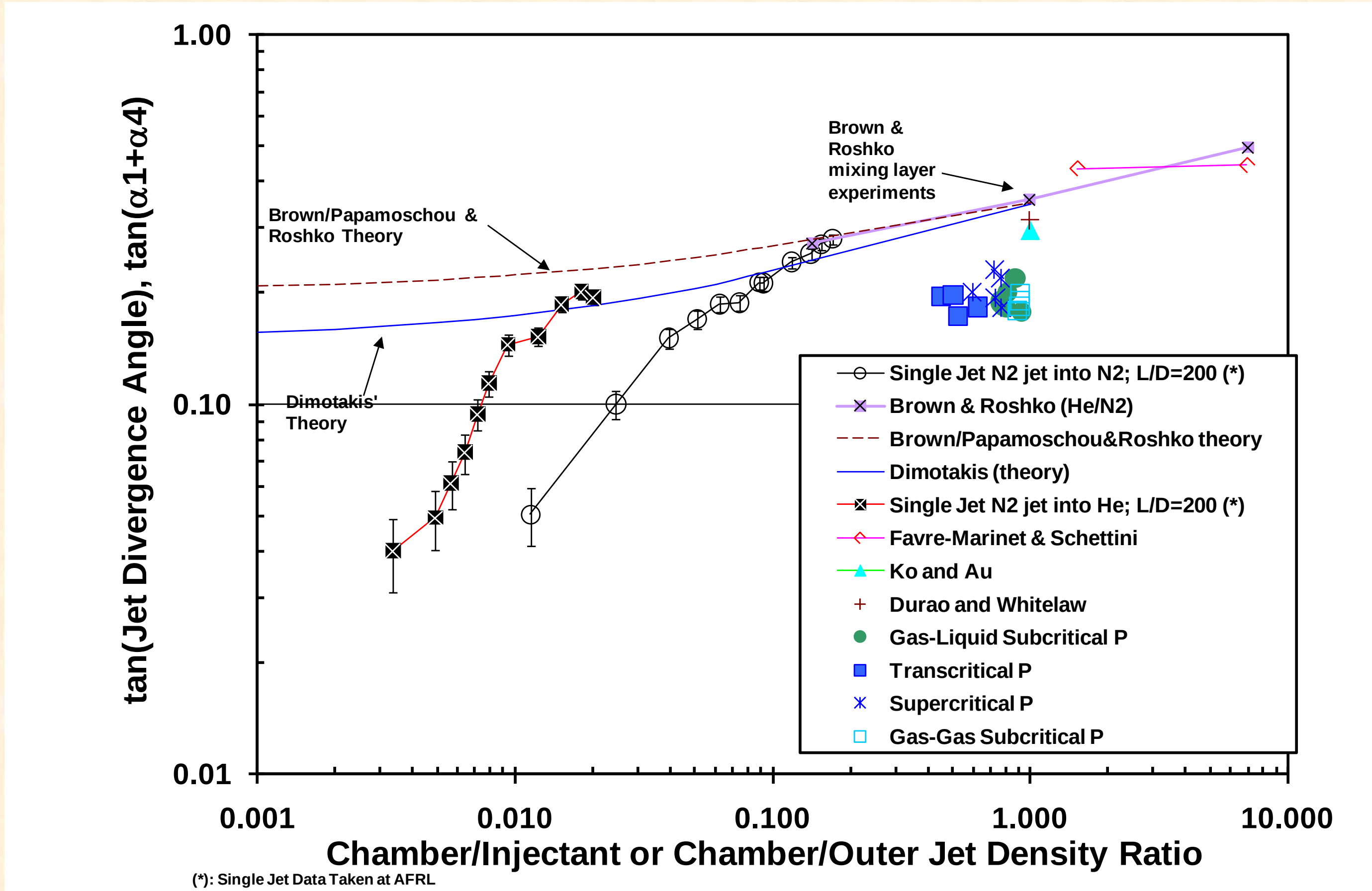

Outer jet spreading angle fairly constant with a mean value of 0.19

Growth rate of the outer jet

www.advtechconsultants.com

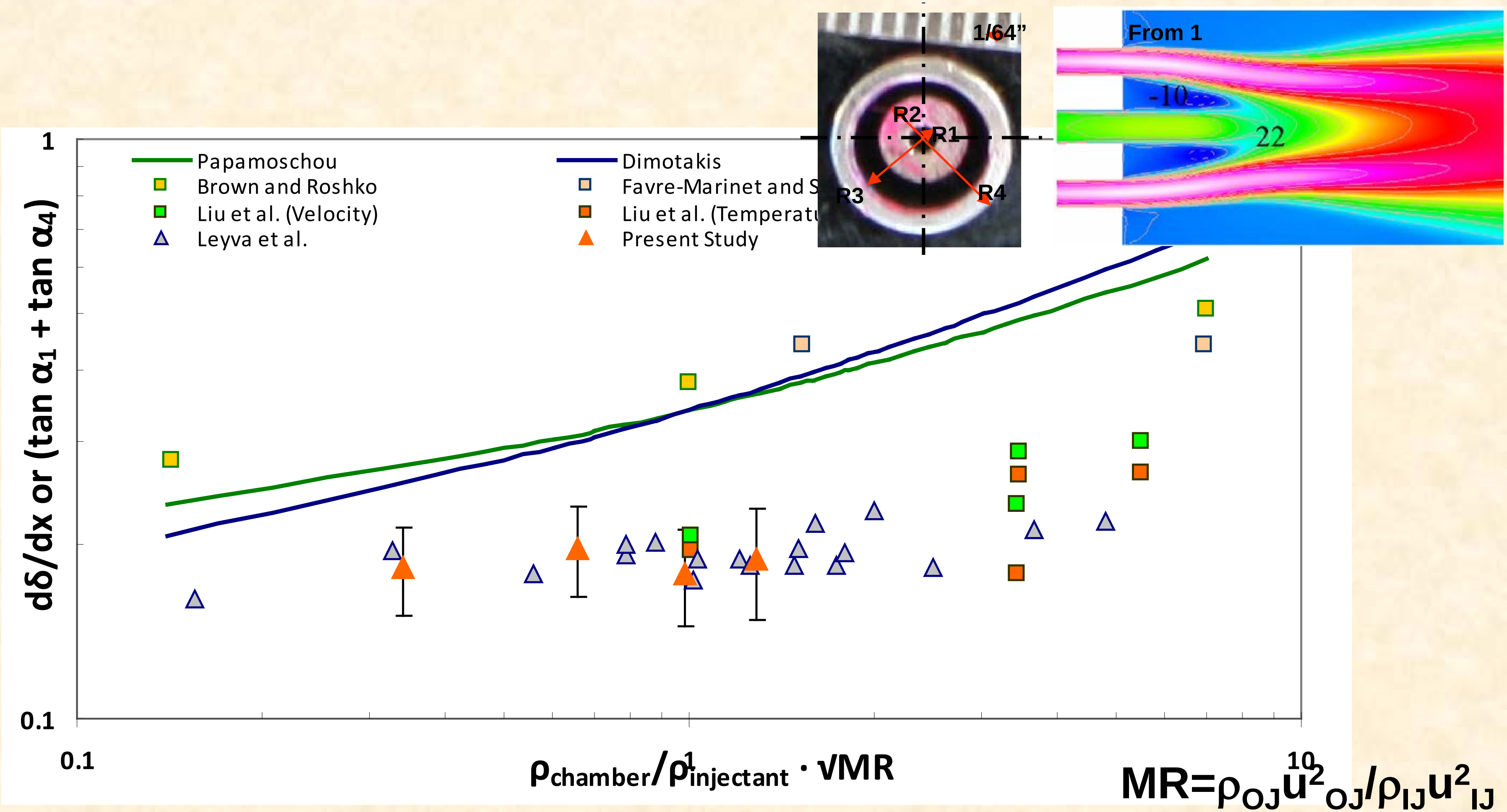

$MR=\rho_{OJ}u^2_{OJ}/\rho_{IJ}u^2_{IJ}$

1.Liu T., Zong, N., Yang, V., "Dynamics of Shear-Coaxial Cryogenic Nitrogen Jets with Acoustic Excitation under Supercritical Conditions", AIAA 2006-759.

Different x-axis groups data from all the pressure regimes

ATC
Advanced Technology Consultants
www.advtechconsultants.com

CFD results from Liu et al.

	case 1	case 2	case 3	case 4
P (MPa)	4.94	10	4.94	10
T_{chm} (K)	233	233	233	233
T_f (K)	191	191	191	191
T_o (K)	132	132	132	132
ρ_f (kg/m^3)	98.8	217.2	98.8	217.2
ρ_o (kg/m^3)	404.0	555.4	404.0	555.4
u_f (m/s)	120	120	65	95
u_o (m/s)	32	32	32	32
u_f / u_o	3.75	3.75	2.03	2.97
$(\rho u)_f / (\rho u)_o$	0.92	1.47	0.50	1.16
$(\rho u^2)_f / (\rho u^2)_o$	3.44	5.50	1.01	3.45
$\dot{m}_f / \dot{m}_o$	11.9	19.0	6.4	15.0
a_f (m/s)	279.6	302.2	279.6	302.2
a_o (m/s)	230.9	441.2	230.9	441.2
M_f	0.43	0.40	0.23	0.31
M_o	0.14	0.08	0.14	0.08
Re_f	3.3E5	5.8E5	1.8E5	4.6E5
Re_o	1.3E5	1.0E5	1.3E5	1.0E5

Re based on R_i and R_o

Table 1 Simulation conditions for analysis of shear-coaxial cryogenic nitrogen mixing process.

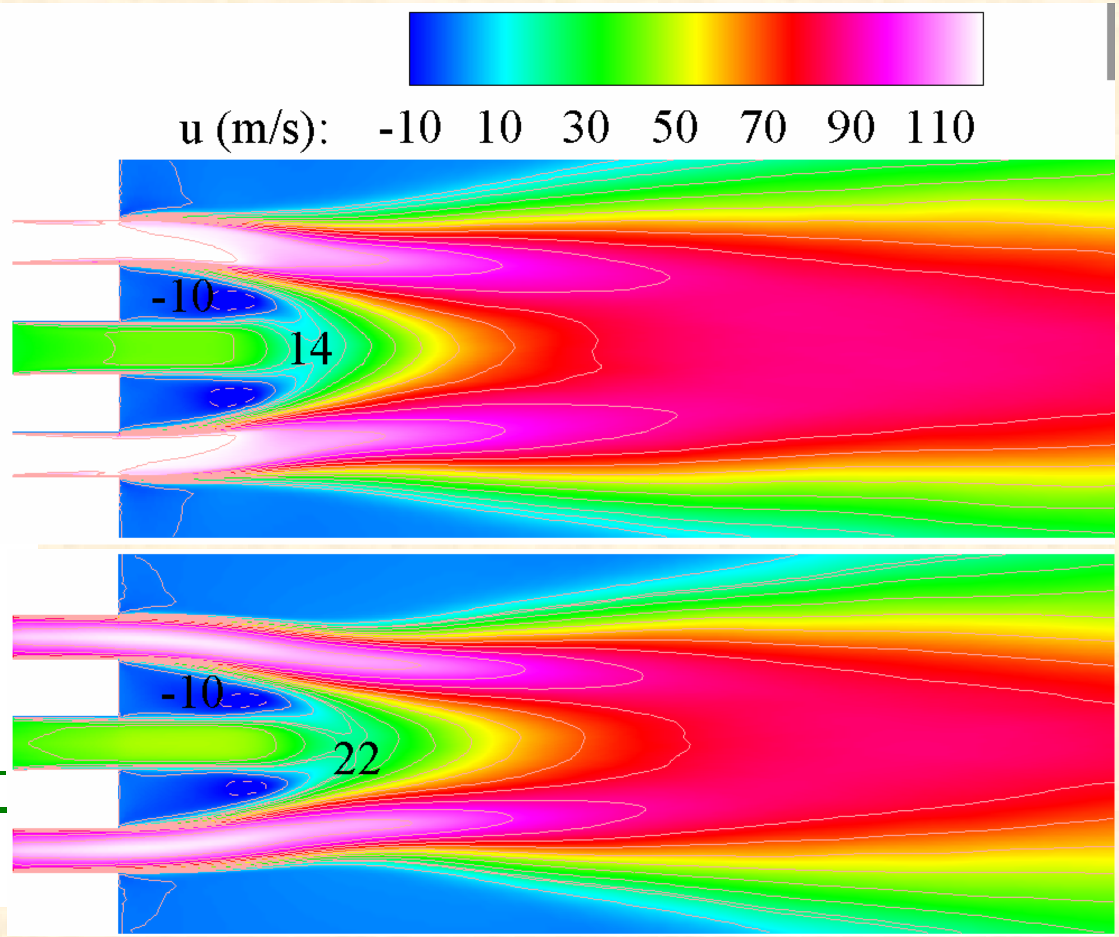

1.Liu T., Zong, N., Yang, V., “Dynamics of Shear-Coaxial Cryogenic Nitrogen Jets with Acoustic Excitation under Supercritical Conditions”, AIAA 2006-759.

Coaxial Jet (acoustic interaction)

ATC Advanced Technology Consultants

www.advtechconsultants.com

Subcritical (P_r=0.63) Coaxial Injector

Frequency: 2700 Hz
Chamber temp: 300 K

Effects of acoustic waves on a coaxial injector under subcritical condition and at core flowrate of 300 mg/s and three different coflow rates of 5, 188, 350 mg/s.

- **As co-flow rate is increased, reduction of the jet diameter even at the injector exit plane is observed**
- **The reduction of the visual jet diameter at the exit plane is due to the warmer GN2 co-flow, affecting the near-wall liquid nitrogen thermodynamic states inside the inner tube which guides the LN2 jet.**
- **One sees a simultaneous fuzziness of the jet boundary covered with a cushion layer of vaporized (lower density) and cold nitrogen.**
- **Measurements of λ_{Sub} agrees with a calculation using the core jet velocity and the acoustic waves oscillation period**

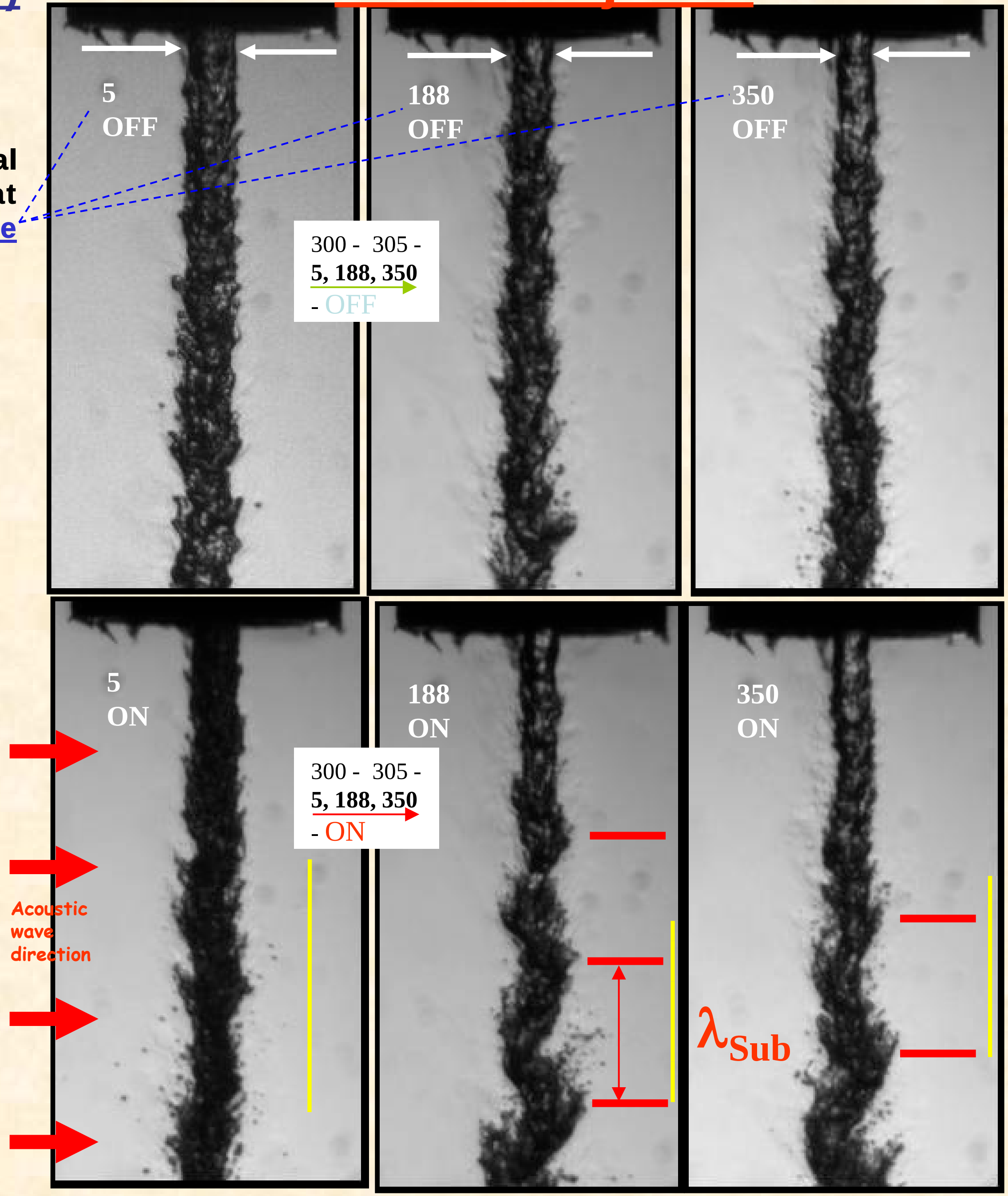

ATC
Advanced Technology Consultants
www.advtechconsultants.com

Supercritical (P_r=1.43) Coaxial Injector

Frequency: 2700 Hz
Chamber temp: 300 K

Effects of acoustic waves on a coaxial injector under supercritical condition and at core flowrate of 300 mg/s and three different coflow rates of 5, 188, 350 mg/s.

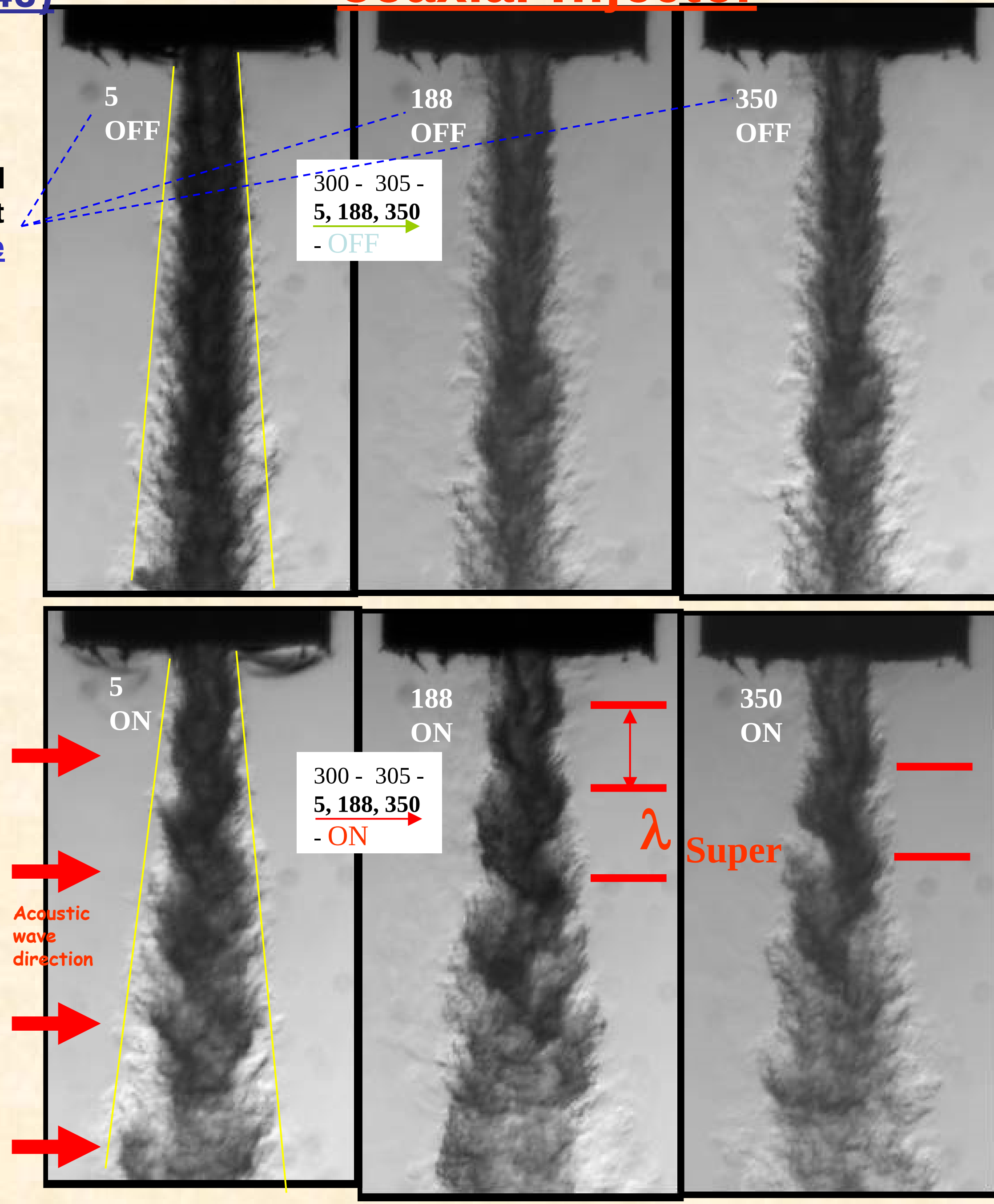

- Increase in the coflow rate alone tends to slightly narrow the jet with no other distinct visual effects
- Effects of the acoustic waves are, not only to increase the initial jet angle, but to again impose a sinusoidal shape to the jet
- $\lambda_{Sub} > \lambda_{Super}$:As the penetration rate of the newly injected fluid is reduced under higher chamber pressures (supercritical), the wavelength should decrease, as seen in the figures

ATC Advanced Technology Consultants

www.advtechconsultants.com

Coaxial Jet Subcritical Pressure

- Movie shows transition from when acoustic field is OFF to ON
- Acoustic driver frequency at 2.98 kHz
- Velocity Ratio = 9.1
- Chamber Pressure = 1.5 MPa
- Momentum Ratio = 3.2
- Framing rate 18.00 kHz

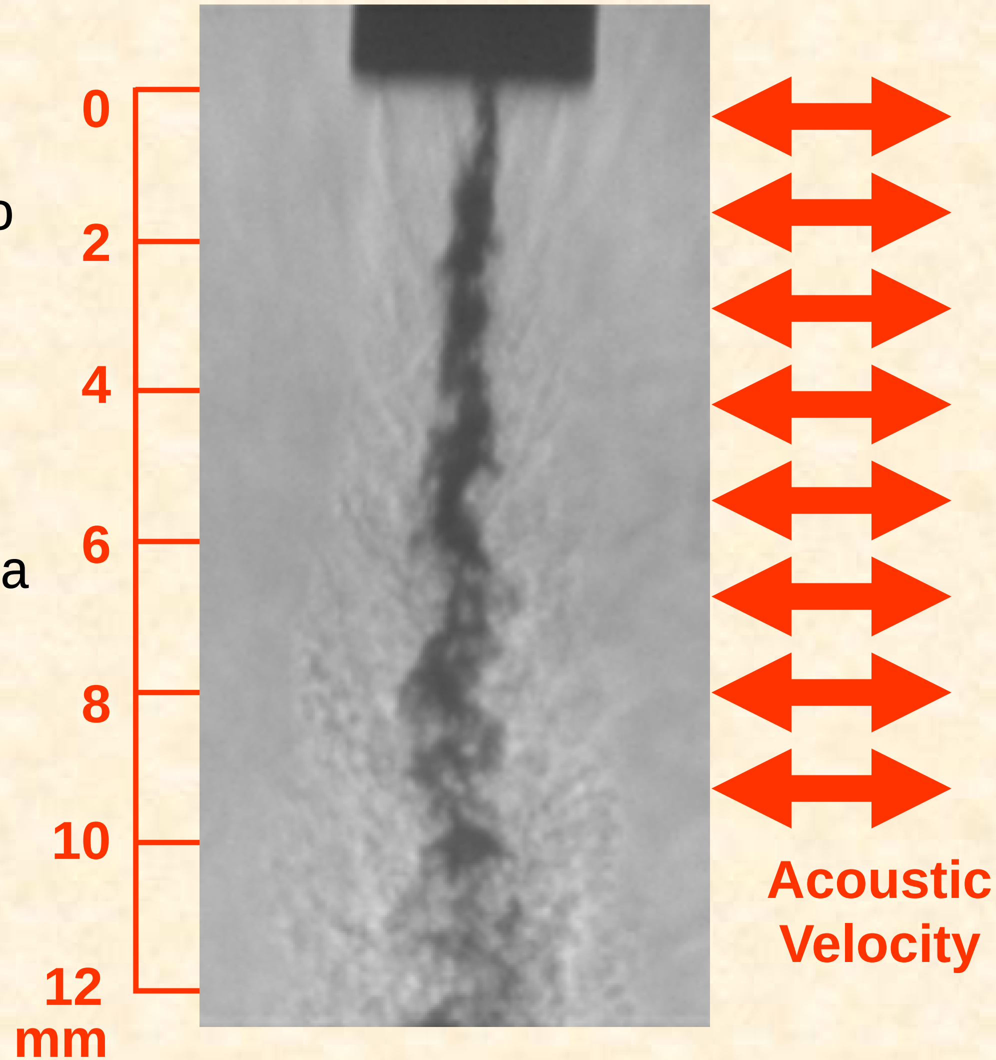

1. Davis, D. W. and Chehroudi, B., 2006. Measurements in an Acoustically-Driven Coaxial Jet under Supercritical Conditions, *AIAA J. of Propulsion and Power*, Vol. 23, No. 2, March-April, pp. 364-374.
2. PhD Thesis work by D. Davis at AFRL Supervised by B. Chehroudi

ATC Advanced Technology Consultants
www.advtechconsultants.com

Coaxial Jet Supercritical Pressure

- Movie shows transition from when acoustic field is OFF to ON
- Acoustic driver frequency at 2.98 kHz
- Velocity Ratio = 4.3
- Chamber Pressure = 4.9 MPa
- Momentum Ratio = 5.1
- Framing rate 18.00 kHz

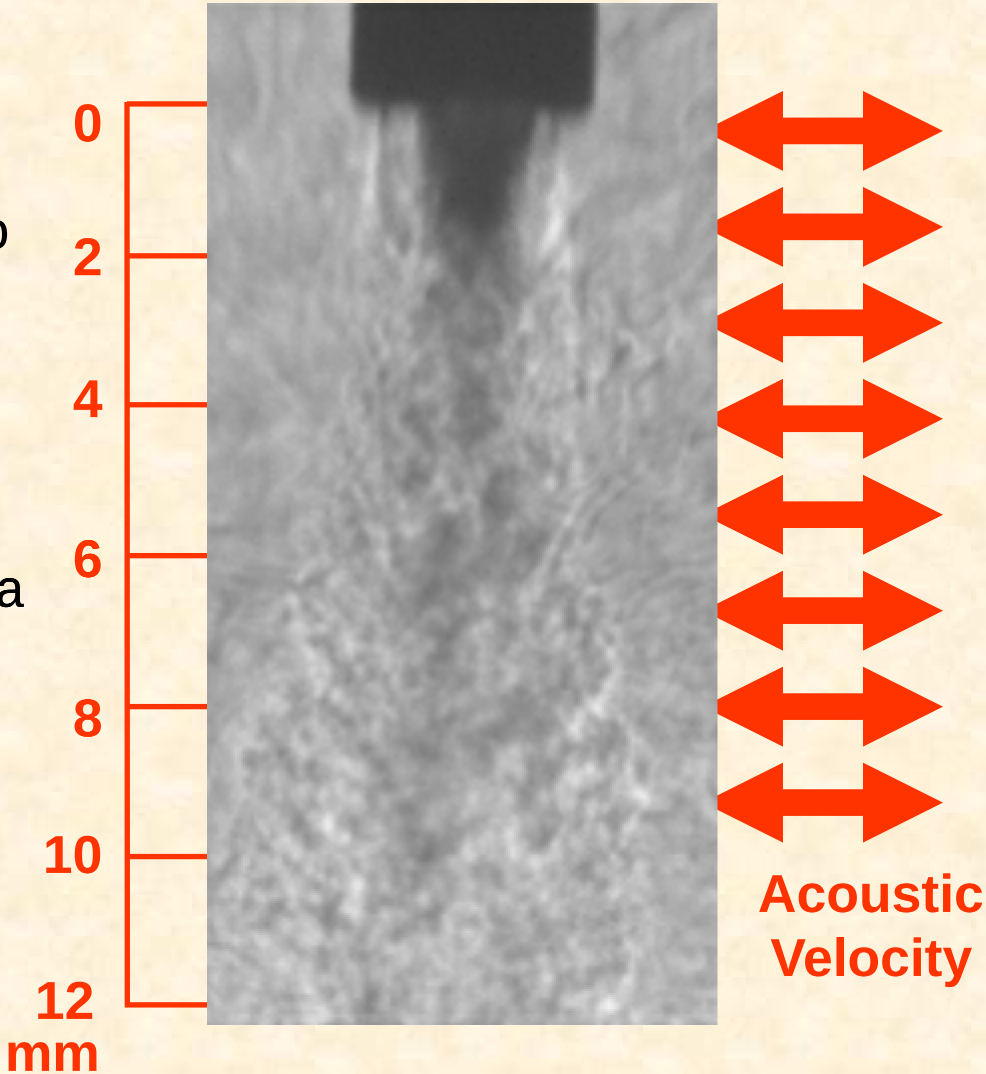

1. Davis, D. W. and Chehroudi, B., 2006. Measurements in an Acoustically-Driven Coaxial Jet under Supercritical Conditions, *AIAA J. of Propulsion and Power*, Vol. 23, No. 2, March-April, pp. 364-374.
2. PhD Thesis work by D. Davis at AFRL Supervised by B. Chehroudi

Mean Dark-Core Length vs. Velocity Ratio (VR)

ATC Advanced Technology Consultants

www.advtechconsultants.com

- **As VR increases, *L/D (normalized mean dark-core length)* decreases and approaches a constant**
- **Mean Dark-core length becomes shorter when acoustic driver is turned ON**

VR: Outer-to-Inner jet Velocity Ratio

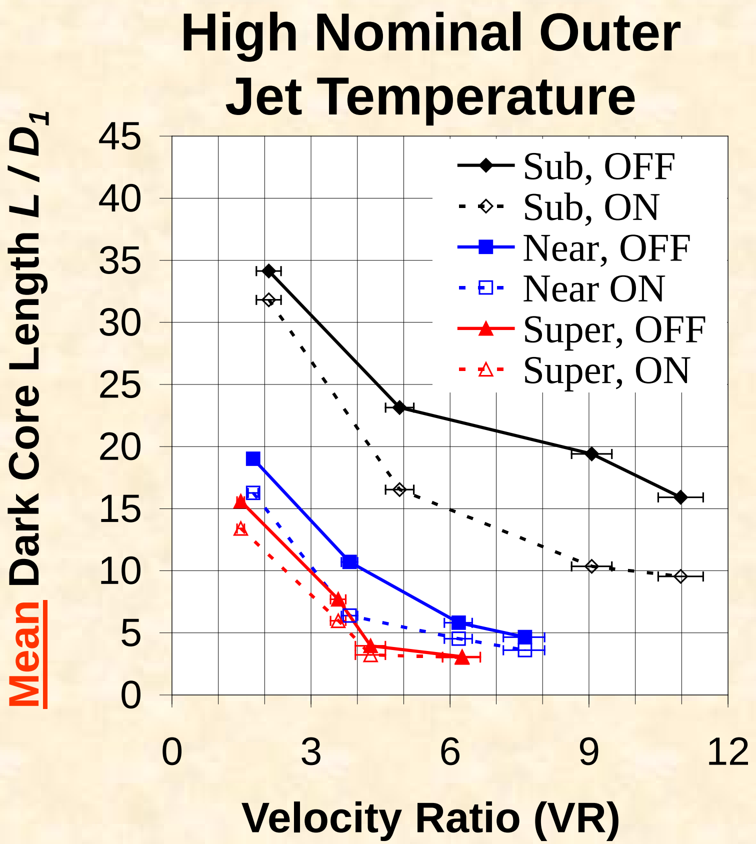

1. Davis, D. W. and Chehroudi, B., 2006. Measurements in an Acoustically-Driven Coaxial Jet under Supercritical Conditions, *AIAA J. of Propulsion and Power*, Vol. 23, No. 2, March-April, pp. 364-374.
2. PhD Thesis work by D. Davis at AFRL Supervised by B. Chehroudi

ATC Advanced Technology Consultants

www.advtechconsultants.com

RMS of Dark-Core Length vs. Velocity Ratio (VR)

- **First time the RMS of core length reported**
- **Intuitively, RMS of dark-core length fluctuations relates in some form to *mixture ratio variations***
- **High VR creates lowest RMS values (implications for combustion instability)**
  - **Inherent insensitivity (stability) of the jet at high VR**

VR: Outer-to-Inner jet Velocity Ratio

RMS: Root-mean- square of core length fluctuations

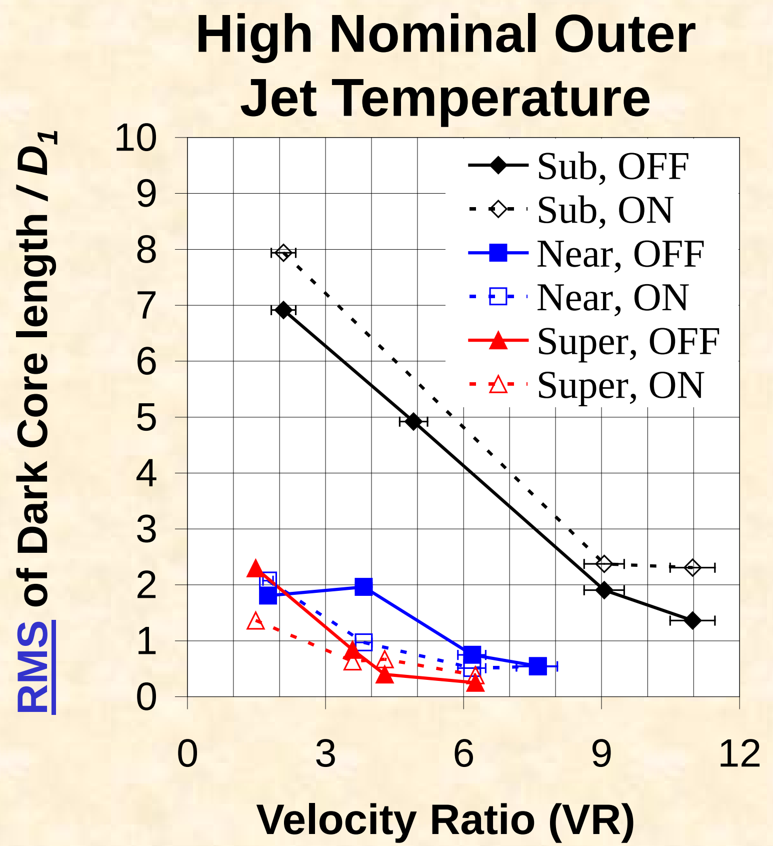

1. Davis, D. W. and Chehroudi, B., 2006. Measurements in an Acoustically-Driven Coaxial Jet under Supercritical Conditions, *AIAA J. of Propulsion and Power*, Vol. 23, No. 2, March-April, pp. 364-374.
2. PhD Thesis work by D. Davis at AFRL Supervised by B. Chehroudi

ATC
Advanced Technology Consultants
www.advtechconsultants.com

AFRL
THE AIR FORCE RESEARCH LABORATORY
LEAD | DISCOVER | DEVELOP | DELIVER

Schematic of the two acoustic sources at 0 and 180 degrees

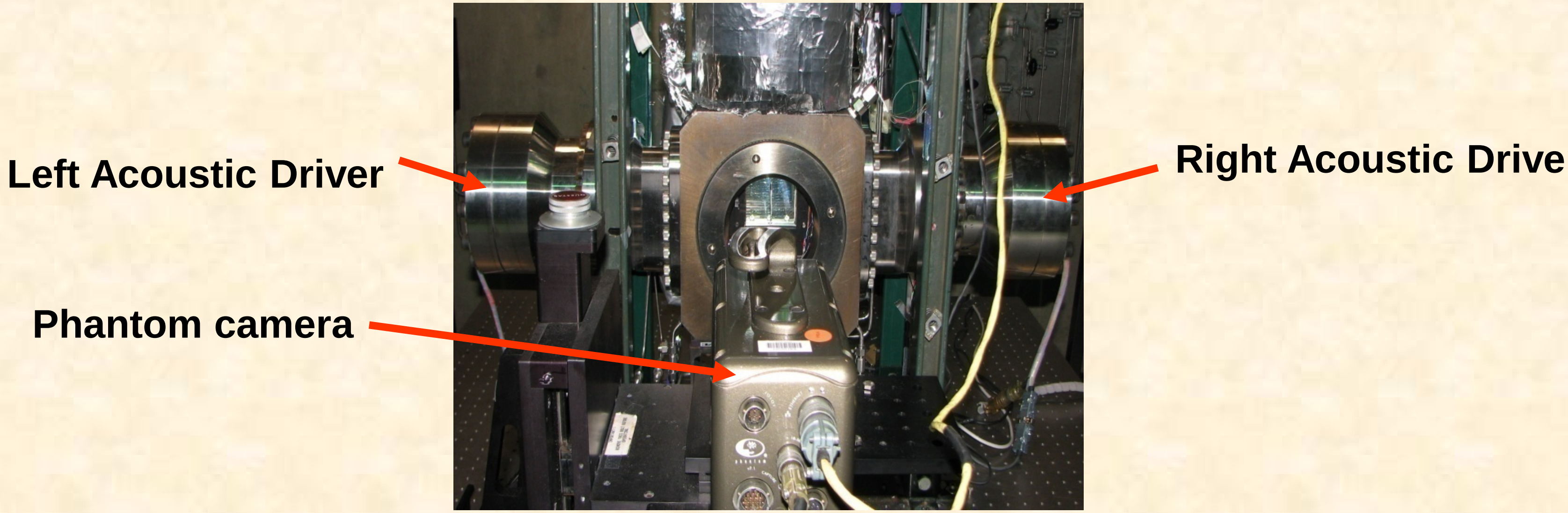

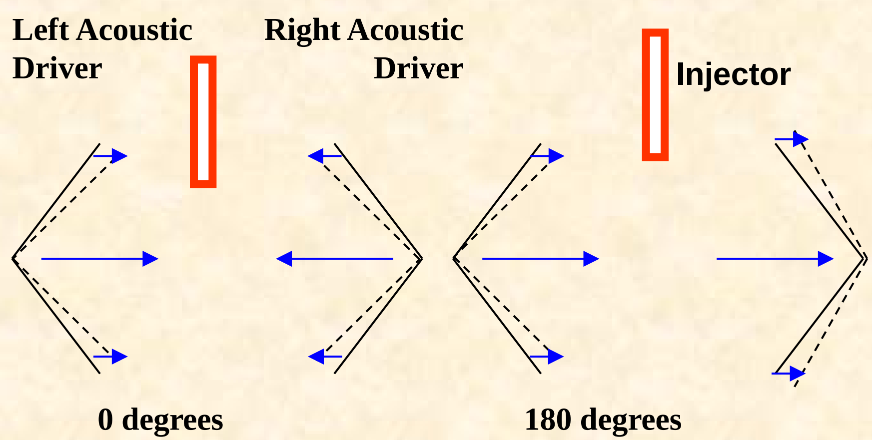

ATC Advanced Technology Consultants

www.advtechconsultants.com

Different phase angles between the two acoustic sources

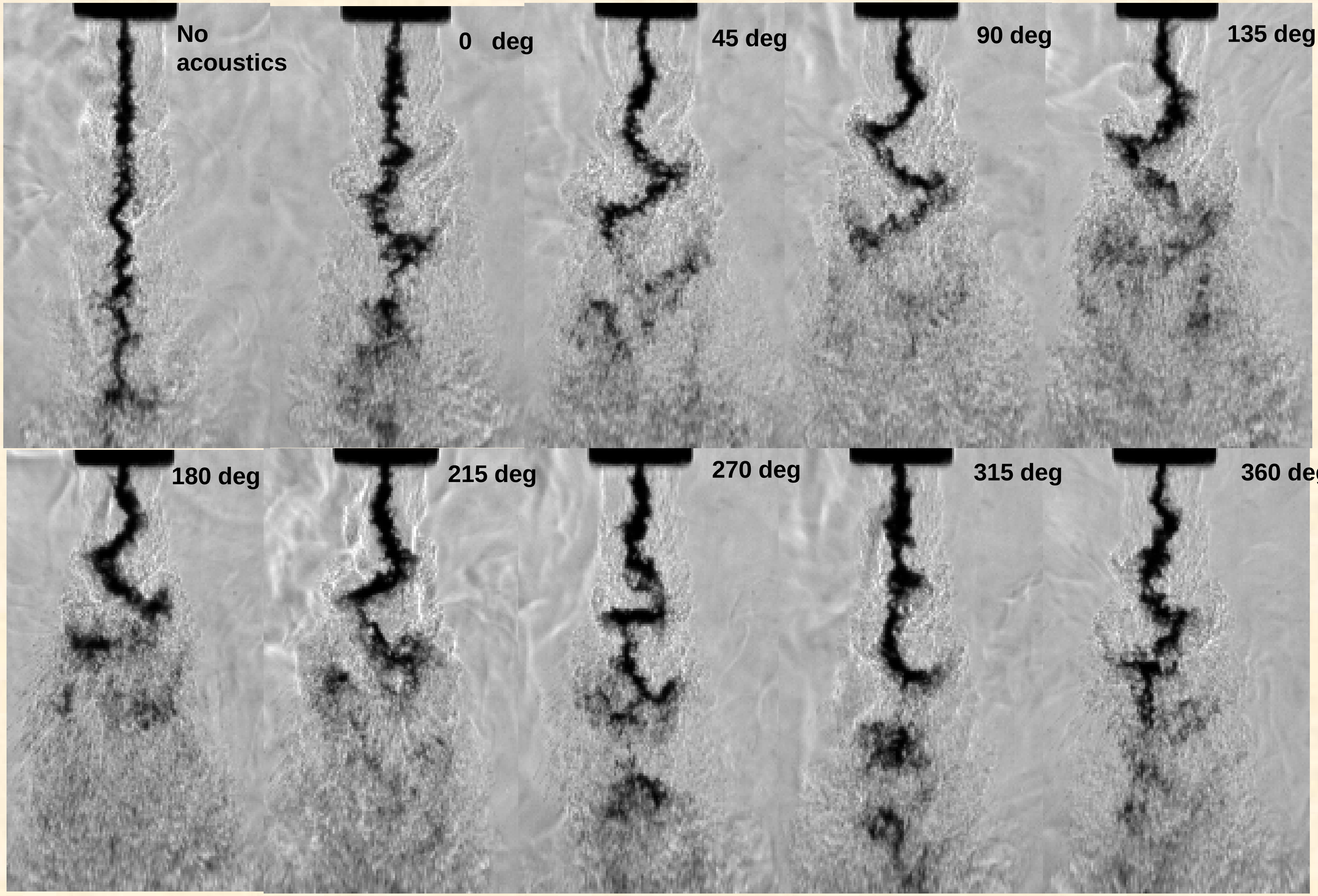

Pchamber =1.5 MPa, MR=2.6, VR=7.6

ATC Advanced Technology Consultants

www.advtechconsultants.com

Combustion Instability in Liquid Rocket Engines

A Unified Injector Sensitivity Theory

B. Chehroudi, PhD

ATC Advanced Technology Consultants

www.advtechconsultants.com

Combustion Instability

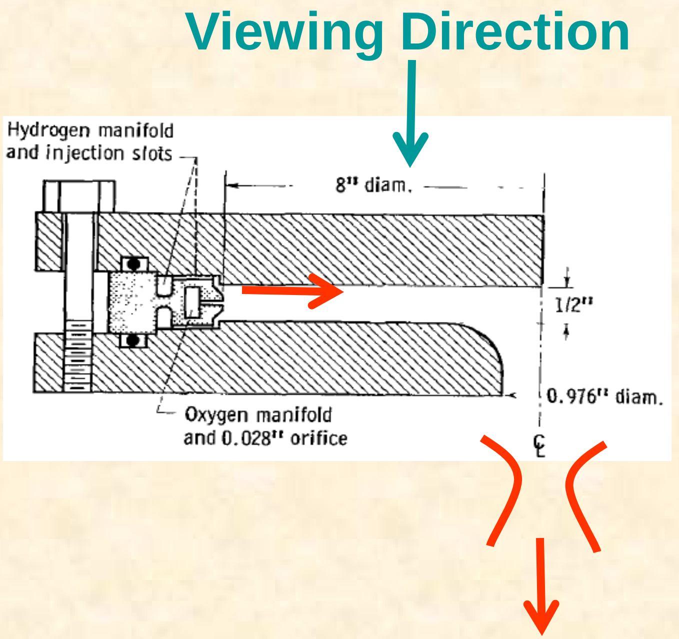

- The LOX core was found to decrease in length during a combustion instability event
- LOX core large scale sinusoidal structure

Heidmann, NASA TN D-2725, 1965
NASA Lewis Film C-226, 1965

Mechanism of Acoustic Combustion Instability (CI) in Liquid Rocket Engines (LRE)

- **In LOX/H2 Engines** (***Coaxial injector***; **RL-10, J-2, J-2S; SSME). Conditions under which CI occurred more commonly (or inevitably):**
  - **Lower velocity ratio (VR) V_{H2}/V_{LOX}**
  - **Sufficiently low temperature of injected hydrogen (Temp Ramping)**
  - **Less recessed oxidizer tubes**
  - **Reduced injector pressure drop**
  - **True mechanism remains obscure**
- **In LOX/HC Engines** (***Impinging jets injector***; **mostly from F-1)**
  - **Sensitivity of jets and formation of spray fans to velocity fluctuations parallel to the injector face**
  - ***Hewitt correlation*** **suggests certain injector parameters (d/V)**
  - **Others (resurge, etc.)**

3.3 Mechanisms in LOX/HC Engines

- Later developments at Aerojet and Penn State led to correlations with the parameter injector orifice diameter/injection velocity (D_j / V_j) to identify the peak injection response.

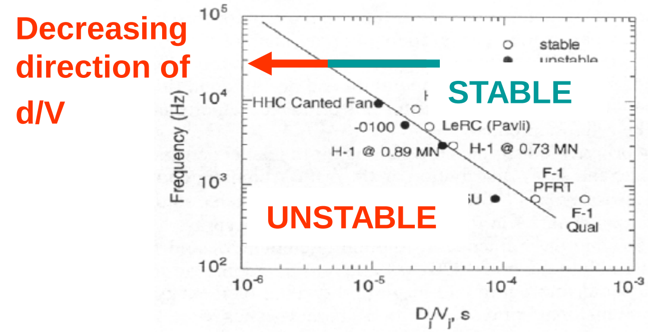

Like-doublet injector (LOX/HC)

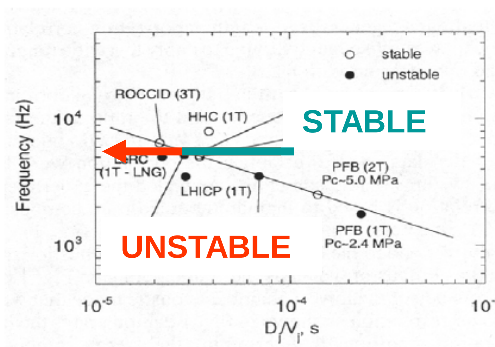

O-F-O injector (LOX/RP-1)

- These results are related to the dynamics of injectors but there is no associated modeling.

From Prof. F. Culick, CalTech

Chehroudi, B. 2009. A Unified Approach on Combustion Instability in Cryogenic Liquid Rockets, 47th AIAA Aerospace Sciences Meeting, AIAA-2009-237, Orlando, Florida, 5-8 January

Dark Core Characteristics is the Key: *Non-reacting* Coaxial Jet & Connection to Multi-Element LRE

ATC Advanced Technology Consultants

www.advtechconsultants.com

From AFRL & PennState: Davis (PhD Thesis), Davis and Chehroudi, and Leyva et al.

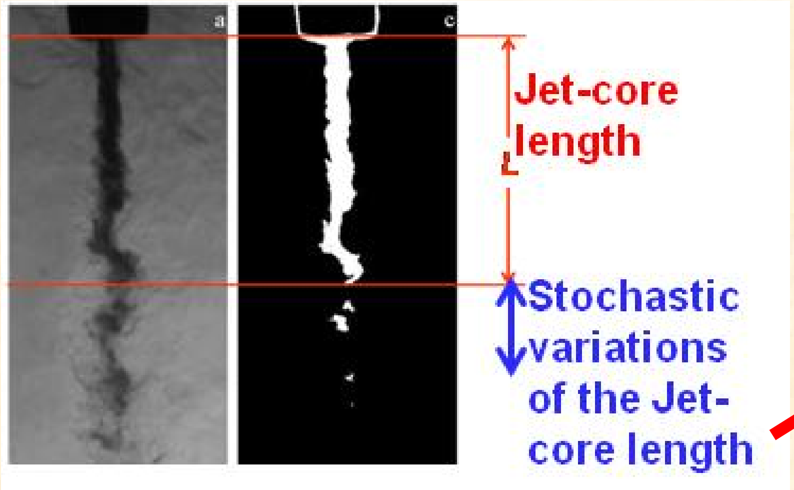

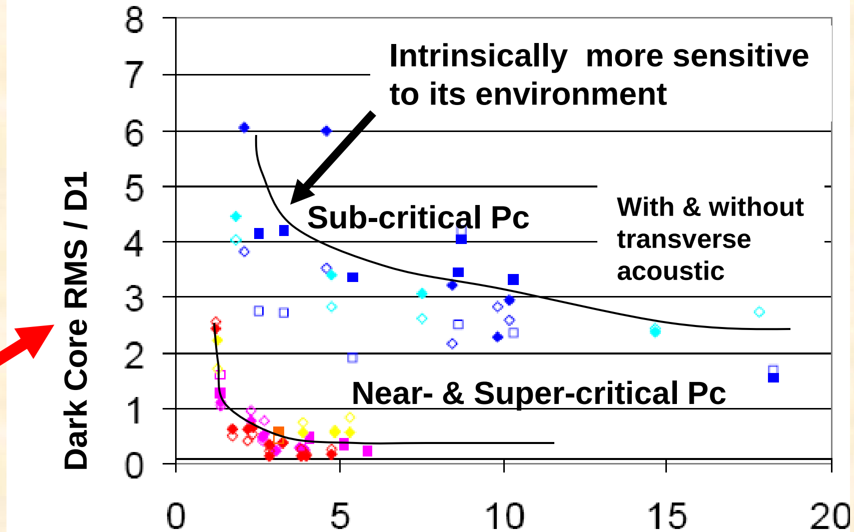

1. RMS of the dark core length oscillations as
   - A reflection of mass fluctuations (first order approximation)
   - Indication of *intrinsic sensitivity* of the injector
2. RMS of the core length variations is much higher at subcritical chamber pressure at all velocity ratios
   - *Intrinsic (higher) sensitivity* at subcritical (see also next slide for consistent result in fired engine)

- Lower RMS at high velocity ratio offered a possible explanation for the enhanced stability observed in LRE (**at high V_{H2}/V_{LOX}**)
- Temperature ramping (**for LRE stability rating**) was linked to its impact on the velocity ratio and hence core length RMS offered an explanation

Chehroudi, B. 2009. A Unified Approach on Combustion Instability in Cryogenic Liquid Rockets, 47th AIAA Aerospace Sciences Meeting, AIAA-2009-237, Orlando, Florida, 5-8 January

Dark Core Characteristics is the Key: Intrinsic Sensitivity of Impinging Jet Injector at Low d/V values

ATC Advanced Technology Consultants

www.advtechconsultants.com

Decreasing direction of d/V

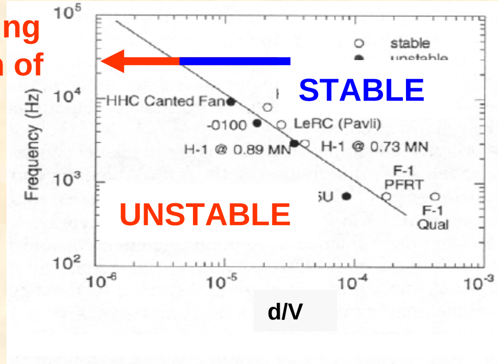

Chehroudi, B. 2009. A Unified Approach on Combustion Instability in Cryogenic Liquid Rockets, 47th AIAA Aerospace Sciences Meeting, AIAA-2009-237, Orlando, Florida, 5-8 January

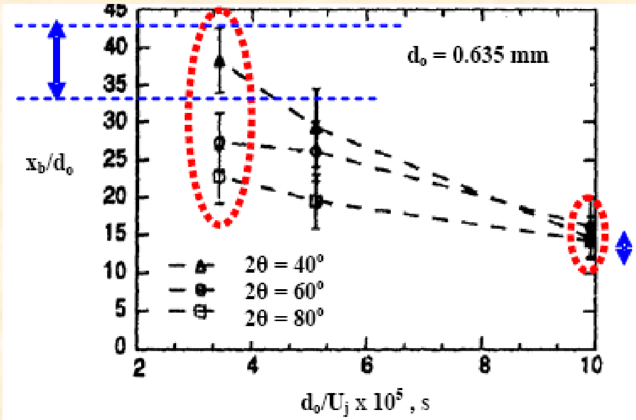

Figure 8. Shows *sheet breakup length* as a function of instability parameter at three different impingement included angles. Much higher sensitivity of the *sheet breakup length* is seen with included angle (2θ) at low dn/V (= d_o/U_j, in the original article) values. Anderson et al. [13].

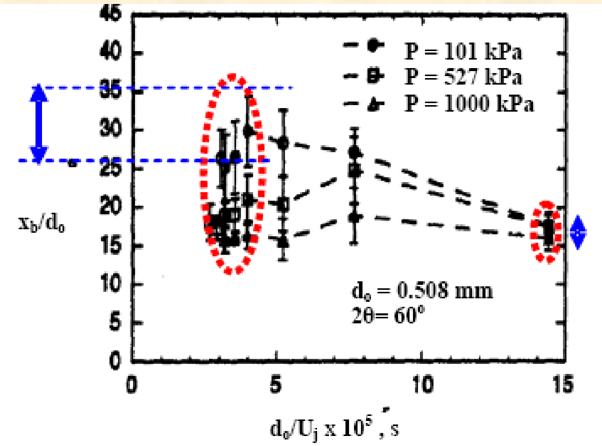

Figure 9. Shows *sheet breakup length* as a function of instability parameter at three different chamber pressures. Much higher sensitivity of the *sheet breakup length* is seen with chamber pressure at low dn/V (= d_o/U_j, in the original article) values. Anderson et al. [13].

Impinging Jets:

- **PennState work in non-reacting setup (*Anderson et al.)***
  - **Higher sensitivity at lower values of d/V**
  - **Higher sensitivity to chamber pressure at low values of d/V**
  - **Intrinsic stability of the impinging jet injector at low d/V values (*for more details see paper*)**

A Unified Injector Sensitivity Theory

ATC Advanced Technology Consultants

www.advtechconsultants.com

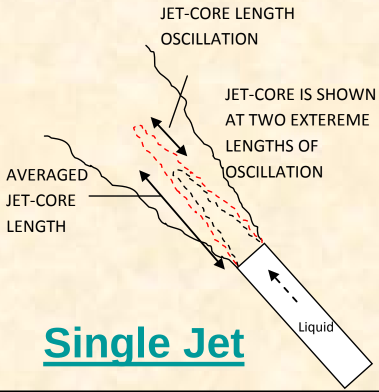

Single Jet

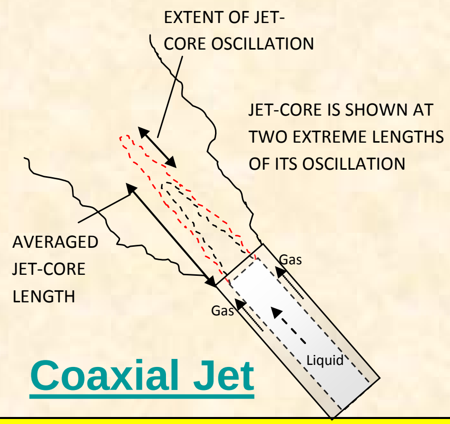

Coaxial Jet

Key Components of the *Unified Theory*:

1. **All share a "dark core" with Mean & RMS, suggesting a unified approach for intrinsic sensitivity of the jet to its environment**

2. **When an important dynamic feature (dark-core or breakup zone) of an injector design becomes sufficiently sensitive to thermofluid parameters of its environment, it is highly likely that this could strengthen the feedback link thought to be critical in the amplification process and hence move the dynamic system into an unstable operating regime.**

3. **See schematic diagram of hypothesis**

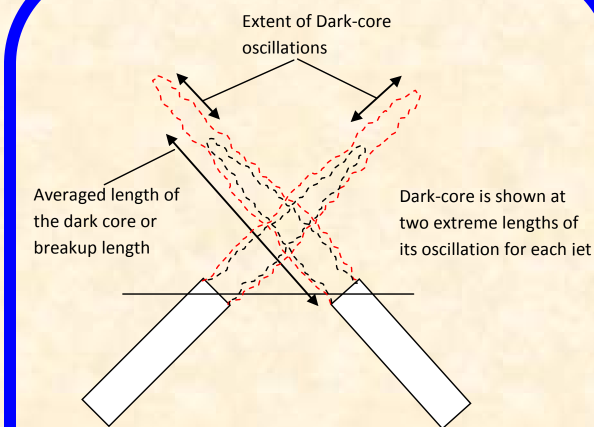

Lowered Intrinsic Sensitivity (e.g., for LOL)

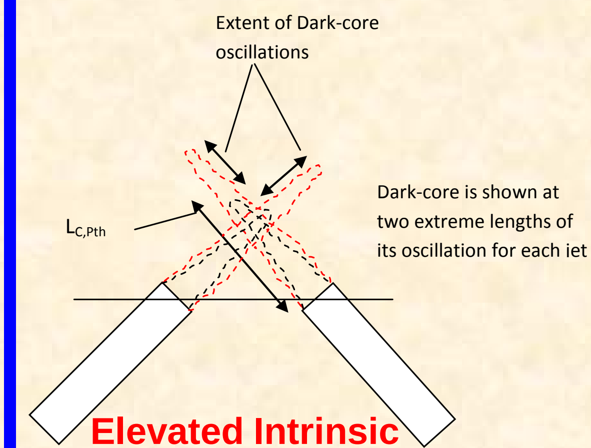

Elevated Intrinsic Sensitivity (e.g., for LOL)

Impinging Jets

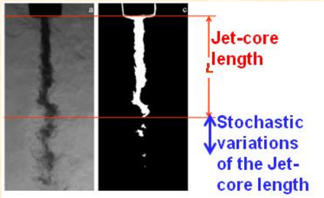

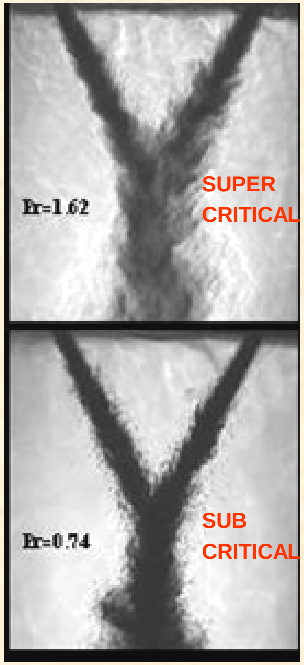

Chehroudi, B. 2009. A Unified Approach on Combustion Instability in Cryogenic Liquid Rockets, 47th AIAA Aerospace Sciences Meeting, AIAA-2009-237, Orlando, Florida, 5-8 January

Supporting Data and Offered Explanations by the *Unified Injector Sensitivity Theory*

ATC
Advanced Technology Consultants
www.advtechconsultants.com

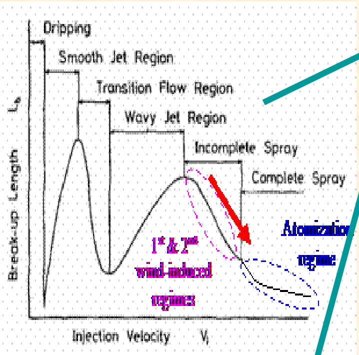

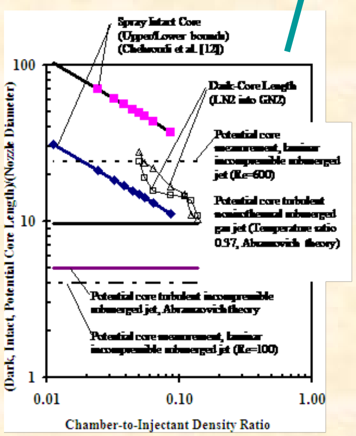

SINGLE JET
Dark-core (Breakup) length
Hiroyasu

IMPINGING JET

Hewitt Stability plot for LOL impinging (d/V)

Comparable pre-impingement distance and Dark-core length

Observed Instability at high chamber pressures for some engine designs (J. Fang)

(Santoro' Group) Impinging jet increasing sensitivity at lower d/V (Anderson et al.)

Prediction for impinging jet rockets using the THEORY

Cavitation& Hydraulic Flip (Hiroyasu)

Dark Core length measurements by DLR and Chehroudi (AFRL)

Unified Injector Sensitivity Theory
Dynamics of the Dark Core length

COAXIAL JET

LRE Stability rating
- Temp Ramping
- Velocity Ratio

DLR work in single-element Rocket
Stable at near- & super-critical
Unstable at subcritical

Physical interpretation of RMS and connection to instability (Culick)

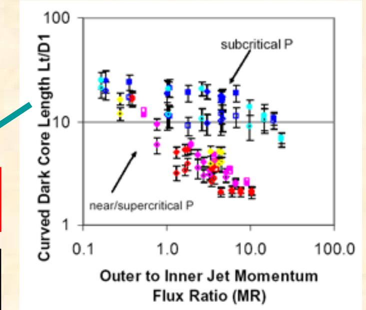

Figure 10. Trend of the Curved Dark Core Length vs.

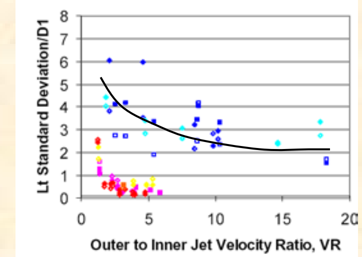

Chehroudi, B. 2009. A Unified Approach on Combustion Instability in Cryogenic Liquid Rockets, 47th AIAA Aerospace Sciences Meeting, AIAA-2009-237, Orlando, Florida, 5-8 January

MANY EXPERIMENTALLY OBSERVED TRENDS ARE CONSISTENT WITH THE THEORY

ATC
Advanced Technology Consultants
www.advtechconsultants.com

Conclusions

- *For the first time*, it was shown, quantitatively, that supercritical single jets grow similar to the incompressible variable-density jets
- 2*(FWHM) of radial profiles measured by Raman is equivalent to Visual jet thickness
- Fractal dimension of the jet at subcritical agrees with those of liquid jets at wind-induced atomization regimes and for supercritical jets is in agreement with values reported for gaseous jets
- A phenomenological model equation is proposed that mimics the experimental data both at subcritical and supercritical conditions
- Dark-core length (for coaxial jets) as a function of outer-to-inner jet momentum flux ratio for subcritical behaves like two-phase flows and for the supercritical like single-phase flows (dual character)
- Interaction of external acoustic field with single and coaxial jets were investigated when jets are located at the velocity antinode (pressure node)
- A *Unified Injector Sensitivity Theory* is proposed
- Unique systematic approach based on dynamic behavior of the "Jet-core length" characterized for single jets (showerhead), coaxial jets, and impinging jets
- This theory, *for the first time*, attempts to propose & unify the underlying mechanism responsible for the sensitivity of different liquid rocket injectors to acoustic field established inside the rocket thrust chamber
- Theory is able to offer plausible explanations for combustion instability observations in liquid rocket engines under sub- and super-critical conditions
- Theory is consistent with the examined (so far) existing body of data from cold to fired single-element tests, as well as able to explain engine data such as Hewitt Stability Correlation (see paper for details)

The End